Copyright Warning & Restrictions

The copyright law of the United States (Title 17, United States Code) governs the making of photocopies or other reproductions of copyrighted material.

Under certain conditions specified in the law, libraries and archives are authorized to furnish a photocopy or other reproduction. One of these specified conditions is that the photocopy or reproduction is not to be "used for any purpose other than private study, scholarship, or research." If a, user makes a request for, or later uses, a photocopy or reproduction for purposes in excess of "fair use" that user may be liable for copyright infringement,

This institution reserves the right to refuse to accept a copying order if, in its judgment, fulfillment of the order would involve violation of copyright law.

Please Note: The author retains the copyright while the New Jersey Institute of Technology reserves the right to distribute this thesis or dissertation

Printing note: If you do not wish to print this page, then select "Pages from: first page # to: last page #" on the print dialog screen

ABSTRACT

THE DESIGN AND OPTIMIZATION OF COOPERATIVE MOBILE EDGE

by
Xueqing Huang

As the world is charging towards the Internet of Things (IoT) era, an enormous amount of sensors will be rapidly empowered with internet connectivity. Besides the fact that the end devices are getting more diverse, some of them are also becoming more powerful, such that they can function as standalone mobile computing units with multiple wireless network interfaces. At the network end, various facilities are also pushed to the mobile edge to foster internet connections. Distributed small scale cloud resources and green energy harvesters can be directly attached to the deployed heterogeneous base stations.

Different from the traditional wireless access networks, where the only dynamics come from the user mobility, the evolving mobile edge will be operated in the constantly changing and volatile environment. The harvested green energy will be highly dependent on the available energy sources, and the dense deployment of a variety of wireless access networks will result in intense radio resource contention. Consequently, the wireless networks are facing great challenges in terms of capacity, latency, energy/spectrum efficiency, and security. Equivalently, balancing the dynamic network resource demand and supply is essential to the smooth network operation.

Leveraging the broadcasting nature of wireless data transmission, network nodes can cooperate with each other by either allowing users to connect with multiple base stations simultaneously or offloading user workloads to neighboring base stations. Moreover, grid facilitated and radio frequency signal enabled renewable energy sharing among network nodes are introduced in this dissertation. In particular, the smart grid

can transfer the green energy harvested by each individual network node from one place to another. The network node can also transmit energy from one to another using radio frequency energy transfer.

This dissertation addresses the cooperative network resource management to improve the energy efficiency of the mobile edge. First, the energy efficient cooperative data transmission scheme is designed to cooperatively allocate the radio resources of the wireless networks, including spectrum and power, to the mobile users. Then, the cooperative data transmission and wireless energy sharing scheme is designed to optimize both the energy and data transmission in the network. Finally, the cooperative data transmission and wired energy sharing scheme is designed to optimize the energy flow within the smart grid and the data transmission in the network.

As future work, how to motivate multiple parties to cooperate and how to guarantee the security of the cooperative mobile edge is discussed. On one hand, the incentive scheme for each individual network node with distributed storage and computing resources is designed to improve network performance in terms of latency. On the other hand, how to leverage network cooperation to balance the tradeoff between efficiency (energy efficiency and latency) and security (confidentiality and privacy) is expounded.

THE DESIGN AND OPTIMIZATION OF COOPERATIVE MOBILE EDGE

by
Xueqing Huang

A Dissertation
Submitted to the Faculty of
New Jersey Institute of Technology
in Partial Fulfillment of the Requirements for the Degree of
Doctor of Philosophy in Electrical Engineering

Helen and John C. Hartmann Department of
Electrical and Computer Engineering

May 2017

APPROVAL PAGE

THE DESIGN AND OPTIMIZATION OF COOPERATIVE MOBILE EDGE

Xueqing Huang

Dr. Nirwan Ansari, Dissertation Advisor — Date
Distinguished Professor, Department of Electrical and Computer Engineering, NJIT

Dr. Cristian Borcea, Committee Member — Date
Department Chair and Professor, Department of Computer Science, NJIT

Dr. Doru Calin, Committee Member — Date
Director/Domain Leader and Bell Labs Fellow, Nokia, NJ
Adjunct Professor, Columbia University

Dr. Abdallah Khreishah, Committee Member — Date
Assistant Professor, Department of Electrical and Computer Engineering, NJIT

Dr. Qing Liu, Committee Member — Date
Assistant Professor, Department of Electrical and Computer Engineering, NJIT

BIOGRAPHICAL SKETCH

Author: Xueqing Huang

Degree: Doctor of Philosophy

Date: May 2017

Undergraduate and Graduate Education:

- Doctor of Philosophy in Electrical Engineering,
  New Jersey Institute of Technology, Newark, NJ, 2017
- Master of Engineering in Communication and Information Systems,
  Beijing University of Posts and Telecommunications, Beijing, P. R. China, 2012
- Bachelor of Engineering in Communication Engineering,
  Hefei University of Technology, Anhui, P. R. China, 2009

Major: Electrical Engineering

Presentations and Publications:

Journals:

X. Huang, T. Han, and N. Ansari, "Smart grid enabled mobile networks: jointly optimizing BS operation and power distribution," *IEEE Transactions on Networking*, doi: 10.1109/TNET.2017.2655462.

X. Huang and N. Ansari, "Resource exchange in smart grid connected cooperative cognitive radio networks," *IEEE Transactions on Vehicular Technology*, doi: 10.1109/TVT.2016.2642902.

X. Huang and N. Ansari, "Content caching and distribution in smart grid enabled wireless networks," *IEEE Internet of Things Journal*, vol. 4, no. 2, pp. 513-520, Apr. 2017.

X. Huang and N. Ansari, "Optimal cooperative power allocation for energy harvesting enabled relay networks," *IEEE Transactions on Vehicular Technology*, vol. 65, no. 4, pp. 2424-2434, Apr. 2016.

X. Huang and N. Ansari, "Joint spectrum and power allocation for multi-node cooperative wireless systems," *IEEE Transactions on Mobile Computing*, vol. 14, no. 10, pp. 2034-2044, Oct. 2015.

X. Huang and N. Ansari, "Energy sharing within EH-enabled wireless communication networks," *IEEE Communications Magazine*, vol. 22, no. 3, pp. 144-149, Jun. 2015.

X. Huang, T. Han, and N. Ansari, "On green energy powered cognitive radio networks," *IEEE Communications Surveys and Tutorials*, vol. 17, no. 2, pp. 827-842, 2nd Quarter, 2015.

H. Li, C. Yang, X. Huang, N. Ansari and Z. Wang, "Cooperative RAN caching based on local altruistic game for single and joint transmissions," *IEEE Communications Letters*, vol. 21, no. 4, pp. 853-856, Apr. 2017.

Q. Cui, P. Kang, X. Huang, M. Valkama, and J. Niemela, "Optimal power allocation for homogeneous and heterogeneous CA-MIMO systems," *Science China Information Sciences (Springer)*, vol. 56, no. 2, pp 1-14, Feb. 2013.

Q. Cui, B. Luo, X. Huang, A. Dowhuszko, and J. Jiang, "Closed form power allocation solution with minimization power consumption for coordinated transmission," *EURASIP Journal on Wireless Communications and Networking (Springer)*, vol. 2012, no. 1, pp. 1-14, 2012.

Q. Cui, X. Huang, B. Luo, X. Tao, and J. Jiang, "Capacity analysis and optimal power allocation for coordinated transmission in MIMO-OFDM systems," *Science China Information Sciences (Springer)*, vol. 55, no. 6, pp 1372-1387, Jun. 2012.

Conferences:

X. Huang and N. Ansari, "Secure multi-party data communications in cloud augmented IoT environment," in *Proceedings of the IEEE International Conference on Communications (ICC)*, May 2017, pp. 1-6.

X. Huang and N. Ansari, "Content caching and user scheduling in heterogeneous wireless networks," in *Proceedings of the IEEE GLOBECOM*, Dec. 2016, pp. 1-6.

Z. Wang, H. Li, X. Huang, and S. Ci, "Modeling and transmission optimization of full-duplex energy harvesting enabled hybrid relaying," in *Proceedings of the IEEE GLOBECOM*, Dec. 2016, pp. 1-7.

X. Huang and N. Ansari, "Data and energy cooperation in relay-enhanced OFDM systems," in *Proceedings of the IEEE ICC*, May 2016, pp. 1-6.

X. Liu, X. Huang and N. Ansari, "Green energy driven user association in cellular networks with dual-battery system," in *Proceedings of the IEEE ICC*, May 2016, Kuala Lumpur, Malaysia.

X. Huang and N. Ansari, "RF energy harvesting enabled power sharing in relay networks," in *Proceedings of the IEEE OnlineGreencomm*, Nov. 2014, pp. 1-6.

T. Han, X. Huang and N. Ansari, "Energy agile packet scheduling to leverage green energy for next generation cellular networks," in *Proceedings of the IEEE ICC*, May 2013, pp. 3650-3654.

Q. Cui, B. Luo, and X. Huang, "Joint power allocation solutions for power consumption minimization in coordinated transmission system," in *Proceedings of the IEEE GLOBECOM Wkshps*, Dec. 2011, pp. 452-457.

X. Huang, Q. Cui, and X. Tao, "Coexistence studies involving LTE-advanced," in *Proceedings of the IEEE International Conference on Broadband Network and Multimedia Technology (IC-BNM)*, Oct. 2010, pp. 273-277.

S. Yang, Q. Cui, X. Huang and X. Tao, "An effective uplink power control scheme in CoMP systems," in *Proceedings of the IEEE Vehicular Technology Conference (VTC)*, Sept. 2010, pp. 1-5.

Patent:

Q. Cui, P. Zhang, X. Huang, Q. Wang, and X. Tao, "Uplink power control scheme for carrier aggregation system," International Patent Application No. PCT/CN2011/081127, filed on Oct. 21, 2011; Chinese Patent No. CN102076072B, granted on Oct. 09, 2013.

To my beloved son, parents, brother, and parents in law. Their encouragement, sacrifices, and love have meant more to me than they can imagine. To my dear husband, Yan, for his unwavering support. This thesis is dedicated to them.

—— Xueqing Huang

ACKNOWLEDGMENT

My deepest gratitude is to my advisor, Dr. Nirwan Ansari. I have been amazingly fortunate to have him give me the freedom and encouragement to explore research ideas while providing excellent guidance. His persistent support and patience helped me overcome many difficult situations throughout my research. Without his continuous help, this dissertation would not have been possible.

To my committee members, Dr. Cristian Borcea, Dr. Doru Calin, Dr. Abdallah Khreishah, and Dr. Gary Liu, I thank them for their time and advisement.

This dissertation is based upon work supported by the National Science Foundation under Grant No. CNS-1320468.

I want to thank my friends – Tao Han, Yan Zhang, Bongho Kim, Thomas Lo, Mina Taheri, Xiang Sun, Abbas Kiani, Xilong Liu, Liang Zhang, Qiang Fan, Ali Shahini, Di Wu, Yi Xu, Ruihua Cheng, Xin Gao, Rui Cao, Jianchen Shan, Qingfeng Liu, Jie Zhang, and many others, who have given me support and encouragement over the last five years.

I would like to extend my gratitude to other faculty and staff members of the Department of Electrical and Computer Engineering for their support throughout my doctoral studies.

TABLE OF CONTENTS

Chapter **Page**

1 INTRODUCTION 1

2 COOPERATIVE WIRELESS DATA TRANSMISSION 6

2.1 Coordinated Transmission Model 8

2.2 Problem Analysis 11

2.2.1 Power Allocation Scheme 12

2.2.2 UE-BS Association Scheme 13

2.2.3 Complexity Reduction Scheme 15

2.3 Joint Spectrum and Power Allocation Algorithm 17

2.4 Simulation Results 19

2.4.1 Two-node System 19

2.4.2 Multi-node System 21

2.5 Summary 22

3 DATA AND ENERGY COOPERATION IN WIRELESS COMMUNICATIONS SYSTEMS 25

3.1 System Model and Problem Formulation 27

3.2 Problem Anslysis 29

3.3 Optimal Power Allocation 33

3.4 Numerical Results 37

3.5 Summary 38

4 WIRED ENERGY AND WIRELESS DATA COOPERATION 40

4.1 System Model 43

4.1.1 Traffic Model 45

4.1.2 Energy Consumption Model 47

4.2 Problem Formulation and Analysis 49

4.2.1 Problem Simplification 51

TABLE OF CONTENTS
(Continued)

Chapter **Page**

4.2.2 Problem Decomposition 53
4.3 An Approximate Solution 56
4.3.1 Wired and Wireless Energy Transfer 56
4.3.2 Analysis of the WUA Problem 57
4.3.3 Solving the WUA Problem 59
4.3.4 Solving the BES Problem 61
4.4 Implementation 61
4.4.1 Wireless Access Network Operation 63
4.4.1.1 Distributive ELLA algorithm 63
4.4.2 Smart Grid Operation 64
4.4.2.1 Distributive algorithm for the BES problem 65
4.5 Simulation Results 65
4.6 Sumamry 69
5 FUTURE WORK 70
5.1 Communications and Storage Resources Trading 70
5.1.1 Communications Resource Trading 70
5.1.2 Storage Resource Sharing 71
5.1.3 Incentive Scheme Design 72
5.2 Secure Multi-party Communications and Computation 73
5.2.1 Physical Layer Security 73
5.2.2 Multi-party Privacy 74
APPENDIX A PROOFS OF LEMMAS 76
A.1 Proof of Lemma 1 76
A.1.1 $M = 2$ 76
A.1.2 $M \geq 3$ 78
A.2 Proof of Lemma 2 80

TABLE OF CONTENTS
(Continued)

Chapter **Page**

A.2.1 $M = 2$, $\boldsymbol{J^{CC}} = [j_{1,2}]$ 80

A.2.2 $M = 3$, $\boldsymbol{J^{CC}} = [j_{1,2}, j_{1,3}, j_{2,3}]$ 80

A.3 Proof of Lemma 3 81

A.4 Proof of Lemma 8 84

A.5 Proof of Lemma 9 85

A.6 Proof of Lemma 10 87

A.7 Proof of Lemma 12 89

APPENDIX B PROOFS OF THEOREMS 91

B.1 Proof of Theorem 1 91

B.2 Proof of Theorem 2 91

BIBLIOGRAPHY 92

LIST OF TABLES

Table		Page
2.1	Comparison Between JSPA and Existing Work	9
4.1	List of Important Notations	44
4.2	On-grid Power Consumption of BSs	69

LIST OF FIGURES

Figure		Page
1.1	Future smart grid powered virtualized wireless access network.	2
2.1	Cooperative wireless system model.	8
2.2	Coordination with relaxed power constraint.	16
2.3	JSPA algorithm.	17
2.4	Total power consumption of the 2-BS cooperative system.	21
2.5	Loss rate of the 2-BS cooperative system.	22
2.6	Total power consumption of the 3-BS cooperative system.	23
2.7	Loss rate of the 3-BS cooperative system.	23
3.1	Cooperative data and energy transmission system.	26
3.2	System capacity versus power budget of RN.	38
4.1	Smart grid enabled mobile network.	41
4.2	On-grid brown energy flow and Inter-BS green energy flow.	45
4.3	Inter-BS green energy flow with the green energy hub.	54
4.4	Wireless energy transfer of traffic offloading.	57
4.5	Wireless energy transfer efficiency vs. ρ_{i^*}.	58
4.6	Distributed ELLA algorithm.	63
4.7	ELLA's convergence.	66
4.8	Coverage area.	67
4.9	On-grid power consumption.	67
4.10	Traffic delivery latency.	68
5.1	Mobile edge with distributed storage resources.	71
5.2	Energy efficiency v.s. data confidentiality.	73
5.3	Energy harvesting enabled physical layer security.	74
5.4	Privacy enhanced cooperative framework.	75
A.1	Power shift in the 2-BS cooperative wireless system.	76

LIST OF FIGURES
(Continued)

Figure **Page**

A.2 Power shift in the 3-BS cooperative wireless system. 78

A.3 UE-BS association in the 2-BS cooperative wireless system. 81

A.4 Spectrum and power coordination in the 3-BS cooperative wireless system. 82

A.5 Solution mapping. 84

A.6 Power supplements among BSs. 86

CHAPTER 1

INTRODUCTION

The mobile and wireless systems have witnessed a massive penetration of wireless devices and an exponential growth in wireless applications. To achieve the expected service requirements with the available radio resources, radio access networks have evolved towards the 5th Generation (5G) [1]. In particular, full duplex radio has been proposed to double the spectrum efficiency [2, 3], and macro cells have been splitted into various small cells powered by low power nodes to enhance the spatial reuse and reduce the energy demand [4–7]. The underlaid device to device communications enables opportunistic spectrum access and direct communications between nearby devices [8–10], and cloudlet has brought cloud resources closer to the end users such that the data centers can be accessed without going through the core network [11–15]. Moreover, energy harvesting (EH) enabled base stations, which take fuel from ambient sources, including wind, solar, wind, and even radio frequency (RF) signals, have been deployed on a small scale [16–18].

Although pushing everything to the edge and bringing in green energy can alleviate the intense demand for radio resources, the achievable energy and spectrum efficiency are approaching the theoretical limits, which are primarily attributed to the interference caused by the ultra-dense cell packing and uncertainties in the availability of spectrum and energy.

To address these challenges, the radio access network is expecting radical changes other than a simple evolution of the previous generations. Virtualizing the wireless access is a promising technological concept to overcome the aforementioned shortcomings [19–21]. Network Function Virtualization (NFV) transforms network appliances to software applications [22, 23] while Software Defined Networking

(SDN) allows a centralized view of a distributed network and more efficient service orchestration and automation by separating *network control and forwarding* (including switches, routers, and firewalls) planes. During this transition towards SDN/NFV and cloud-based telecommunication environment, network operators propose cloud-based service delivery, including cloud-radio access network (C-RAN) [24] and mobile-central office re-architected as datacenter (M-CORD) [25].

Meanwhile, future wireless access systems are expected to be powered by the smart grid, a modernized electrical grid which provides efficient control of the delivery and use of electricity [26]. As the smart grid advances and develops, green power farms that harvest energy from green sources, e.g., solar energy and wind energy, can substantially reduce carbon footprints. Also, the penetration of distributed green energy capitalization allows consumers to contribute their clean energy back to the grid [27–29]. In this way, the green energy can be transmitted and shared within the whole wireless network and the smooth operation of the network can be guaranteed [30].

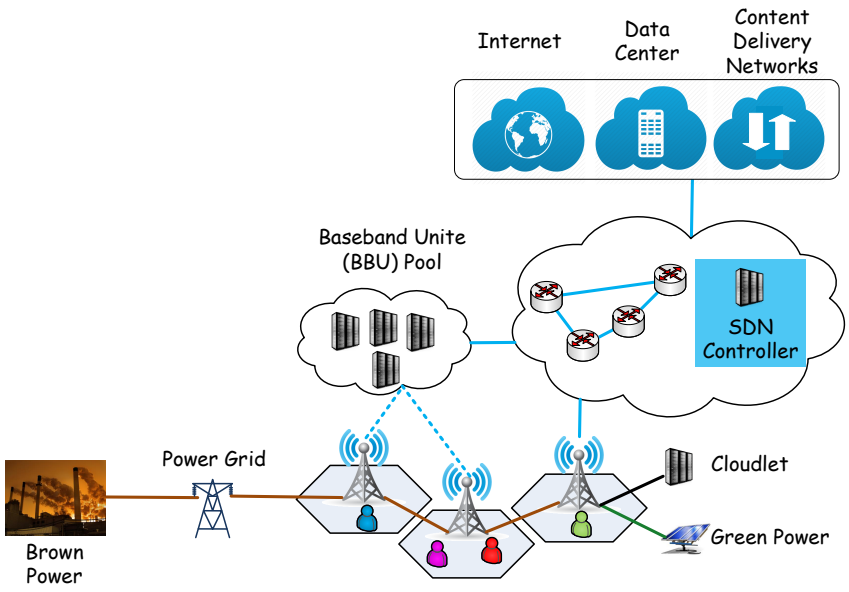

Figure 1.1 Future smart grid powered virtualized wireless access network.

As shown in Figure 1.1, the wireless access network consists of multi-tier legacy physical base stations with diverse power budgets. Besides the physical wireless architecture, the hierarchical cloud resources are deployed in the field or connected to the switches or routers, and the SDN controller includes a set of actions, such as radio communications resources and storage resources management. The smart grid will distribute and deliver not only the brown energy generated by the traditional power plants, but also the green energy either produced by the big scale centralized energy harvesting farms or the distributed smaller energy harvesters.

With cloud and radio resources distributively located at mobile edge, it is desirable to know how to cooperatively manage the network resources, such that the network performances, in terms of energy efficiency, system throughput, network latency, and security, are globally optimized. To improve the energy efficiency of the wireless access network, the framework of cooperative data transmission is proposed in Chapter 2, where each user equipment (UE) can simultaneously connect to multiple base stations (BSs). For the downlink cooperative data transmission (CoMP) system, the radio resources, in terms of power and spectrum, are cooperatively optimized to minimize the total transmission power of the network while maintaining the quality of service (QoS) requirement. First, the conjecture is proven such that for the system with arbitrary M cooperative BSs and N UEs, the minimum total power consumption can always be achieved when the number of *multi-BS UEs* (UEs that are powered by multiple BSs) is limited by $M-1$. Second, the UE-BS association scheme is derived to determine the clusters of multi-BS UEs as well as the clusters of *individual-BS UEs* (UEs that are powered by individual BSs). Third, a complexity reduction scheme is proposed to improve the efficiency of the joint spectrum and power allocation algorithm (JSPA).

In addition to the cooperative data transmission scheme, diverse renewable energy sources can be leveraged to improve energy efficiency. In Chapter 3, radio

frequency (RF) energy harvester is deployed to allow network nodes share energy wirelessly. To maximize the network capacity, an orthogonal frequency division multiplexing (OFDM) based cooperative relay system is proposed, where the relay node not only can forward the data to the destination node, but is also capable of transferring energy to the source node. In particular, to maximize the overall system capacity in multiple subchannels and multiple time slots while meeting the power constraints, a power allocation optimization problem is formulated and solved in three steps. Step one, at each data transmission and data forwarding cycle, the total transmission power of relay is split into two parts, one for data forwarding and the other as power supplement for the source node. Step two, according to the analysis, during each cycle, once all of the subchannels are sorted in a certain order, the relay node will only provide forwarding power to the subchannels with index greater than a certain value. Meanwhile, the incentive for the relay node to provide power supplement should be strong enough such that relay chooses not to simultaneously transmit data and energy. Step three, an equivalent convex constrained optimization problem is formulated and the solution is derived by solving the Lagrange function. The solution takes the form of water-filling in combination with a cooperative feature.

In Chapter 4, smart grid is introduced to conduct green energy flows among base stations. For the wireless access network equipped with distributed green energy harvesters, to improve the energy efficiency of the network, the energy consumption and green energy supply of the network have to be balanced. The base station either can cooperate with each other by either offloading user traffic or sharing the green energy directly via the smart grid infrastructure. In particular, to minimize the on-grid brown power consumption, the traffic load in the network and the green power flow in the grid are jointly optimized in three steps. Initially, the energy sharing efficiency of traffic offloading and that of grid facilitated energy transfer are compared. It has been shown that the wireless energy sharing efficiency will decrease

with the traffic load, while the wired energy sharing efficiency is determined by the grid structure. Next, when the traffic load is less than the threshold, traffic load is optimized without considering the green power flow. Thirdly, the energy flow is derived based on the traffic load obtained in the second step.

In Chapter 5, as future research work, the incentive and security issues of the cooperative framework are introduced. Briefly, the communication and storage resource trading is discussed among the multiple parties to motivate the cooperation. Finally, both the physical layer security scheme and the privacy preserving light weight communication and computation protocol are discussed.

CHAPTER 2

COOPERATIVE WIRELESS DATA TRANSMISSION

To improve the system performance and make the best use of the system resource, cooperative transmission leverages the broadcast nature of wireless communications such that some nodes in wireless networks can help each other to transmit signals for better quality via spatial diversity or higher data rates through spatial multiplexing [18]. In this chapter, for the green radios with multiple cooperative nodes and node-specific power budget, we aim to minimize the total transmission power consumption of the system while guaranteeing the UE-specific QoS requirement in terms of throughput.

The next-generation cellular networks, including cloud radio access networks (C-RAN) and software defined wireless networks (SDN), have proposed to enable cooperative transmission through the base band unit pool [31] and the controller [32]. One typical technology that has already been adopted by 3GPP Long Term Evolution is coordinated multi-point (CoMP) transmission [33]. As illustrated in Figure 2.1a, the adjacent outer cells and cell edge users can be considered as a new virtual cell (shaded area). This virtual cell is surrounded by multiple inner cells, has multiple base stations (BSs) serving as power sources, and works on the outer band (allocated by the fractional frequency reuse scheme [34]) or major subcarriers (allocated by the soft frequency reuse scheme [35]). The features of multiple power sources and shared spectrum have motivated the coordination transmission, which is considered as an effective tool to improve the coverage of high data rates and the cell-edge throughput.

In addition to the cellular networks with simultaneous multiple data transmissions, cooperative communications has been widely adopted in ad-hoc networks and cognitive networks [36], where cooperative sequential data transmissions

play a major role. As illustrated in Figure 2.1b, the destination node (DN) combines the signal transmitted by the source node (SN) in the first time slot and the forwarding signal transmitted by the relay node in the second time slot. Network coding based two-way relay schemes with decoding (decode-and-forward) and without decoding (amplify-and-forward, denoise-and-forward, compress-and-forward) have been introduced to implement cooperative communications [37]. Although the capacity of the relay network and that of point-to-point cellular network are different, the inherent cooperative diversity of relay network can save energy by combining the signals received from different spatial paths and consecutive time slots [38]. Without loss of generality, we focus on the cellular network in this chapter.

To capitalize on the internal flexibility of FDMA/OFDMA in power loading across the frequency channels/subcarriers, and the external flexibility in multiple nodes serving as power sources, the resource allocation scheme for cooperative wireless systems can dynamically assign the limited resources (spectrum and power) to deliver the best quality of service to customers at the lowest cost; that is, the available resources are allocated to the user who can best exploit the resources according to the current channel state information (CSI). This multi-node multi-UE diversity gained from dynamic resource allocation improves the performance of cooperative wireless systems. We investigate a new joint spectrum and power allocation scheme for a cooperative downlink multi-user system using the frequency division multiple access scheme, in which arbitrary M BSs coordinately allocate their resources to each UE.

With the assumption that multi-BS UE (user being served by multiple BSs) would require the same amount of spectrum from these BSs, we conclude that when the number of multi-BS UEs is limited by $M-1$, the resource allocation scheme can always guarantee the minimum overall transmit power consumption while meeting the throughput requirement of each UE and also each BS's power constraint. Then, to decide the clusters of multi-BS UEs and the clusters of individual-BS UEs (users being

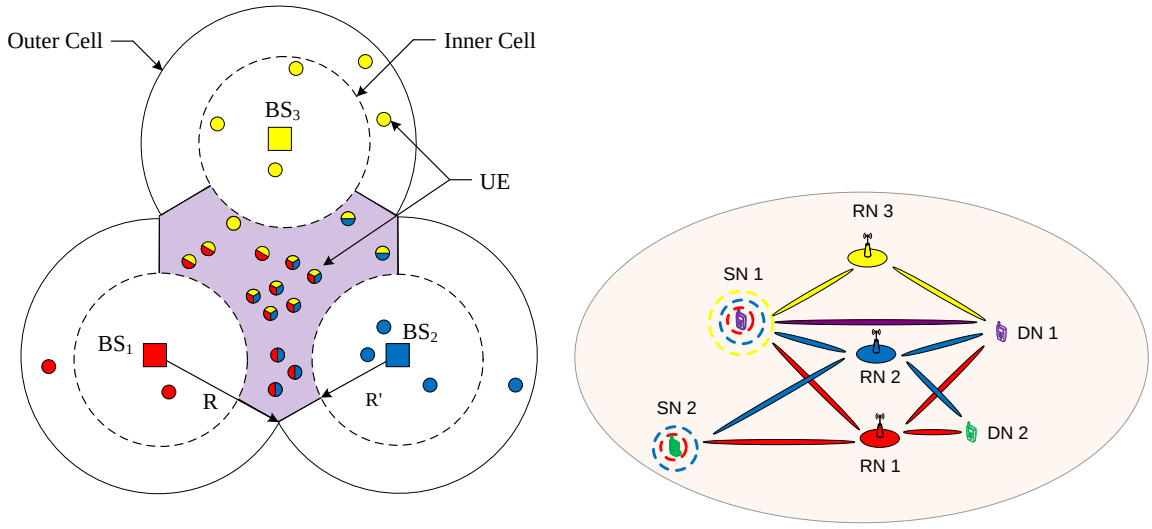

(a) (b)

Figure 2.1 Cooperative wireless system model.

served by individual BSs), we propose a UE-BS association scheme and a complexity reduction scheme. Finally, a novel joint spectrum and power allocation algorithm is proposed to minimize the total power consumption.

The major features that distinguish our work from the previous state-of-the-art works with similar system scenarios are summarized in Table 2.1. Since JSPA does not require UEs to have the capability to be served by all of the BSs, it is applicable to any cooperative networks where mobile UEs can move out of the coverage of certain BSs. Since JSPA is proven to be optimal, it outperforms the existing algorithms, and its low-complexity is desirable for the practical operation of the cooperative networks, such as the online resource allocation schemes which cope with mobile UEs.

2.1 Coordinated Transmission Model

Consider a cooperative downlink multi-user system, in which M BSs coordinately assign spectrum and allocate power to N users located in the coordinative zone, as depicted in Figure 2.1. Each user feeds back the instantaneous CSI to its

Table 2.1 Comparison Between JSPA and Existing Work

BS No.	Alg.	Maximum No. of Multi-BS UE	Serving BS Candidates	OPT	CPX
2	MRT [39]	N	2	Sub-opt	Low
	JMPC [40]	1		Opt	High
	JSPA		Varying		Low
M	MRT	N	M	Sub-opt	Low
	JMPC	1			High
	JSPA	$M-1$	Varying	Opt	Low

corresponding BS via a feedback channel. Through the back-haul channels, which can be optical fiber or out of band microwave links, each BS has access to the data and control information (such as CSI) of associated users [41]. Note that when M or N is very large, acquisition of CSI and data information of each UE at each cooperative BS is very challenging for the back-haul links and feedback channels. Therefore, we assume BSs have partial access to control and data information, i.e., the data transmission of the user is dynamically coordinated only among those BSs who have gained access to this UE.

To simplify the mathematical derivation, we assume each BS has the same power constraint P_0 and share the same overall bandwidth B_0. Since multiple access technologies based on frequency division allocate orthogonal spectrum among UEs to avoid interference, B_0 is divided into N distinct and nonoverlapping flat fading channels with various bandwidths, one for each UE. As compared with the co-channel separation method such as zero-forcing in [42], the orthogonal spectrum sharing method is not necessarily less efficient in terms of spectrum usage because the cell edge

users are highly likely to be in the low SINR region caused by inter-cell interference. In addition, for the central area of each cell, they can all utilize the same spectrum resources, such as inner band and minor subcarriers in [34], [35], [43]. However, to ensure tractability of our analysis, the joint resource allocation of UEs located in the coordinated zone and central area is left for our future work.

Furthermore, if UE j is a multi-BS UE, the serving BSs would allocate the same channel to this UE, so that without shifting frequency, UE j can optimally receive its information from the assigned channel with maximal-ratio combining (MRC) [44], [45]. Thus, the achievable throughout of the j-th user given by the AWGN Shannon Capacity (sum rate) is expressed as

$$R_j = B_j \log_2 \left(1 + \frac{\sum_{i=1}^{M} P_{i,j} |H_{i,j}|^2}{{\sigma_j}^2} \right) \tag{2.1}$$

where B_j is the bandwidth assigned to the j-th channel, ${\sigma_j}^2 = N_0 B_j$ represents the power of additive white Gaussian noise at the j-th channel, $P_{i,j}$ denotes the allocated transmission power from BS i to the j-th channel, and $H_{i,j}$ denotes the corresponding channel gain between BS i and the j-th channel.

The goal here is to minimize the total transmission power of the system while meeting each user's throughput requirement R_j^S as well as each BS's power and spectrum constraints. The circuit energy consumption associated with data reception in the UE side is generally modeled as a constant, especially with given data rate and no frequency shifting in each UE [46]. For the circuit energy consumption incurred by data transmission at the BS side, we also adopt the simplified constant model [47]; this is due to the fact that in addition to the UEs in the coordinated zone, each BS has to serve the UEs located in the central area of each cell, and so BSs are likely to remain active. As a result, only the transmission power of all of the BSs is considered

in the following problem formulation.

$$\begin{aligned} P_{overall} &= \min \sum_{i=1}^{M} \sum_{j=1}^{N} P_{i,j} \\ s.t. \quad & R_j = R_j^S, \ j \in \mathcal{N} \\ & \sum_{j=1}^{N} P_{i,j} \leq P_0, \ i \in \mathcal{M} \\ & \sum_{j=1}^{N} B_j = B_0 \end{aligned} \tag{2.2}$$

where $\mathcal{M} = \{1, \cdots, M\}$, $\mathcal{N} = \{1, \cdots, N\}$. Owing to the limitation in the feedback/back-haul channels or severe channel attenuation, if UE j cannot be associated with BS i or has moved out of the coverage of BS i, then we set $H_{i,j} = 0$.

For the sake of mathematical abbreviation, we denote $\gamma_{i,j} = (P_0|H_{i,j}|^2)/(N_0 B_0)$, $x_{i,j} = P_{i,j}/P_0$ and $y_j = B_j/B_0$. Note that $\gamma_{i,j}$ is the signal to noise ratio (SNR) associated with BS i over the total bandwidth B_0 when the entire power P_0 is allocated to the j-th UE. $x_{i,j}$ and $y_{i,j}$ represent the power and bandwidth allocation ratio, and $R_j^S/B_0 = R_j'$. Since the logarithm is monotonically increasing, the objective function (2.2) combined with the constraints can be described as follows:

$$\begin{aligned} Z = & \min_{\{\mathbf{X},\mathbf{Y}\}} \sum_{i=1}^{M} \sum_{j=1}^{N} x_{i,j} \\ s.t. \quad & \sum_{i=1}^{M} \gamma_{i,j} x_{i,j} = (2^{R_j'/y_j} - 1) y_j, \ j \in \mathcal{N} \\ & \sum_{j=1}^{N} x_{i,j} \leq 1, \ i \in \mathcal{M} \\ & \sum_{j=1}^{N} y_j = 1 \end{aligned} \tag{2.3}$$

where $\mathbf{X} = \{x_{i,j} \,|i \in \mathcal{M}; j \in \mathcal{N}\}$, $\mathbf{Y} = \{y_j \,|j \in \mathcal{N}\}$, and $Z = P_{overall}/P_0 \leq M$ represents the total power consumption ratio.

2.2 Problem Analysis

As discussed in [40], finding the global optimal solution of the power allocation problem is very complicated. Solving (2.3) is even more challenging due to the

non-convexity of the joint optimization of spectrum and power. In order to achieve the minimum power consumption, we first decouple the power allocation problem from the spectrum allocation problem.

2.2.1 Power Allocation Scheme

The main result of this chapter is to prove that the number of multi-BS UEs in the optimal solution is limited by $M-1$, as stated in the following Lemma.

Lemma 1. *For any spectrum allocation scheme* $\mathbf{Y}$*, there exists an optimal power allocation with at least* $(M-1)(N-1)$ *elements of* $\mathbf{X}$ *being zero.*

The proof of Lemma 1 is provided in Appendix A.1. The observation presented in Lemma 1 simplifies the joint spectrum and power allocation problem greatly, because 1) the power allocation is decoupled from the spectrum allocation, which enables versatile access technologies, such as FDMA or OFDMA system; 2) the number of BS-UE links in the system, i.e., the number of non-zero elements in $\mathbf{X}$, is limited within the range of $[N, N+M-1]$.

Remark 1. *Define the* SNR ratio *between (BS* i*, UE* j*) link and (BS* i'*, UE* j*) link as*

$$\gamma_{i,i'}^{j} = \frac{\gamma_{i,j}}{\gamma_{i',j}} \tag{2.4}$$

According to the power shifting argument *in Appendix A.1, if* $\gamma_{i,i'}^{j}$ *allows a feasible power shifting that will decrease the total power consumption, then the corresponding power allocation is not optimal.*

Conclusively, power shifting argument can be used as an initial assessment to determine whether UE j should be associated with BS i, i' or both, and we will elaborate this in the next section.

2.2.2 UE-BS Association Scheme

To satisfy the QoS requirements, each user j should be associated with at least one BS i such that $x_{i,j}y_j > 0$. Since the number of non-zero elements in $\mathbf{X}$ is limited (Lemma 1), the majority of UEs will be associated with one BS only. According to the channel conditions, we will address the UE-BS association problem such that the complexity of finding the zero elements is further decreased.

Suppose there is no power limit for each BS, to minimize the power consumption of the system, the intuitive association scheme for each UE is to find the BS with the best channel condition. With this scheme, UE j will be powered by BS i only, where

$$i = \arg \max_{k \in \{1,2,\cdots,M\}} \{\gamma_{k,j}\} \tag{2.5}$$

Thus, UEs will be divided into M clusters denoted by *initial disjoint clusters* $\{J_i^0 \,|i \in \mathcal{M}\}$, where the i-th cluster, J_i^0, consists of UEs, which prefer to be powered by BS i.

With the introduction of BS-specific power budget, BS i may not be able to power all of the UEs in cluster i, and other BSs will provide power coordination. Let $J_i^{i'}$ be the cluster consisting of UEs that 1) belong to J_i^0, and 2) are powered by BS i' (partially or being taken over completely). Then, *new disjoint clusters* $\{J_i \,|i \in \mathcal{M}\}$ will be formed, where J_i consists of UEs that are powered by BS i only.

Remark 2. *Since $J_i^{i'} \neq \Phi$ implies there is power shortage in BS i, $J_{i'}^i = \Phi$. Let $\overline{J_i^{i'}} = J_i^0 \backslash J_i^{i'}$ be the UE cluster which consists of UEs that are not taken over by BS i'. If $\bigcup_{i' \in M \backslash i} \overline{J_i^{i'}} \subset J_i^0$, then BS i would not take UEs from any other BSs, i.e., $\bigcup_{i' \in M \backslash i} J_{i'}^i = \Phi$, so $J_i = \bigcap_{i' \in M \backslash i} \overline{J_i^{i'}}$.*

Since the stability of clusters depends on the SNR ratio $\gamma_{i,i'}^{j}$ in (2.4), a *common candidate (CC) vector* $\boldsymbol{J^{CC}}$ can be defined for the disjoint clusters

$$\begin{aligned}\boldsymbol{J^{CC}} = [j_{1,2}, \quad & j_{1,3}, \quad \cdots \quad j_{1,M}, \\ & j_{2,3}, \quad \cdots \quad j_{2,M}, \\ & \ddots \quad \vdots \\ & \qquad\qquad j_{M-1,M}]\end{aligned}$$

where each element $j_{i,i'}$ is the multi-BS UE candidate that is commonly powered by BS i and i'.

For any $i \in \{1, \cdots, M-1\}$ and $i' \in \{i+1, \cdots, M\}$, we require $j_{i,i'}$ in $\boldsymbol{J^{CC}}$ to satisfy the following inequality

$$\min_{j \in J_i} \gamma_{i,i'}^{j} \geq \gamma_{i,i'}^{j_{i,i'}} > \max_{j \in J_{i'}} \gamma_{i,i'}^{j} \tag{2.6}$$

where for the initial cluster J_i^0 and $J_{i'}^0$, the corresponding $j_{i,i'}$ satisfies $\gamma_{i,i'}^{j_{i,i'}} \geq 1 > \gamma_{i,i'}^{1+j_{i,i'}}$.

Lemma 2. *To minimize the power consumption, the CC vector which satisfies (2.6) always exists for the optimal clusters* $\{J_i \,|\, i \in \mathcal{M}\}$.

The proof of Lemma 2 is provided in Appendix A.2. A very important point to be noticed from Lemma 2 is that multi-BS UEs are all in $\boldsymbol{J^{CC}}$ because at most one UE will be associated with both BS i and BS i'. Thus,

$$|\mathrm{UNI}(\boldsymbol{J^{CC}})| \leq M - 1$$

where UNI($\bullet$) consists of unique elements in $\bullet$.

Let J_i^{mul} be the multi-BS UE candidates that are simultaneously powered by BS i and other BSs. Then, we will have

$$J_i^{mul} = (\bigcup_{i'=i+1}^{M} j_{i,i'} \bigcup_{i'=1}^{i-1} j_{i',i}) \backslash (\bigcup_{i'=1}^{M} J_{i'}) \tag{2.7}$$

$$\begin{cases} x_{i,j} = (2^{R'_j/y_j} - 1)y_j/\gamma_{i,j}, & j \in J_i \\ x_{i,j} = 0, & j \notin J_i \bigcup J_i^{mul} \end{cases} \tag{2.8}$$

As we can see, by revealing the relationship between J_i and $\boldsymbol{J^{CC}}$, Lemma 2 can further differentiate the non-zero and zero variables of $\mathbf{X}$.

2.2.3 Complexity Reduction Scheme

Instead of iteratively solving (2.3) for every $\boldsymbol{J^{CC}}$ that satisfies (2.6), we try to find the possible optimal $\boldsymbol{J^{CC}}$ by considering the model of a 2-BS system, which can be used as the reference for the more complicated cooperative system involving three or more BSs.

For the initial disjoint clusters, suppose we relax the power constraint for BS i_1 and set the power limit of the other BS i_2, $\{i_1, i_2\} = \{1, 2\}$, (2.3) becomes:

$$\begin{aligned} Z = \min & \sum_{j \in J_1^0} \frac{(2^{\frac{R'_j}{y_j}} - 1)y_j}{\gamma_{1,j}} + \sum_{j \in J_2^0} \frac{(2^{\frac{R'_j}{y_j}} - 1)y_j}{\gamma_{2,j}} \\ s.t. \quad & \sum_{j \in J_{i_1}^0} (2^{R'_j/y_j} - 1)y_j/\gamma_{i_1,j} \leq +\infty \\ & \sum_{j \in J_{i_2}^0} (2^{R'_j/y_j} - 1)y_j/\gamma_{i_2,j} \leq 1 \\ & \sum_{j=1}^{N} y_j = 1 \end{aligned} \tag{2.9}$$

where $x_{i,j} = 0$ if $j \notin J_i^0$, and $x_{i,j}$ is given in (2.8) if $j \in J_i^0$.

As we can see, (2.9) is convex over $\mathbf{Y}$. By Lagrange dual function, we can derive the closed form solution expressed in the Lambert-W function [48], or utilize various algorithms designed for the convex problem to approach the optimal solution [49].

As shown in Figure 2.2, the relaxed solutions can be represented in the two dimensional coordinates $S_i = (\sum_{j \in J_1^0} x_{1,j}, \sum_{j \in J_2^0} x_{2,j})$, where S_i is the solution to (2.9) with BS i having no power budget. $S_i > (1, 1)$ means the power consumption of

BS i is greater than 1, i.e., S_i is located outside of the square region bound by $(1,1)$. $S_i \leq (1,1)$ implies S_i is located within the region bound by $(1,1)$.

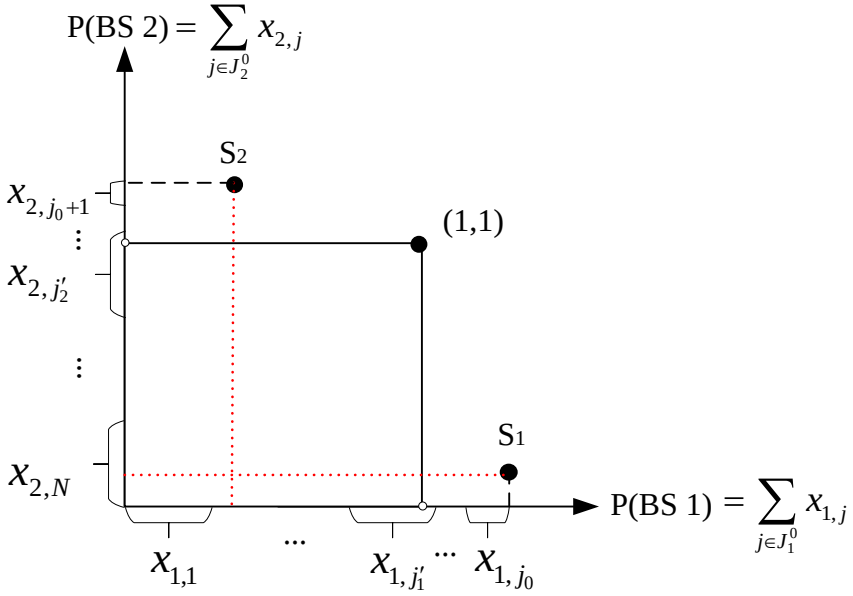

Figure 2.2 Coordination with relaxed power constraint.

Lemma 3. *Suppose UEs are sorted in the descending order of* $\gamma_{1,2}^j$, $\boldsymbol{J^{CC}} = [j_{1,2}]$.
1) If $S_1 = S_2$, *then* S_i *is the optimal solution.*
2) If $S_1 > (1,1)$, *then there exists* $j_1' \in J_1^0$ *such that* $\sum_{j=1}^{j_1'-1} x_{1,j} \leq 1$, $\sum_{j=1}^{j_1'} x_{1,j} > 1$, *then* $j_{1,2} \geq j_1'$.
3) If $S_2 > (1,1)$, *then there exists* $j_2' \in J_2^0$ *such that* $\sum_{j=j_2'+1}^{N} x_{2,j} \leq 1$, $\sum_{j=j_2'}^{N} x_{2,j} > 1$, *then* $j_{1,2} \leq j_2'$.

The proof of Lemma 3 is provided in Appendix A.3. By relaxing the power constraint of a BS, Lemma 3 can limit the range of $j_{1,2}$, so that the complexity of finding the optimal solution is much lower than iterating through every possible $\boldsymbol{J^{CC}}$.

Remark 3. *For any disjoint clusters* $\{J_i \,|i \in \mathcal{M}\backslash\{i_1, i_2\}\}$ *with* $M \geq 3$, *we can limit the range of* j_{i_1,i_2} *by using Lemma 3.*

The details of how to apply Lemma 3 are provided in the next section.

2.3 Joint Spectrum and Power Allocation Algorithm

Since $J_i^0 \subseteq J_i$ implies BS i may provide power coordination to other BSs, $M - \sum_{i=1}^{M} 1\{J_i^0 \subseteq J_i\}$ BSs will receive power coordination, where $1\{\bullet\} = 0$ if $\bullet$ is false and 1 otherwise. Consequently, for any $\{J_i, J_i^{mul} | i \in \mathcal{M}\}$ which satisfies Lemma 2, the

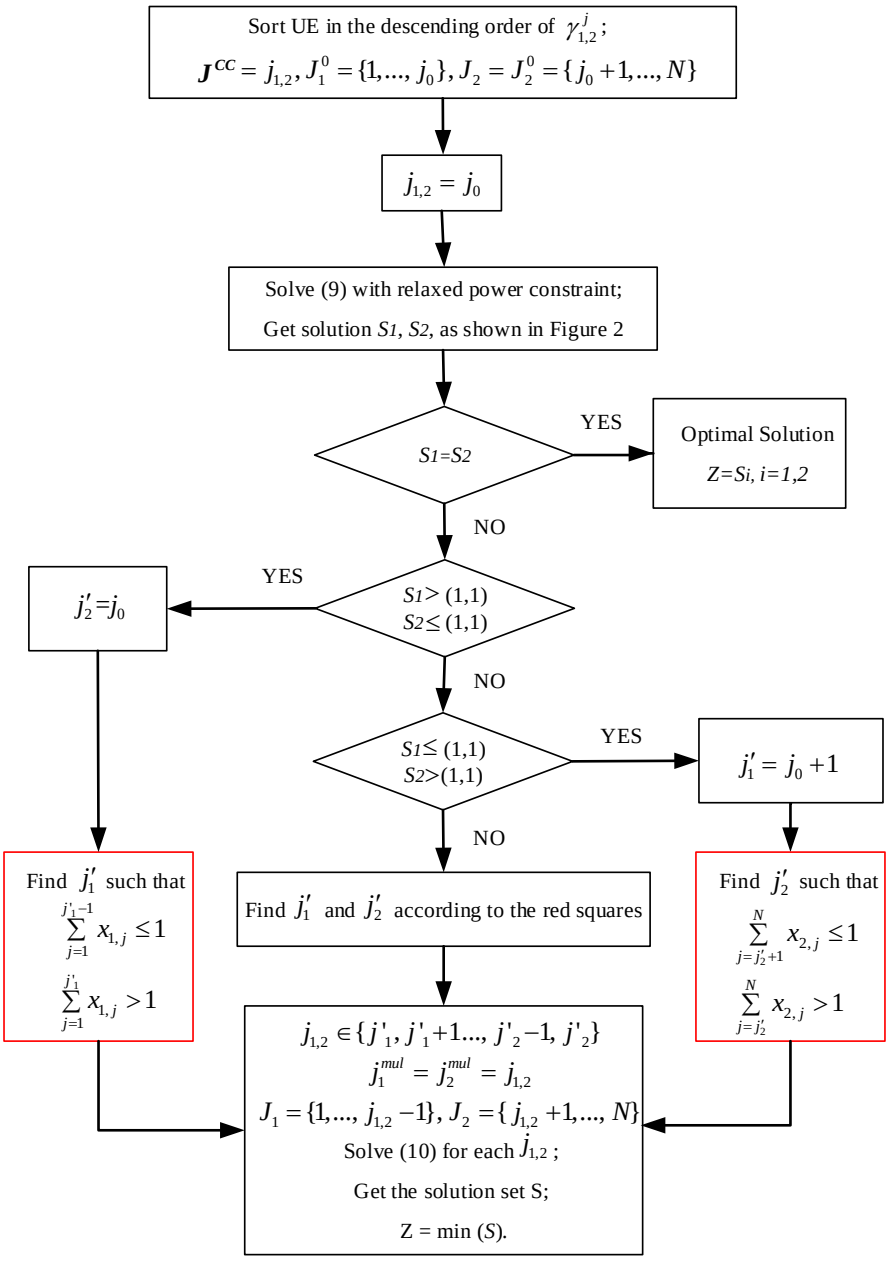

Figure 2.3 JSPA algorithm ($M = 2$).

objective function in (2.3) can be transformed into

$$\begin{aligned}
&\min \sum_{i=1}^{M}\Big(\sum_{j\in J_i}\frac{(2^{\frac{R'_j}{y_j}})y_j}{\gamma_{i,j}}+\sum_{j\in J_i^{mul}}x_{i,j}\Big)1\{J_i^0\subseteq J_i\}+M-\sum_{i=1}^{M}1\{J_i^0\subseteq J_i\}\\
&s.t.\quad \sum_{j\in J_i}\frac{(2^{\frac{R'_j}{y_j}}-1)y_j}{\gamma_{i,j}}+\sum_{j\in J_i^{mul}}x_{i,j}\le 1,\ i\in\mathcal{M}\\
&\qquad \sum_{i=1}^{M}\gamma_{i,j}x_{i,j}=(2^{R'_j/y_j}-1)y_j,\ j\in\bigcup_{i=1}^{M}J_i^{mul}\\
&\qquad \sum_{j=1}^{N}y_j=1
\end{aligned}\tag{2.10}$$

where $x_{i,j}$ is given in (2.8), and if $1\{J_i^0\subseteq J_i\}=0$, the first constraint is satisfied with equality, i.e., $\sum_{j\in J_i}(2^{R'_j/y_j}-1)y_j/\gamma_{i,j}+\sum_{j\in J_i^{mul}}x_{i,j}=1$.

Algorithm 1: JSPA algorithm: UE-BS association

for $\boldsymbol{J^{CC}}$ *with* $|UNI(\boldsymbol{J^{CC}})|\le M-1$ **do**
- $\mathcal{M}=\{1,\cdots,M\}$, $\mathcal{N}=\{1,\cdots,N\}$;
- According to (2.5), get J_i^0, $i\in\mathcal{M}$, $j\in\mathcal{N}$;
- $\overline{J_i^{i'}}=J_i^0$, $i\in\mathcal{M}$, $i'\in\mathcal{M}\backslash i$;
- $J_i, J_i^{mul}=\Phi$, $i\in\mathcal{M}$;
- **while** $\bigcup_{i\in\mathcal{M}}J_i\bigcup_{i\in\mathcal{M}}J_i^{mul}\neq\mathcal{N}$ **do**
  - $\mathcal{N}\leftarrow\mathcal{N}\backslash\bigcup_{i\in\mathcal{M}}J_i$;
  - $\mathcal{M}\leftarrow\mathcal{M}\backslash\{i\in\mathcal{M}:\bigcup_{i'\in\mathcal{M}\backslash i}\overline{J_i^{i'}}\subset J_i^0\}$;
  - Update J_i^0, $i\in\mathcal{M}$, $j\in\mathcal{N}$;
  - **for** $i\in\mathcal{M}$ **do**
    - $\mathcal{M}'=\{1,\cdots,M\}\backslash i$;
    - $\overline{J_i^{i'}}=\{j\in J_i^0:\gamma_{i,i'}^{j}>\gamma_{i,i'}^{j_{i,i'}}\}$, $i'\in\mathcal{M}'$;
    - $J_i\leftarrow J_i\bigcup\{\bigcap_{i\in\mathcal{M}'}\overline{J_i^{i'}}\}$;
  - According to (2.7), get J_i^{mul}, $i\in\mathcal{M}$, $j\in\mathcal{N}$;
- Return $\{\boldsymbol{J^{CC}}, J_i, J_i^{mul}|i\in\{1,\cdots,M\}\}$;

Based on Lemmas 1-3, we first present the joint spectrum and power allocation (JSPA) algorithm with $M=2$. Similar to (2.9), for each $j_{1,2}$ in Figure 2.3, (2.10) is also a convex optimization problem with $N+2$ variables $\{\mathbf{Y}, x_{1,j_{1,2}}, x_{2,j_{1,2}}\}$. With

arbitrary M, the two procedures to achieve the optimal resource allocation are given in Alg. 1 and Alg. 2, where Alg. 1 is used to find the multi-BS UE candidates that satisfy Lemma 2, and Alg. 2 will iterate the output candidates that satisfy Lemma 3 until the corresponding optimal UE-BS association scheme that minimizes the overall power consumption is found.

2.4 Simulation Results

We assume that 20 independent and identically distributed (i.i.d.) Rayleigh-faded users are uniformly located within the shaded zone (see Figure 2.1). R is 1000 m and the inner cell radius R' is 600 m. The distance-dependent path loss model is $L(d) = 128.1 + 37.6 \lg(d)$ dB, d in km, and $N_0 = -174$ dBm/Hz. For the sake of simplicity, we assume $B_0 = 1$, and each BS's power constraint is $P_0 = 1$.

The performances of the proposed JSPA algorithm and JMPC algorithm in [40] are averaged over 1,000 independent snapshots by *Monte-Carlo* simulation. The throughput requirement of each UE is defined as

$$R_j = \epsilon R_j^0, \ \epsilon > 0 \tag{2.11}$$

where R_j^0 is generated according to (2.1), with all of the N users being assigned equal spectrum and power (ESP) from each BS.

2.4.1 Two-node System

As pointed out in Table 2.1, for $M = 2$, both JSPA and JMPC are optimal in the sense of power allocation. For easy comparison, we assume the system-specific throughput requirement of JMPC is divided among all of the UEs, i.e., UE-specific R_j^S in (2.11). Then, as shown in Figure 2.4, JSPA outperforms JMPC in the total power consumption. The reason is that JSPA supports flexible spectrum allocation, while JMPC adopts equal bandwidth allocation for all UEs.

Algorithm 2: JSPA algorithm: Complexity reduction

$Z = M$;
for $i_1, i_2 \in \{1, \cdots, M\}$, $i_2 > i_1$ **do**
    $\mathcal{M} \leftarrow \{1, \cdots, M\} \backslash \{i_1, i_2\}$;
    for $\{J_i, J_i^{mul} | i \in \mathcal{M}\}$ *returned by Alg. 1* **do**
        $\mathcal{N} \leftarrow \{1, \cdots, N\} \backslash \{\bigcup_{i \in \mathcal{M}} J_i \bigcup_{i \in \mathcal{M}} J_i^{mul}\}$;
        Sort UE in the descending order of γ_{i_1,i_2}^{j};
        Update J_i^0, $i \in \{i_1, i_2\}$, $j \in \mathcal{N}$;
        In (2.10), $J_i \leftarrow J_i^0$, $i \in \{i_1, i_2\}$;
        Keep power budgets of BSs other than i_1/i_2;
        Get the relaxed solutions to (2.10): S_{i_1}/S_{i_2};
        if $S_{i_1} > (1,1)$, $S_{i_2} \leq (1,1)$ **then**
            Get j'_{i_1} according to Lemma 3, $j'_{i_2} = \max_{j \in J_{i_1}^0} \{j\}$;
        else if $S_{i_2} > (1,1)$, $S_{i_1} \leq (1,1)$ **then**
            Get j'_{i_2} according to Lemma 3, $j'_{i_1} = \max_{j \in J_{i_1}^0} \{j\} + 1$;
        else if $S_{i_1} > (1,1)$, $S_{i_2} > (1,1)$ **then**
            Get j'_{i_1}, j'_{i_2} according to Lemma 3;
        else if $S_{i_1} \leq (1,1)$, $S_{i_2} \leq (1,1)$ **then**
            $j'_{i_1} = j'_{i_2} = \max_{j \in J_{i_1}^0} \{j\}$;
        for $\{J_i, J_i^{mul}\}$ *returned by Alg. 1* **do**
            if $j_{i_1,i_2} \in \{j'_{i_1}, \cdots, j'_{i_2}\}$ **then**
                Get the solution to (2.10): S;
                $Z \leftarrow \min\{Z, S\}$;
return Z;

Figure 2.5 indicates that with $\epsilon > 1$, there will be loss, i.e., the system fails to support all of the N users' throughput requirements with its maximum power and spectrum resources. Apparently, the loss rate must be zero with $\epsilon \leq 1$ and the loss rate will increase with ϵ. Since JSPA always consumes less or equal power, the loss rate is smaller accordingly.

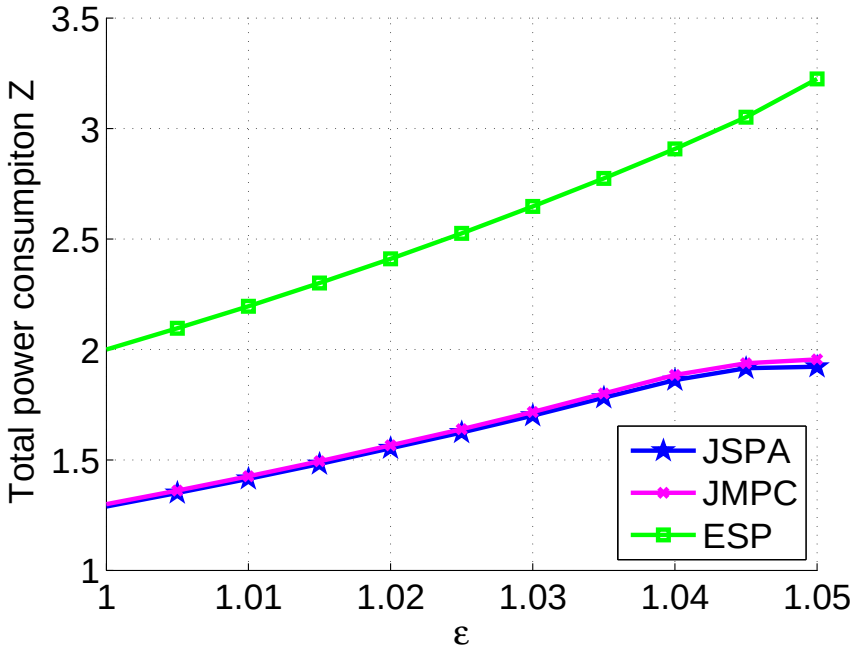

Figure 2.4 Total power consumption of the 2-BS cooperative system.

2.4.2 Multi-node System

To verify the point that for $M \geq 3$, JSPA is optimal while JMPC is sub-optimal in the sense of power allocation, we assume instead of UE-specific throughput requirement and spectrum allocation, JSPA requires UE-common bandwidth allocation and system-specific throughput requirement (sum of R_j in (2.11)).

As we can see in Figures 2.6 and 2.7, JSPA always achieves the best performance, both in total power consumption and the loss rate, even when it does not enable flexible spectrum allocation. The gain will increase with the randomness of R_j rather than with the simultaneous increase/decrease with bigger/smaller ϵ. The randomness

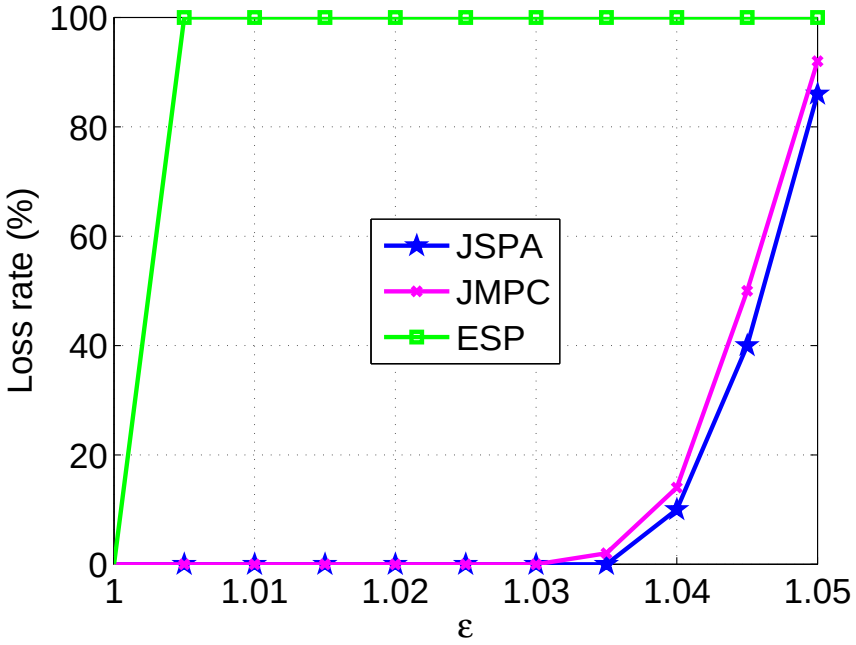

Figure 2.5 Loss rate of the 2-BS cooperative system.

make it less likely for one BS to exceed the power limit, when it provides spectrum or power to help the overloaded BS. Since JSPA and JMPC are compared in the same enviorment, we can conclude that under the perfect coordinated transmission between the multiple BSs, the proposed JSPA algorithm provides a significant reduction in the power consumption.

2.5 Summary

In this chapter, we have investigated the joint spectrum and power allocation problem in minimizing the overall transmit power consumption while meeting the throughput requirements of each UE and each BS's power constraint for a cooperative downlink multi-user system. By using a new approach with "power shifting" and "common candidate vector", we have shown analytically that the number of multi-BS UEs should be limited by the number of BSs. Moreover, we have also proposed the UE-BS association scheme and the corresponding complexity reduction scheme, which determines the serving BSs for each UE based on channel conditions and

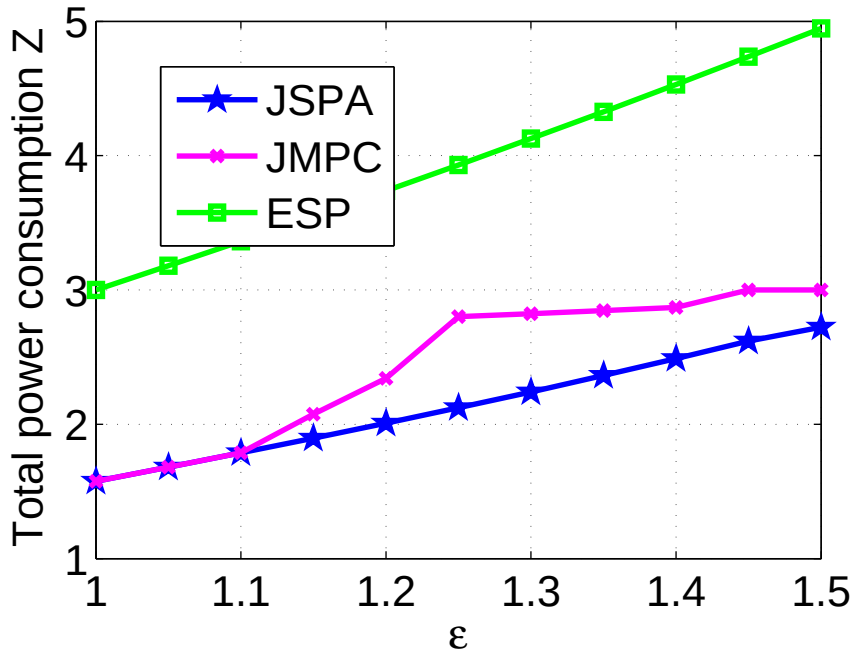

Figure 2.6 Total power consumption of the 3-BS cooperative system.

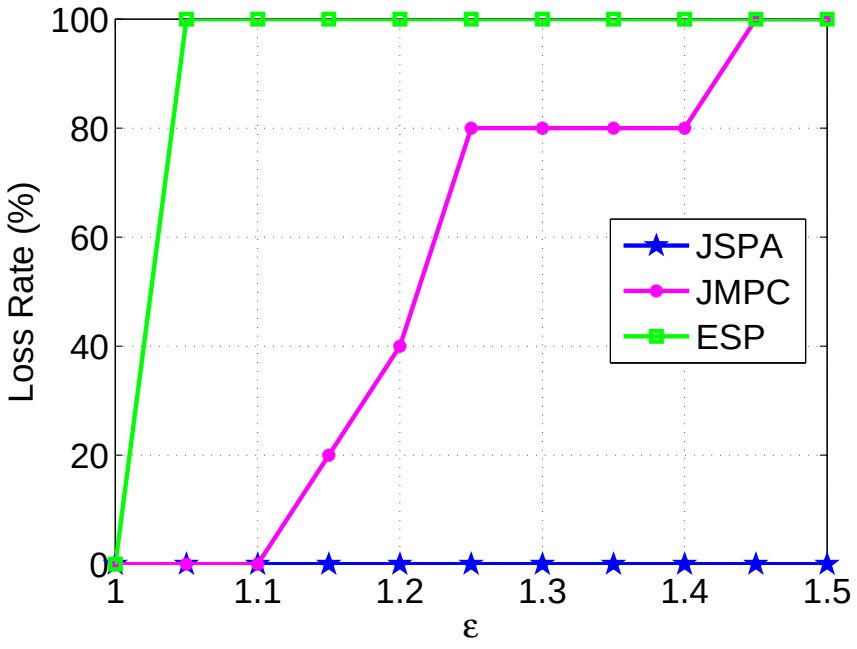

Figure 2.7 Loss rate of the 3-BS cooperative system.

the constraints in the optimization problem. Finally, a novel joint spectrum and power allocation algorithm, proven to yield the minimum total power consumption, is proposed. In the future, the capacity of the feedback/back-haul channel, the

resource allocation scheme for the users located in the non-coordinated zone, and more sophisticated circuit energy consumption model of both BSs and UEs can be taken into consideration in which case the theoretical results can be directly applied to the realistic wireless communication system. Meanwhile, although the system model is based on the downlink cellular network, the derived results are applicable for various networks with cooperative features: multiple power sources and shared spectrum.

CHAPTER 3

DATA AND ENERGY COOPERATION IN WIRELESS COMMUNICATIONS SYSTEMS

Greening wireless access networks is receiving much attention because explosive surge of mobile data traffic in wireless edge consumes a significant amount of energy [18]. On one hand, the wireless access networks can continually improve the energy utilization, so that reduced energy consumption may result in reduced interference and improved system performances [50]. On the other hand, renewable green energy can be capitalized to power these networks, and thus, enhances our climate, health, and economy [51].

As far as energy utilization is concerned, cooperative data transmission uses multiple serving nodes to transmit signals to the same end device, so that the useful signals are strengthened while the experienced interference is lessened. Cooperative data transmission is generally classified into two categories: coordinated and sequential cooperative data transmission. The former means multiple serving nodes transmit simultaneously, such as the coordinated multipoint (CoMP) transmission [52], and the latter indicates the data transmission of serving nodes occurs one after another, such as the network coding based relay schemes [53].

As compared with traditional wireless access networks which mainly rely on non-renewable brown energy, energy harvesting techniques have the potential to liberate the network from energy related inhibition. To overcome the dynamics of green energy sources and ensure long-term, uninterrupted network operation, energy cooperation schemes have been designed so that the energy can be shared among multiple devices [30]. With the deployment of smart grid, wireless access nodes can share each other's energy directly. With radio frequency (RF) energy harvesting, one node's energy storage can be transferred to another node wirelessly. To study the throughput gain

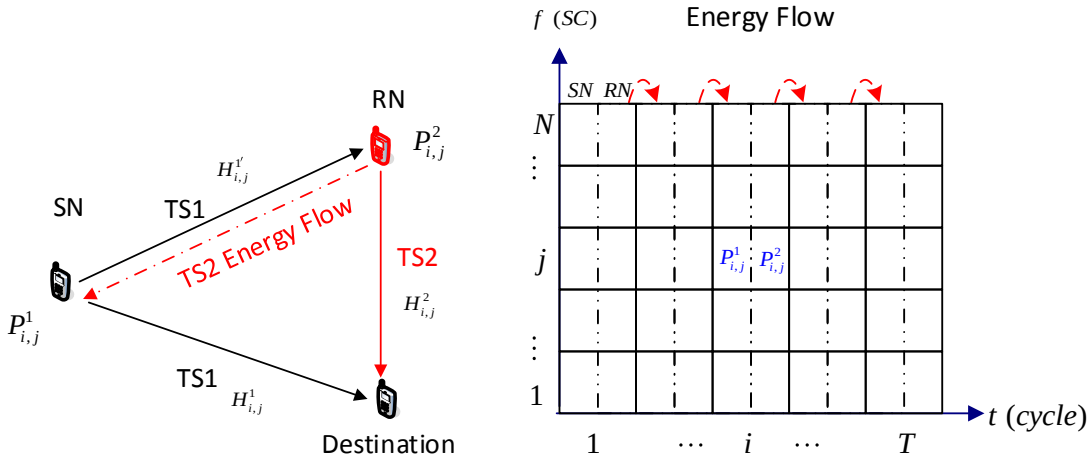

(a) (b)

Figure 3.1 Cooperative data and energy transmission system.

derived from energy cooperation, power allocation schemes have been designed for various systems, including multiple access channel [54] and two way channel [55].

In the next generation green wireless access network, the evolved more flexible system architecture will enable the cooperative data transmission among different network tiers, ranging from macro cells to device to device communications [52]. Moreover, the introduction of network function virtulization and software defined network will reduce the overhead associated with coordinating the energy and data information among multiple serving nodes. The cooperation of data and energy has been studied in the smart-grid powered CoMP system [56], and RF energy harvesting enabled relay system [51, 53, 57–59].

In this work, we extend our work in [53] by considering a relay-enhanced OFDM system consisting of a RF energy harvesting source node (SN) and a cooperative decode-and-forward (DF) relay node (RN), which are transmitting and forwarding in multiple fading subchannels and multiple time slots. For such a system, we propose and investigate a novel power allocation scheme such that the system capacity is

maximized while the power constraints of both source node and relay are satisfied in each time slot. We show that the corresponding optimization problem can be solved by splitting the total transmission power of relay into two parts, one for data forwarding and the other for providing additional power supplement for the source node. In particular, our analysis indicates that there exists the *last common channel*, which separates the subchanels only powered by SN and the subchannels powered by both SN and RN. For a given set of last common subchannels, a closed form solution is derived, and the corresponding optimal power allocation scheme is presented. Numerical results show that for given parameters the proposed cooperative water-filling algorithm provides the optimal performance.

3.1 System Model and Problem Formulation

Suppose the system capacity is measured over $\mathcal{T} = \{1, \cdots, T\}$ cycles, where each data transmission and forwarding cycle consists of two consecutive time slots (TSs), and T can be the delay requirements of data traffic. As illustrated in Figure 3.1, in each odd TS, SN transmits data to the relay node and the destination node (DN), while in the even TS, RN forwards the signal received in the previous TS. SN can harvest energy from the forwarding signals and facilitate the data transmission in the next cycles.

The total bandwidth occupied by SN is divided into $\mathcal{N} = \{1, \cdots, N\}$ subchannels (SCs), each with bandwidth of B, and the block-fading channel response $H_{i,j}^{k}$, $i \in \mathcal{T}$, $j \in \mathcal{N}$, is approximately constant within two time slots and flat within each narrow-band subchannel. More specifically, $k = 1$ refers to the SN-DN link and $k = 2$ the RN-DN link, and $H_{i,j}^{1'}$ denotes the corresponding subchannel gain between SN and RN.

Before the first cycle starts, the amount of the green/brown energy acquired by SN and RN is assumed to be $P^1_{\max}$ and $P^2_{\max}$, respectively.[1] Denote $P^k_{i,j}$ as the ratio between the transmission power allocated to the j-th subchannel at the i-th cycle and P^1_{max}, where $k = 1$ refers to the power source being SN, and $k = 2$ the power source being DF-RN. Note that $P^k_{i,j}$ is referred to as the power allocation for the rest of the paper. Thus, at the i-th cycle, the AWGN Shannon Capacity associated with the j-th subchannel can be expressed as follows [60].

$$c_{i,j} = \frac{B}{2}\log_2(1 + \min\{P^1_{i,j}\gamma^{1'}_{i,j}, \sum_{k=1}^{2} P^k_{i,j}\gamma^k_{i,j}\}) \tag{3.1}$$

where at the i-th cycle, $\gamma^k_{i,j} = \left|H^k_{i,j}\right|^2 P^1_{\max}/(N_0 B)$ is the SNR associated with the SN-DN link ($k = 1$) as well as that of the RN-DN link ($k = 2$), when the j-th subchannel is allocated the entire power of SN. $\gamma^{1'}_{i,j}$ is the corresponding SNR associated with the SN-RN link. $N_0 B$ represents the power of white noise.

Note that we assume $\gamma^{1'}_{i,j} > \gamma^1_{i,j}$, $i \in \mathcal{T}, j \in \mathcal{N}$, so that RN receives more information than DN in the first TS, and forwarding in the second TS has the potential to improve $c_{i,j}$ [61], [62].

Our aim is to maximize the total capacity while meeting the power constraint of each node.

$$\begin{aligned} C = & \max_{\{P^1_{i,j}, P^2_{i,j}\}} \sum_{i=1}^{T}\sum_{j=1}^{N} c_{i,j} \\ s.t. \quad & C^t_{SN} : \sum_{i=1}^{t}\sum_{j=1}^{N} P^1_{i,j} \le 1 + \sum_{i=1}^{t-1}\sum_{j=1}^{N} \beta_{i,j} P^2_{i,j}, t \in \mathcal{T} \\ & C_{RN} : \sum_{i=1}^{T}\sum_{j=1}^{N} P^2_{i,j} = P^2_{tot} \end{aligned} \tag{3.2}$$

where C^t_{SN} denotes the power constraint of SN at cycle t, and C^T_{SN} is satisfied with equality because SN will use all its energy to increase the capacity. C_{RN} represents the

[1]The terms of power and energy are used interchangeably in this chapter because the power consumption and energy storage are all measured within each TS.

power budget of RN, and $P^2_{tot} = P^2_{\max}/P^1_{\max}$. $\beta_{i,j} = \eta\left|H^{1'}_{i,j}\right|^2$ is the overall RF energy harvesting efficiency, with η denoting the energy harvesting efficiency factor [63]. $\beta_{T,j} = 0$ because the energy harvested in the last cycle cannot be utilized for future data transmission.

3.2 Problem Anslysis

According to [53], the channel capacity $c_{i,j}$ can be maximized when $P^1_{i,j}\gamma^{1'}_{i,j} = \sum_{k=1}^{2} P^k_{i,j}\gamma^k_{i,j}$, and it is intuitive to define a threshold $P^{th}_{i,j}$ such that at the i-th cycle, the capacity of the j-th channel will increase with $P^2_{i,j}$ if $P^2_{i,j} \leq P^{th}_{i,j}$. Meanwhile, when $P^2_{i,j} > P^{th}_{i,j}$, SN can also harness more energy from the forwarding signals. Hence, we can divide $P^2_{i,j}$ based on $P^{th}_{i,j}$.

$$\begin{cases} P^2_{i,j} = p_{i,j} + \alpha_{i,j} \\ \alpha_{i,j} = [P^2_{i,j} - P^{th}_{i,j}]^+ \\ P^{th}_{i,j} = [P^1_{i,j}\gamma'_{i,j}]^+ \\ \gamma'_{i,j} = (\gamma^{1'}_{i,j} - \gamma^1_{i,j})/\gamma^2_{i,j} \end{cases} \tag{3.3}$$

where $[\bullet]^+ = \max\{\bullet, 0\}$. $p_{i,j}$ is for *data forwarding* and $\alpha_{i,j}$ is for *power supplement*.

With the separation between $p_{i,j}$ and $\alpha_{i,j}$, the definition of capacity $c_{i,j}$ in (3.1) becomes

$$c_{i,j} = \frac{B}{2}\log_2(1 + P^1_{i,j}\gamma^1_{i,j} + p_{i,j}\gamma^2_{i,j}) \tag{3.4}$$

Remark 4. *At cycle i, $i \in \mathcal{T}$, RN can aggregate the power supplements to one single* **aggregation channel** *(AGC) $j^i_{\max}$ as follows:*

$$\begin{cases} j^i_{\max} = \arg\max\limits_{j\in\mathcal{N}} \beta_{i,j} \\ \alpha_{i,j} = \begin{cases} 0, & j \neq j^i_{\max} \\ \alpha_i \geq 0, & j = j^i_{\max} \end{cases} \end{cases} \tag{3.5}$$

where $j^i_{\max}$ is the subchannel with the maximum energy harvesting efficiency, and α_i is the total power supplement provided by RN at cycle i.

Suppose at each cycle i, all of the N subchannels are sorted in ascending order of $\beta_{i,j} + \gamma_{i,j}$, where $\gamma_{i,j}$ is the **SNR ratio** between the RN channel and SN channel, $\gamma_{i,j} = \gamma^2_{i,j}/\gamma^1_{i,j}$. Then, the following properties are obtained for the optimal power allocation.

Lemma 4. *At each cycle i, $i \in \mathcal{T}$, there exists a* **last common channel** *(LCC) j^*_i, such that*

$$p_{i,j} = \begin{cases} 0, & j < j^*_i \\ \in [0, P^{th}_{i,j^*_i}], & j = j^*_i \\ P^{th}_{i,j}, & j > j^*_i \end{cases} \tag{3.6}$$

Proof.

At the i-th cycle, when the relay node has to choose between two subchannels, the subchannel with higher $\gamma^2_{i,j}$ and $\beta_{i,j}$ will always be chosen because higher $\gamma^2_{i,j}$ will yield greater capacity and greater $\beta_{i,j}$ means more harvested energy for the source node.

Consequently, when the power allocated by SN to all of the subchannels are given, the relay node will start from the subchannel with the highest index, allocate power to the threshold, and then move on to the previous subchannel. The process will continue until a certain subchannel j^*_i is reached, and RN decides to stop.

□

Lemma 5. *When there exists power supplement at the i-th AGC, i.e., $\alpha_i > 0$, the maximum total capacity can be guaranteed when all of the LCCs j^*_I, $\forall I \in \mathcal{T}$ satisfy the following inequalities:*

$$j^i_{\max} > j^*_i \tag{3.7}$$

$$\beta_i > \begin{cases} \beta_{I,j_I^*} + \gamma_{I,j_I^*}, \textit{if } p_{I,j_I^*} < P^{th}_{I,j_I^*} \\ \beta_{I,j_I^*-1} + \gamma_{I,j_I^*-1}, \textit{if } p_{I,j_I^*} = P^{th}_{I,j_I^*} \end{cases} \tag{3.8}$$

where β_i is the maximum overall energy harvesting efficiency at cycle i, i.e., $\beta_i = \beta_{i,j^i_{max}}$.

Proof.

Based on the definition of power supplement in (3.3), $\alpha_i > 0$ indicates $p_{i,j^i_{\max}} = P^{th}_{i,j^i_{\max}}$. According to (3.6) in *Lemma 4*, there must be $j^i_{\max} > j^*_i$.

By the definition in (3.3), α_i will only increase the harvested energy, while $p_{i,j}$ can transmit both energy and data simultaneously. Essentially, when RN has a certain amount of power x, will RN spend x as power supplement or forwarding power? We conduct the following comparison in terms of the energy storage of SN.

1) If RN uses x as power supplement at cycle i, the energy harvested by SN is

$$x\beta_i \tag{3.9}$$

2) If RN uses x as forwarding power at cycle $I \in \mathcal{T}$ and subchannel $J \in \mathcal{N}$, the energy saved by SN is

$$x\beta_{I,J} + \Delta P^1_{I,J} = x\beta_{I,J} + x\gamma_{I,J} \tag{3.10}$$

where $x\beta_{I,J}$ is the harvested energy, and to guarantee that the capacity of subchannel J in (3.4) remains the same, $\Delta P^1_{I,J}$ is the additional energy that SN will have to spend, if there is no x amount of forwarding power. The amount of $\Delta P^1_{I,J}$ is determined as follows.

$$P^1_{I,J}\gamma^1_{I,J} + (x + p_{I,J})\gamma^2_{I,J} = (P^1_{I,J} + \Delta P^1_{I,J})\gamma^1_{I,J} + p_{I,J}\gamma^2_{I,J},$$

where $x + p_{I,J} < P^{th}_{I,J}$.

Thus, if RN provides power supplement at cycle i, (3.9) must be greater than (3.10). That is

$$\beta_i > \beta_{I,J} + \gamma_{I,J} \tag{3.11}$$

where the forwarding power at cycle I subchannel J does not reach the threshold.

Since subchannels are sorted in ascending order of $\beta_{i,j} + \gamma_{i,j}$, if $\alpha_i > 0$, we just need to guarantee (3.11) will hold for the last common channel J_I^* or $J_I^* - 1$. Hence, (3.8) is proved.

□

The intuition behind *Lemma 4* is that with a given power budget, RN will prefer to spend it in the subchannels with better channel condition and greater harvesting efficiency. *Lemma 5* suggests that the power gain provided by power supplement α_i should be strong enough such that RN does not spend it in the suchannel which can simultaneously transfer information and energy.

From the characteristics of optimal α_i in *Lemma 5* and the aggregation method in *Remark 4*, we have the following remark regarding decreasing number of *supplement power* variables.

Remark 5. *Define* $A_0 = \{i|\alpha_i = 0\}$ *as the* **AGC set** *with power supplements that are equal to zero. Then,* $i \in A_0$*, if any of the following conditions are satisfied: 1) there eixsts* $I < i$ *with* $\beta_I \geq \beta_i$*; 2)* $j_i^* \geq j_{max}^i$*; 3) there eixsts* $I \in \mathcal{T}$ *with* $\beta_{I,j_I^*-1} + \gamma_{I,j_I^*-1} \geq \beta_i$*; 4)* $i = T$*.*

Suppose the **AGC set** $\overline{A}_0 = \{i|\alpha_i > 0\}$ contains non-zero power supplement, then the **Equality set** $A_1 = \{I|C_{SN}^I$ in (3.2) is satisfied with equality$\}$ can always be found as follows.

Lemma 6. *For any* $i_1, i_2 \in \overline{A}_0$*,* $i_1 < i_2$*, the maximum total capacity can be guaranteed when there exists* $I \in A_1$*, where* $i_1 < I \leq i_2$*.*

Proof. When $\alpha_{i_1}, \alpha_{i_2} > 0$, there must be $\beta_{i_1} < \beta_{i_2}$ (*Remark 5*). In particular, as compared with α_{i_1}, SN will harvest more energy with greater α_{i_2}. This means α_{i_1} only exists because SN is in power shortage between cycle $i_1 + 1$ and i_2. Meanwhile, the amount of α_{i_1} should be just enough to support the data transmission from cycle $i_1 + 1$ to cycle i_2.

□

Remark 6. *Sort $\overline{A}_0$ in ascending order as $\overline{A}_0 = \{i_1, i_2, \cdots, i_{|\overline{A}_0|}\}$. For the k-th element i_k in $\overline{A}_0$, the corresponding k-th element can be found in A_1, where $i_k < I_k \leq i_{k+1}$. Moreover, $T \in A_1$.*

Based on the above analysis, the $2NT$ variables in (3.2) can be reduced to less than $(N+1)T$ variables $\{P^1_{i,j}, p_{i,j^*_i}\}$. For any given set of LCCs $\{j^*_i | i \in \mathcal{T}\}$, and the corresponding A_0, A_1 given in *Remarks 5-6*, the total capacity can be simplified as follows.

$$\begin{aligned}
\frac{2C}{B} = \max_{\{P^1_{i,j}, p_{i,j^*_i}\}} & \sum_{i=1}^{T} \Big\{ \log_2(1 + P^1_{i,j^*_i}\gamma^1_{i,j^*_i} + p_{i,j^*_i}\gamma^2_{i,j^*_i}) + \\
& \sum_{j=1}^{j^*_i-1} \log_2(1 + P^1_{i,j}\gamma^1_{i,j}) + \sum_{j=j^*_i+1}^{N} \log_2(1 + P^1_{i,j}\gamma^{1'}_{i,j}) \Big\} \\
s.t. \quad & C^t_{SN} : \sum_{i=1}^{t}\sum_{j=1}^{N} P^1_{i,j} \leq 1 + \sum_{i=1}^{t-1}\sum_{j=j^*_i+1}^{N} \beta_{i,j}\gamma'_{i,j}P^1_{i,j} + \sum_{i=1}^{t-1}\beta_i\alpha_i + \sum_{i=1}^{t-1}\beta_{i,j^*_i}p_{i,j^*_i},\ t \in \mathscr{T} \\
& C_{RN} : \sum_{i=1}^{T}(p_{i,j^*_i} + \alpha_i + \sum_{j=j^*_i+1}^{N} \gamma'_{i,j}P^1_{i,j}) = P^2_{tot} \\
& TC_i : p_{i,j^*_i} \leq P^1_{i,j^*_i}\gamma'_{i,j^*_i},\ i \in \mathscr{T}
\end{aligned} \tag{3.12}$$

where α_i is either zero ($i \in A_0$), or it can be represented as a function of $\{P^1_{i,j}, p_{i,j^*_i}\}$ using the C^I_{SN} in A_1. The threshold constraint TC_i is defined in (3.3).

3.3 Optimal Power Allocation

To achieve the maximum capacity, we assign an index set $\{j^i_{LCC} | i \in \mathcal{T}\}$ to LCCs in (3.12), where j^i_{LCC} represents the corresponding order of j^*_i when LCCs are sorted in ascending order of $\beta_{i,j^*_i} + \gamma_{i,j^*_i}$.

Lemma 7. *For any two consecutive cycles $i_1, i_2 \in \mathcal{T}$, $i_1 < i_2$,*
1) If $j^{i_1}_{LCC} \geq j^{i_2}_{LCC}$, then at least one of the following constraints is satisfied with equality.

$$p_{i_1,j^*_{i_1}} \leq P^{th}_{i_1,j^*_{i_1}},\ p_{i_2,j^*_{i_2}} \geq 0 \tag{3.13}$$

2) If $j^{i_1}_{LCC} < j^{i_2}_{LCC}$, then at least one of the following constraints is satisfied with equality.

$$p_{i_1,j^*_{i_1}} \geq 0,\ p_{i_2,j^*_{i_2}} \leq P^{th}_{i_2,j^*_{i_2}},\ C^{i_2-1}_{SN} \text{ in (3.12)} \tag{3.14}$$

Proof. 1) According to *Lemma 4*, when $j_{LCC}^{i_1} \geq j_{LCC}^{i_2}$, at least one of the constraints in (3.13) holds with equality.

2) When $j_{LCC}^{i_1} < j_{LCC}^{i_2}$, suppose none of the conditions in (3.14) holds with equality, then it is feasible that SN allocates more power to channel $j_{i_1}^*$ in the i_1-th cycle, and RN allocates more power to channel $j_{i_2}^*$ in the i_2-th cycle.

The above mentioned power shifting will decrease the power consumption of either SN or RN and it will continue until one of the conditions in (3.14) is honored. □

Remark 7. *Suppose LCC I has the highest index, then 1) If $p_{I,j_I^*} < P_{I,j_I^*}^1 \gamma'_{I,j_I^*}$, and C_{SN}^{I-1} is not satisfied with equality, then $p_{i,j_i^*} = 0, i \in \mathcal{T} \backslash I$.*
2) If $p_{I,j_I^*} < P_{I,j_I^*}^1 \gamma'_{I,j_I^*}$, and C_{SN}^{I-1} is satisfied with equality, then $p_{i,j_i^*} = 0, i \in \{I+1, \cdots, T\}$.

From the characteristics of optimal LCC in *Lemma* 4 and *Remark* 4, we have the cooperative water-filling (WF) algorithm in Algorithm 3.

$$
\begin{aligned}
\tfrac{2C}{B} = \max_{\{P_{i,j}^1, p_{I,j_I^*}\}} & \left\{ \sum_{I \in I^*} \log_2(1 + P_{I,j_I^*}^1 \gamma_{I,j_I^*}^1 + p_{I,j_I^*} \gamma_{I,j_I^*}^2) + \sum_{\substack{i=1 \\ i \notin I^*}}^{T} \log_2(1 + P_{i,j_i^*}^1 \gamma_{i,j_i^*}^1) + \right. \\
& \left. \sum_{i=1}^{T} \sum_{j=1}^{j_i^*-1} \log_2(1 + P_{i,j}^1 \gamma_{i,j}^1) + \sum_{i=1}^{T} \sum_{j=j_i^*+1}^{N} \log_2(1 + P_{i,j}^1 \gamma_{i,j}^{1'}) \right\} \\
s.t. \quad & \sum_{i=1}^{t} \sum_{j=1}^{N} P_{i,j}^1 \leq 1 + \sum_{i=1}^{t-1} \sum_{j=j_i^*+1}^{N} \beta_{i,j} \gamma'_{i,j} P_{i,j}^1 + \sum_{i \in \overline{A}_0} \beta_i \alpha_i \mathbf{1}_{\{t \geq i+1\}} + \\
& \sum_{I \in I^*} \beta_{I,j_I^*} p_{I,j_I^*} \mathbf{1}_{\{t \geq I+1\}}, t \in \mathcal{T} \\
& \sum_{I \in I^*} p_{I,j_I^*} + \sum_{i=\overline{A}_0} \alpha_i + \sum_{i=1}^{T} \sum_{j=j_i^*+1}^{N} \gamma'_{i,j} P_{i,j}^1 = P_{tot}^2 \\
& p_{I,j_I^*} \leq P_{I,j_I^*}^1 \gamma'_{I,j_I^*}, I \in I^*
\end{aligned}
\tag{3.15}
$$

where $\mathbf{1}_{\{x\}}$ is the indicator function, which is 1 when x is true and 0 otherwise. Equation (3.15) is a convex optimization problem consisting of concave objective

Algorithm 3: Cooperative-WF algorithm

$C^* = \emptyset$;
$\mathcal{T} = \{1, \cdots, T\}$;
for *LCC set* $\{j_i^* | i \in \mathcal{T}\}$ **do**
    $A = \{i | \alpha_i = 0, i \in \mathcal{T}\}$ (*Remark 5*);
    for A_0*: Superset of* A **do**
        $\alpha_i = 0, i \in A_0$;
        $\overline{A}_0 = \mathcal{T} \backslash A_0$;
        for A_1*: Equality set for* $\overline{A}_0$ (Remark 6) **do**
            $I^* = \emptyset$;
            while $\mathcal{T} \neq \emptyset$ **do**
                $I = \{i \in \mathcal{T} | j_{LCC}^i = |\mathcal{T}|\}$;
                $I^* = \{I^*, I\}$;
                if $I - 1 \in A_1$ **then**
                    $p_{i,j_i^*} = 0, i \in \{I + 1, \cdots, T\}$;
                    $\mathcal{T} = \{1, \cdots, I - 1\}$;
                else
                    $\mathcal{T} = \emptyset$;
            Calculate C according to (3.15);
            $C^* = \{C^*, C\}$;
Return $C^* = \max\{C^*\}$;

function and linear constraints [57], and the Lagrange function is defined in (3.16),

$$\begin{aligned}\mathcal{L} = &-\tfrac{2C}{B} + \sum_{t\in A_1}\mu_t\Big(\sum_{i=1}^{t}\sum_{j=1}^{N}P_{i,j}^1 - 1 - \sum_{i\in\overline{A}_0}\beta_i\alpha_i\mathbf{1}_{\{t\geq i+1\}} - \sum_{i=1}^{t-1}\sum_{j=j_i^*+1}^{N}\beta_{i,j}\gamma'_{i,j}P_{i,j}^1 - \\ &\sum_{I\in I^*}\beta_{I,j_I^*}p_{I,j_I^*}\mathbf{1}_{\{t\geq I+1\}}\Big) + \eta\Big(\sum_{I\in I^*}p_{I,j_I^*} + \sum_{i\in\overline{A}_0}\alpha_i + \sum_{i=1}^{T}\sum_{j=j_i^*+1}^{N}\gamma'_{i,j}P_{i,j}^1 - P_{tot}^2\Big) + \\ &\sum_{i=1}^{T}\sum_{j=1}^{N}\delta_{i,j}P_{i,j}^1 + \sum_{I\in I^*}\delta_I^* p_{I,j_I^*}\end{aligned} \tag{3.16}$$

where the Lagrange multipliers $\delta_{i,j}$ and δ_I^* are due to the constraint that $P_{i,j}^1, p_{I,j_I^*} \geq 0$.

Note that the same constraints apply for $\alpha_i, i \in \overline{A}_0$. However, they are non-zero power supplements and therefore are excluded. Moreover, since Cooperative-WF algorithm sweeps through all the LCC sets, we assume the threshold constraints are not satisfied with equality for each LCC set and therefore are excluded in the Lagrangian function. Similarly, we exclude the constraints $C_{SN}^t, t \notin A_1$.

The solution to Karush-Kuhn-Tucker conditions is given in (3.17).

$$\begin{aligned}p_{I,j_I^*} &= \left[\frac{ln2}{-\sum_{t\in A_1}\mu_t\mathbf{1}_{\{t\geq I+1\}}\beta_{I,j_I^*}+\eta} - \frac{1+P_{I,j_I^*}^1\gamma_{I,j_I^*}^1}{\gamma_{I,j_I^*}^2}\right]^+, I\in I^* \\ P_{i,j}^1 &= \begin{cases}\left[\frac{ln2}{\sum_{t\in A_1}\mu_t\mathbf{1}_{\{t\geq I\}}} - \frac{1+p_{I,j_I^*}\gamma_{I,j_I^*}^2}{\gamma_{I,j_I^*}^1}\right]^+, & I\in I^* \\ \left[\frac{ln2}{\sum_{t\in A_1}\mu_t\mathbf{1}_{\{t\geq i\}}} - \frac{1}{\gamma_{i,j}^1}\right]^+, & i\notin I^*, j\in\{1,\cdots,j_i^*\} \\ & i\in I^*, j\in\{1,\cdots,j_i^*-1\} \\ \left[\frac{ln2}{\sum_{t\in A_1}\mu_t\left(\mathbf{1}_{\{t\geq i\}}-\mathbf{1}_{\{t\geq i+1\}}\beta_{i,j}\gamma'_{i,j}\right)+\eta\gamma'_{i,j}} - \frac{1}{\gamma_{i,j}^{1'}}\right]^+, & else\end{cases} \\ \eta &= \sum_{t\in A_1}\mu_t\mathbf{1}_{\{t\geq i+1\}}\beta_i, i\in\overline{A}_0\end{aligned} \tag{3.17}$$

As we can see, the optimal power allocation takes the form of traditional water-filling and also has a cooperative nature in the sense that $P_{i,j}^1$ and p_{I,j_I^*} are correlated. The optimal solution can be obtained by getting a set of $\{\eta, \mu_t\}$ that simultaneously fulfills the equal power constraints C_{SN}^t, $t \in A_1$, and C_{RN}. Similar to the water-filling procedure, an algorithmic solution can be found such that the power allocation

satisfies the remaining non-equal power constraints and threshold constraints in (3.15) [57, 58].

3.4 Numerical Results

In this section, we provide numerical results for the studied cooperative relay setting and illustrate the derived optimal policy. We assume that the cycle length is 1 ms, noise spectral density is $N_0 = -174$ dBm/Hz and the system consists of total $N = 6$ subchannels, each with bandwidth of $B = 180$ KHz. Moreover, the harvesting efficiency is set as $\eta = 0.8$, and the power budget of SN is normalized as $P^1_{max} = 1$ W. For the channel model, we assume $H = -20d^{-3}h$ consists of both path-loss attenuation and Rayleigh fading, where 3 is the path-loss exponent, and -20 dB is the average signal power attenuation at a reference distance of 1 m. h is an exponential random variable with unit mean denoting the Rayleigh fading, and d is the length of each link in m. The length of the SN-DN link, SN-RN link, RN-DN link are 50 m, 10 m, and 40 m respectively.

The performances of the proposed Cooperative-WF algorithm and the Separate-WF algorithm are shown in Figure 3.2. Cooperative-WF algorithm with $\eta = 0$ implies that SN cannot share RN's energy since there is no RF energy harvesting functionality. Similarly, the Separate-WF algorithm only employs data cooperation. SN and RN will individually use the traditional water-filling algorithm to allocate power.

As expected, the proposed power allocation scheme is shown to be optimal both at low power constraint and high power constraint. With $P^2_{tot} = 0$, there is neither data cooperation or energy cooperation between SN and RN for all algorithms, and the second time slot of each cycle is wasted. Also, we should note that for the Separate-WF algorithm, when P^2_{tot} increases, C may decrease or remain the same. The reason is that when $P^2_{tot} \geq 5$ in Figure 3.2, RN may allocate more power to the j-th subchannel with better RN-DN link condition (higher $\gamma^2_{i,j}$). When $c_{i,j}$ is

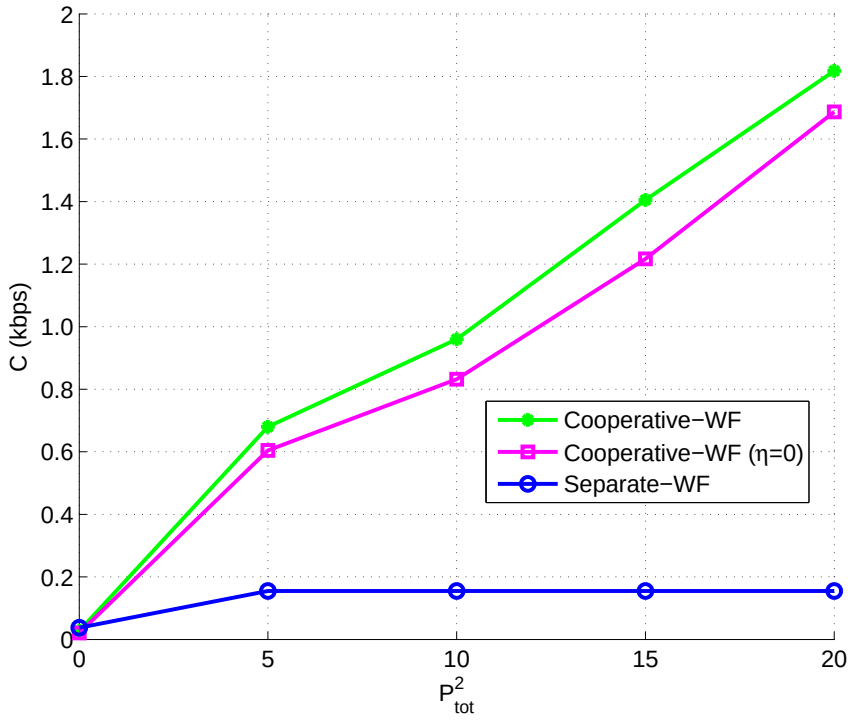

Figure 3.2 System capacity versus power budget of RN ($T = 5$).

determined by the smaller $P^1_{i,j}\gamma^{1'}_{i,j}$, the increased $P^2_{i,j}\gamma^2_{i,j}$ will not improve the capacity. However, this is not the case for the Cooperative-WF algorithm. In fact, C will always increase with P^2_{tot} due to the cooperative features of the system.

3.5 Summary

In this chapter, for the OFDM based cooperative relay system, where the relay node not only can forward the data to the destination node, but is also capable of transferring energy to the source node, we have derived the closed form solution to optimally allocate power for a relay-enhanced data and energy cooperative ODFM system, and a novel power allocation scheme has been proposed to achieve the maximum network capacity. Considering the flexibility of the system, the cooperative power allocation results can be extended to scenarios with wired energy sharing or multiple DF-RNs, which are left for our future research endeavors.

In particular, to maximize the overall system capacity in multiple subchannels and multiple time slots while meeting the power constraints, a power allocation optimization problem is formulated and solved in three steps. First, at each data transmission and data forwarding cycle, we split the total transmission power of relay into two parts, one for data forwarding and the other as power supplement for the source node. Then, our analysis indicates that at each cycle, once all of the subchannels are sorted in a certain order, the relay node will only provide forwarding power to the subchannels with index greater than a certain value. Meanwhile, the incentive for the relay node to provide power supplement should be strong enough such that relay chooses not to simultaneously transmit data and energy. Finally, an equivalent convex constrained optimization problem is formulated and the solution is derived by solving the Lagrange function. The solution takes the form of water-filling in combination with a cooperative feature.

CHAPTER 4

WIRED ENERGY AND WIRELESS DATA COOPERATION

Owing to the direct impact of greenhouse gases on the earth environment and the climate change, the energy consumption of Information and Communications Technology (ICT) is becoming an environmental and thus, social and economic issue [53, 64, 65]. Mobile networks are among the major energy guzzlers of communication networks, and their contributions to the global energy consumption increase rapidly. Therefore, greening mobile networks is crucial to reducing the carbon footprints of ICT [66–69].

As green energy technologies advance, green energy such as sustainable biofuels, solar and wind energy can be readily utilized to power BSs. Telecommunications companies such as Ericsson and Nokia Siemens have designed green energy powered BSs for mobile networks [70, 71]. By adopting green energy powered BSs, mobile service providers may save on-grid power consumption, and thus, reduce their CO_2 emissions [72–74]. However, since the green energy generation is not stable, green energy may not be a reliable energy source for mobile networks. Therefore, future mobile networks are likely to adopt hybrid energy supplies: on-grid brown power and green energy. Green energy is utilized to reduce the on-grid brown power consumption and thus, reduce the CO_2 emissions while on-grid brown power is utilized as a backup power source. To achieve energy efficient wireless data transmission, Hong and Zhu [75] proposed to power wireless access networks with smart grid, where in addition to the green energy generator equipped in each BS, the radial structure power distribution networks are adopted to connect the BSs. Both the power flows in the smart grid and beamforming vectors are investigated for the wireless access network with/without cooperative data transmission.

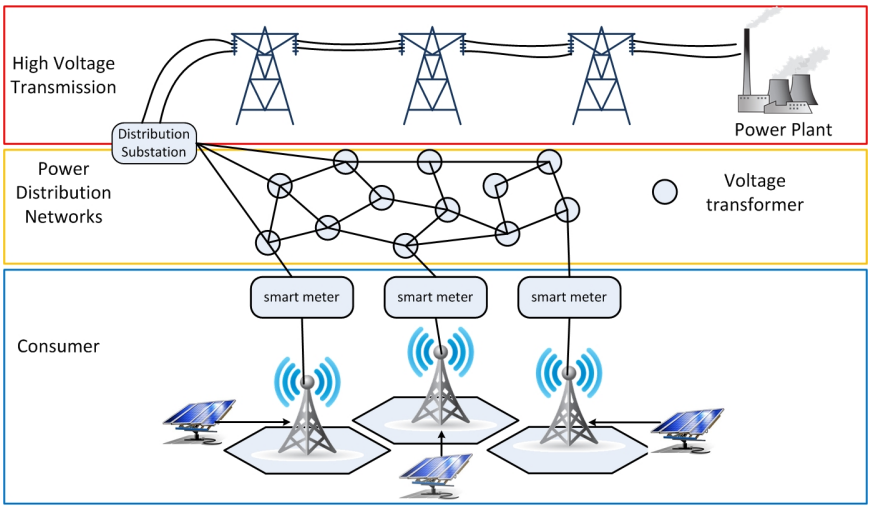

Figure 4.1 Smart grid enabled mobile network.

In smart grid, electricity can be traded among distributed power generators and consumers [28, 29, 76]. Powered by smart grid, mobile networks are able to buy electricity from different power generators according to energy market information and optimize their BS operation to minimize their operating expenses [18, 30, 77]. Via smart grid, the surplus green energy generated by a BS can be shared with other BSs to reduce the on-grid brown power consumption of mobile networks [78]. Considering both green energy and smart grid, the power supplies of future mobile networks are shown in Figure 4.1. In the network, BSs have three power supplies: the power generated from the green energy generator in individual BSs, the power shared from other BSs, and the brown power generated from the remote power plant. The power generated from the remote power plant is the least efficient because of the energy loss during the power transmission and distribution. We refer to the power generated from the remote power plant as on-grid brown power.

Considering the broadcast nature of wireless communications, in addition to the wired energy transfer facilitated by the grid architecture, energy can be shared among multiple BSs through wireless energy transfer based methods, such as traffic offloading [30]. Wired energy transfer not only 1) is limited by the availability of

grid architecture, but also 2) suffers from energy transfer loss caused by the grid equipment, such as power transformer and transmission line. Wireless energy transfer, on the other hand, 1) is constrained within a certain geographical area, owing to the wireless channel attenuation between the mobile user and the base station that will share the energy, and 2) suffers from energy loss in the sense that the offloaded traffic always requires more energy, as compared with the original associated nearest BS.

To minimize the on-grid brown power consumption of mobile networks, we propose to jointly investigate wired energy transfer and wireless energy transfer in the smart grid powered wireless access network. Wired energy transfer is controlled by the power distribution scheme, and the BS operation controls the UE-BS association scheme so that energy can be shared among BSs without wired energy transfer. Although the optimization of the BS operation [79], the green energy utilization [72], and the power distribution [80] are well studied separately, the joint **B**S operation and **P**ower distribution **O**ptimization (BPO) problem is not well investigated.

Within the coverage of the proposed wireless access network, the distribution network of smart grid will not only deliver power resources to base stations, but also to residential customers and other industuries, of which the load is very difficult to model. The complex topology of the power distribution network makes it very difficult to solve the full power flow among the whole distribution network [81]. Consequently, the BPO problem conducts analytic study on how much power is consumed by each base station and how much power is injected to/withdrawn from the grid. The detailed scheduling of the power flow will be carried out by the smart grid, and is out of the scope of this dissertation.

Solving the BPO problem is challenging due to the complex coupling of the BS operation, the green energy utilization, and the power distribution. We propose an approximate solution which decomposes the BPO problem into two subproblems: the weighted user-BS association (WUA) problem and the BS energy sharing (BES)

problem. By addressing the WUA problem, we realize the energy efficiency aware BS operation. By solving the BES problem, we optimize the power sharing among BSs and thus minimize the BSs' on-grid power consumption. The important notations are summarized in Table 4.1.

4.1 System Model

In this chapter, we consider a mobile network with $\mathcal{B} = \{1, \cdots, N\}$ BSs. Each BS can draw brown energy from the connected smart grid. In addition to brown energy, the BSs are equipped with independent energy harvesting system that generates electricity from green energy sources, such as solar. The green energy generation rate in the i-th BS is denoted as E_i. Owing to the disadvantages of "banking" green energy [82], we assume the "harvest-use" structure is adopted for each energy harvester, i.e., the green energy cannot be stored [18]. However, the harvested green energy is not wasted even if it is not used immediately by the BS that generated it. Facilitated by the grid architecture, the individually harvested green energy can be shared among BSs, indicated as bi-directional inter-BS energy flows in Figure 4.2, where $\delta_{i,j}$ is the amount of energy transferred from BS i to BS j, and $\delta_{j,i}$ is the other way around. The smart grid can be considered as a virtual battery for the green energy harvested from all BSs. Note that it is not necessary to have a direct grid link between any BS i and BS j.

In the network, the i-th BS will always transmit with the maximum power $P_i^t, i \in \mathcal{B}$.[1] 1) To reduce carbon footprints, BSs will utilize the harvested green energy E_i first. 2) When green energy in a BS is not sufficient to satisfy this amount of energy demand, the BS can draw power from the other BSs which have surplus green energy, i.e., $\sum_{j \in \mathcal{B} \setminus i} \delta_{j,i}$. 3) If the BS's energy demand is still not satisfied, the BS consumes on-grid brown power, which is pulled from the remote power plant through the high

[1]The downlink power control scheme of an LTE system is very limited. The transmission power can be assumed to be constant over the entire bandwidth [83].

Table 4.1 List of Important Notations

$\mathcal{A}$	Network coverage area
$\mathcal{B}$	BS set, including N BSs
$\mathcal{B}^o$	Set of BSs which consume on-grid brown power
$\mathcal{B}^g$	Set of BSs which have surplus green energy
x	UE location
$\boldsymbol{\delta}$	$\delta_{i,j}$: Power supplement from BS i to BS j through grid
$\boldsymbol{\eta}(x)$	$\eta_i(x)$: Binary association indicator of UE x and BS i
$\widetilde{\boldsymbol{\eta}}(x)$	$\widetilde{\eta}_i(x)$: Maximum SINR association indicator of UE x and BS i
$\boldsymbol{\rho}$	ρ_i: Traffic load (utilization rate) of each BS i
$\widetilde{\boldsymbol{\rho}}$	$\widetilde{\rho}_i$: Traffic load of BS i with maximum SINR association scheme
$r_i(x)$	Data rate of UE at x if associated with BS i
$r(\boldsymbol{\eta}, x)$	Data rate of UE at x if associated to a BS according to $\boldsymbol{\eta}$
$\widetilde{r}(x)$	Maximum achievable data rate of UE at x
τ_i	Latency ratio of BS i
τ^*	Maximum allowable latency ratio
P_i	Total power consumption of BS i
P_i^t	Transmission power of BS i
P_i^s	Static power consumption of BS i
P_i^o	On-grid power consumption of BS i
E_i	Available green power at BS i
$\theta_{i,j}$	Power transfer efficiency between BS i to BS j
$\theta_{0,i}$	Power transfer efficiency from main grid to BS i
θ	Approximate wired energy transfer efficiency ratio
$\widetilde{\boldsymbol{\omega}}$	$\widetilde{\omega}_i$: Wireless energy transfer efficiency threshold of BS i
ζ, ψ	Backtracking line search parameters
ξ_k	Step size at the k-th iteration

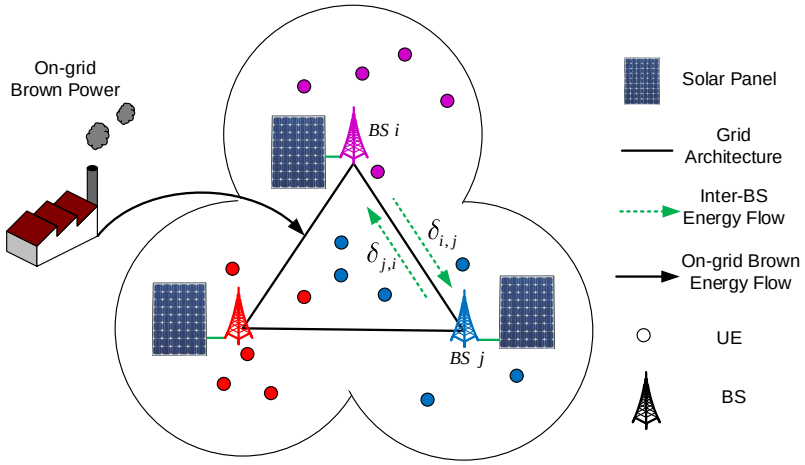

Figure 4.2 On-grid brown energy flow and Inter-BS green energy flow.

voltage transmission line, the distribution substations, and the power distribution network.

4.1.1 Traffic Model

Assume N BSs are deployed to provide data service to an area $\mathcal{A}$. We assume that the traffic arrives according to a Poisson process with the arrival rate per unit area at location x equaling to $\lambda(x)$, and the traffic size per arrival has a general distribution with average value of $s(x)$, thus resulting in a total $\lambda(x)s(x)$ average traffic load. Assuming a mobile user at location x is associated with the i-th BS, then the user's data rate $r_i(x)$ can be generally expressed as a logarithmic function of the instantaneous signal to interference plus noise ratio, $SINR_i(x)$, according to the Shannon Hartley theorem [79],

$$r_i(x) = log_2(1 + SINR_i(x)) \tag{4.1}$$

Here,

$$SINR_i(x) = \frac{P_i^t g_i(x)}{\sigma^2 + \sum_{j \in \mathcal{B}, j \neq i} P_j g_j(x)} \tag{4.2}$$

where σ^2 denotes the noise power level, and $g_i(x)$, $i \in \mathcal{B}$, is the channel gain between BS i and UE located in x, including the path loss and the shadowing fading.

As we can see, the service rate for UE located at x and associated with the i-th BS is

$$\mu_i(x) = \frac{r_i(x)}{s(x)} \tag{4.3}$$

Assuming mobile users are uniformly distributed in the area, the overall utilization rate of the i-th BS can be expressed as follows.

$$\rho_i = \int_{x \in \mathcal{A}} \eta_i(x) \frac{\lambda(x)}{\mu_i(x)} dx \tag{4.4}$$

where $\boldsymbol{\eta}(x) = (\eta_1(x), \cdots, \eta_N(x))$ is an association indicator function. If $\eta_i(x) = 1$, the user at location x is associated with the i-th BS; otherwise, the user is not associated with the i-th BS. For the maximum SINR association scheme $\widetilde{\boldsymbol{\eta}}(x) = (\widetilde{\eta}_1(x), \cdots, \widetilde{\eta}_N(x))$, user at x will only connect to the base station which yields the maximum $SINR_i(x)$. Note that the value of ρ_i indicates the fraction of time during which the i-th BS is busy transmitting data; in particular, we also uses ρ_i to indicate the amount of traffic load of BS i.

The traffic served by the i-th BS, i.e., $\int_{x \in \mathcal{A}} \lambda(x) \eta_i(x) dx$, which is the sum of the traffic arrivals from its coverage area, is a Poisson process, and the user departure rate $\mu_i(x)$ follows a general distribution. Consequently, the BS realizes an $M/G/1$ queuing system. Assuming mobile users share the BS's radio resource and are served based on the round robin fashion, the traffic delivery in the BS can be modeled as an $M/G/1 - PS$ (processor sharing) queue.

According to [84], the average traffic delivery time, including waiting time and service time, for the user in the i-th BS is

$$T_i(x) = \frac{1}{\mu_i(x)(1 - \rho_i)} \tag{4.5}$$

Denote $\tau_i(x)$ as the latency ratio that measures how much time a user at location x must be sacrificed in waiting for a unit service time.

$$\tau_i(x) = \frac{T_i(x) - \frac{1}{\mu_i(x)}}{\frac{1}{\mu_i(x)}} = \frac{\rho_i}{1-\rho_i} \tag{4.6}$$

where $1/\mu_i(x)$ is the service time.

According to (4.6), $\tau_i(x)$ only depends on the traffic load in the i-th BS. Therefore, all the users associated with BS i have the same latency ratio. Thus, we define

$$\tau_i = \frac{\rho_i}{1-\rho_i} \tag{4.7}$$

as the latency ratio of the i-th BS. A smaller τ_i indicates that the i-th BS introduces less latency to its associated users.

4.1.2 Energy Consumption Model

The BS's power consumption consists of two parts: the static power consumption and the dynamic power consumption [50]. The static power consumption is the power consumption of a BS without any traffic load. The dynamic power consumption refers to the additional power consumption caused by traffic load in the BS, which can be well approximated by a linear function of the traffic load [85]. Denote P_i^s as the static power consumption of the i-th BS. Then, the i-th BS's power consumption can be expressed as

$$P_i = \beta_i \rho_i + P_i^s \tag{4.8}$$

Here, β_i is the linear coefficient which reflects the relationship between the traffic load and the dynamic power consumption in the i-th BS. β_i includes the transmission power P_i^t in Equation (4.2) and power efficiency related to the physical equipment, such as power amplifier.

For the wired energy transfer scheme among the wireless access networks, instead of using Kirchhoffs Current Law (KCL), Kirchhoffs Voltage Law (KVL) and nodal analysis method to approximate the power flows [86], we assume when an individual energy harvester (green energy powered BS) feeds its excess green energy back to the grid, it can obtain a certain amount of credit from the grid. The credit can be used by other cooperative harvesters (other BSs) with insufficient green energy in the system (wireless access networks) to purchase the on-grid energy. The relationships between the green energy, on-grid brown energy and energy credit are approximated as wired energy transfer efficiency as follows.

$$\begin{cases} \theta_{0,i} = \theta^T_{0,i}\theta^D_{0,i} = \theta^T_{0,i}\theta^{PT}_{0,i}\theta^{PL}_{0,i} \in (0,1) \\ \theta_{i,j} = \theta_{j,i} = \theta^{PT}\theta^{PL}_{i,j} = \theta^{PT}\theta^{PL}_{j,i} \in (0,1),\ i \neq j \end{cases} \tag{4.9}$$

where $\theta_{0,i}$ is the brown power transmission efficiency reflecting the power loss of transferring power from the remote power plant and the i-th BS, and $\theta_{i,j}$ refers to the green power transmission efficiency of using green energy harvested by i-th BS at the j-th BS.

$\theta_{0,i}$ includes both the *transmission loss* $\theta^T_{0,i}$ and the *distribution loss* $\theta^D_{0,i}$ [87]. The transmission loss is incurred during the process of moving large amounts of power over high voltage and long distance. The distribution system consists of the substations and feeder lines that take power from the high voltage grid and progressively step down the voltage, and eventually enter the base station. Essentially, power distribution loss considers both the efficiency of *power transformer* $\theta^{PT}_{0,i}$ and the efficiency of *power transmission line* $\theta^{PL}_{0,i}$.

The wired power transfer among BSs only occur in the energy distribution system; namely, $\theta_{i,j}$ consists of both 1) θ^{PT}, the efficiency of *grid-tie inverter*, which

is assumed to be the same for all BSs [2], and 2) the efficiency of power line between the two BSs $\theta_{i,j}^{PL}$.

Moreover, we assume the grid is smart in the sense that when energy is transferred from one location to another, the direct energy transfer efficiency is always the highest among all the possible energy transfer routes between these two grid connected locations. Consequently, the energy transfer efficiency in (4.9) exhibits the following characteristics.

$$\begin{cases} \theta_{0,i} \geq \theta_{0,j}\theta_{j,i} \\ \theta_{i_1,i_2} \geq \theta_{i_1,i}\theta_{i,i_2} \end{cases} \tag{4.10}$$

The above assumption is reasonable because if the energy efficiency $\theta_{0,i}$ is less than $\theta_{0,j}\theta_{j,i}$, the smart grid will first transfer energy to BS j, and then to BS i. Eventually, we will have $\theta_{0,i} = \theta_{0,j}\theta_{j,i}$. Similarly, there is no need to transmit directly between BSs i_1 and i_2 without the intermediate node i, if θ_{i_1,i_2} is less than $\theta_{i_1,i}\theta_{i,i_2}$.

Thus, the on-grid brown power consumption in the i-th BS is

$$P_i^o = \frac{\{P_i - (E_i + \sum_{j\in\mathcal{B}} \delta_{j,i}\theta_{j,i} - \sum_{j\in\mathcal{B}} \delta_{i,j})\}^+}{\theta_{0,i}} \tag{4.11}$$

where the positive function $\{\bullet\}^+ = \max\{\bullet, 0\}$, and $\delta_{i,i} = 0$. $\sum_{j\in\mathcal{B}} \delta_{j,i}$ is the amount of green energy received from other BSs. $\sum_{j\in\mathcal{B}} \delta_{i,j}$ is the amount of green energy transmitted to other BSs.

4.2 Problem Formulation and Analysis

In jointly optimizing the BS operation and the power distribution, the network aims to minimize the on-grid power consumption while satisfying the mobile users' quality of service (QoS) requirement, which refers to the average traffic delivery latency in

[2]Grid-tie inverter is capable of converting direct current (DC) sources such as solar panels or small wind turbines into alternating current (AC) for tying with the grid. Grid-tie inverter will not be a necessity when the AC distribution system is replaced by the DC distribution system.

this chapter. The joint **B**S operation and **P**ower distribution **O**ptimization (BPO) problem can be formulated as

$$\min_{(\boldsymbol{\rho},\boldsymbol{\delta})} \sum_{i\in\mathcal{B}} P_i^o = \sum_{i\in\mathcal{B}} \frac{\{P_i-(E_i+\sum_{j\in\mathcal{B}}\delta_{j,i}\theta_{j,i}-\sum_{j\in\mathcal{B}}\delta_{i,j})\}^+}{\theta_{0,i}} \tag{4.12}$$

$$s.t. \qquad 0 \le \tau_i \le \tau^*, i \in \mathcal{B} \tag{4.13}$$

where τ^* is the maximum allowable latency ratio for satisfying users' QoS requirements in the network. $\boldsymbol{\rho} = (\rho_1, \rho_2, \cdots, \rho_N)$, and

$$\boldsymbol{\delta} = \begin{pmatrix} 0, & \delta_{1,2}, & \cdots, & \delta_{1,N} \\ \delta_{2,1}, & 0, & \cdots, & \delta_{2,N} \\ \vdots, & \vdots, & \ddots, & \vdots \\ \delta_{N,1}, & \delta_{N,2}, & \cdots, & 0 \end{pmatrix} \tag{4.14}$$

where $\delta_{i,j}\delta_{j,i} = 0$. This indicates that when BS i provides green energy to BS j, then BS j will not simultaneously transmit energy back to BS i, because energy loss is incurred during green energy transferring process.

Suppose with the maximum SINR association scheme $\widetilde{\boldsymbol{\eta}}(x)$, the traffic load of each BS is $\widetilde{\boldsymbol{\rho}} = (\widetilde{\rho}_1, \cdots, \widetilde{\rho}_N)$. To ensure the area defined in (4.13) is feasible, we assume τ^* is at least greater than the latency ratio corresponding to $\widetilde{\boldsymbol{\rho}}$.

To solve the BPO problem, the traffic load assigned to each BS and the power sharing among the BSs should be optimized. A BS's traffic load is determined by the user-BS association scheme. The power transmission efficiency of the power grid is one of the factors in determining the optimal user-BS association. The optimal power sharing depends on the BSs' traffic load, the green energy generation rate, and the power transmission efficiency. Owing to the complex coupling of these variables and parameters, solving the BPO problem is challenging.

4.2.1 Problem Simplification

Similar to the link capacity concept in the wired/wireless data transmission network, the capacity to flow power on a line or a group of lines of the smart grid can also be limited and dynamic [88]. Consequently, in reality, the power flows among BS pairs depend not only on the available energy and energy transfer efficiency, but also on other power injections and withdrawals using the power lines in between. In the power grid, injection shift factor (ISF) is used to approximate the change in active-power flow across a transmission line due to a change in active-power generation or load at a particular bus. Based on ISF, line flow distribution factors, such as the power transfer distribution factor (PTDF), can be derived to model the relative change in power flow on a particular line due to a change in injection and corresponding withdrawal at a pair of buses. More recently, the Generalized ISF has been proposed to predict active-power line flows during the transient period following a disturbance [89].

Both PTDF and Generalized ISF are linear power flow models designed to maintain the grid balance [90]. Since it is known empirically that, given a fixed topology and ignoring controllable device limits, the linear factors are relatively insensitive to the levels of injections and withdrawals [91], we assume that the power flows among the BS pairs in the wireless access network is separated from the other power injections or loads in the smart grid. With this assumption, the characteristics of power supplements provided by each BS are presented in the following Lemmas.

Lemma 8. *For any given power consumption scheme $\boldsymbol{\rho}$, there exists an optimal power supplements profile $\boldsymbol{\delta}$, such that the power supplements provided by each BS will not exceed its own available green energy.*

$$\sum_{j\in\mathcal{B}} \delta_{i,j} \leq E_i + \sum_{j\in\mathcal{B}} \delta_{j,i}\theta_{j,i},\ i \in \mathcal{B}$$

Lemma 9. *For any given power consumption scheme $\boldsymbol{\rho}$, there exists an optimal power supplements profile $\boldsymbol{\delta}$, such that each BS will never receive green power supplement from one BS while providing power supplement to another BS.*

$$(\sum_{j\in\mathcal{B}}\delta_{i,j})(\sum_{j\in\mathcal{B}}\delta_{j,i})=0,\ i\in\mathcal{B}$$

The proofs can be found in Appendices A.4-A.5. The results presented can be anticipated from (4.10) because the direct route between two nodes is the most efficient in terms of energy transfer. fly, to minimize the total on-grid energy consumption, the grid and BSs will choose the direct path to reduce the power loss.

The observation presented in Lemmas 8 and 9 simplifies the BPO problem as follows: if the i-th BS consumes on-grid brown power, then $\sum_{j\in\mathcal{B}}\delta_{i,j}=0$, and the corresponding P_i^o is redefined as follows.

$$P_i^o=\frac{P_i-E_i-\sum_{j\in\mathcal{B}^g}\theta_{j,i}\delta_{j,i}}{\theta_{0,i}},i\in\mathcal{B}^o \tag{4.15}$$

where $\mathcal{B}^o$ and $\mathcal{B}^g$ are the set of BSs which consume on-grid brown power and the set of BSs which have surplus green energy, respectively. $\mathcal{B}^o=\{i|P_i>E_i,\ i\in\mathcal{B}\}$ and $\mathcal{B}^g=\{i|P_i\leq E_i,\ i\in\mathcal{B}\}$.

The corresponding problem in (4.12) is reformulated as follows.

$$\min_{(\boldsymbol{\rho},\boldsymbol{\delta},\mathcal{B}^o,\mathcal{B}^g)}\sum_{i\in\mathcal{B}^o}\frac{P_i-E_i-\sum_{j\in\mathcal{B}^g}\theta_{j,i}\delta_{j,i}}{\theta_{0,i}} \tag{4.16}$$

$$s.t.\qquad 0\leq\rho_i\leq\frac{\tau^*}{1+\tau^*},i\in\mathcal{B} \tag{4.17}$$

$$\mathcal{B}^o\cap\mathcal{B}^g=\emptyset \tag{4.18}$$

$$\mathcal{B}^o\cup\mathcal{B}^g=\mathcal{B} \tag{4.19}$$

$$\sum_{j\in\mathcal{B}^o}\delta_{i,j}\leq E_i-P_i,i\in\mathcal{B}^g \tag{4.20}$$

$$\sum_{j\in\mathcal{B}^g}\theta_{j,i}\delta_{j,i}\leq P_i-E_i,i\in\mathcal{B}^o \tag{4.21}$$

where the constraint in (4.17) is mapped from $0 \leq \tau_i \leq \tau^*$, based on the definition of the average latency ratio given in (4.7), and $\widetilde{\boldsymbol{\rho}} \leq \tau^*/(1+\tau^*)$. The constraint in (4.21) is introduced to eliminate the positive function of the objective function of the BPO problem, and

$$\boldsymbol{\delta} = \begin{cases} \delta_{i,j} \geq 0,\ i \in \mathcal{B}^g, j \in \mathcal{B}^o \\ 0,\ else \end{cases}$$

4.2.2 Problem Decomposition

Given a BS's green energy generation rate and the power transmission efficiency of power grid in the objective function of (4.16), the first component of the on-grid brown power consumption $(P_i - E_i)/\theta_{0,i}$ is determined by the BS's power consumption while the second component $\sum_{j\in\mathcal{B}^g} \theta_{j,i}\delta_{j,i}/\theta_{0,i}$ is determined by the power sharing among the BSs.

For the second component, according to Chapter 10 in [92], the efficiency of transferring power from the remote power plant to BS i is much lower than the efficiency of power line between BS i and other BSs.

$$\theta_{0,i} \ll \theta_{i,j}^{PL},\ \forall j \in \mathcal{B}\backslash i \tag{4.22}$$

Since wireless access networks encourage the usage of the carbon neutral green energy rather than the on-grid brown energy, in addition to the physical wired energy transfer loss, the carbon emission factor will also render small $\theta_{0,i}$ and large $\theta_{i,j}^{PL}$. Consequently, the energy loss ratio of any BS can be approximated as the same, denoted by θ.

$$\theta \simeq \theta^{PT}\frac{\theta_{i,j}^{PL}}{\theta_{0,i}} = \frac{\theta_{i,j}}{\theta_{0,i}},\ \forall j \in \mathcal{B}\backslash i \tag{4.23}$$

where all BSs have the same grid-tie efficiency θ^{PT} in (4.9).

With this approximation, the system model in Figure 4.2 is transformed into an equivalent system shown in Figure 4.3, where the green energy hub collects all the

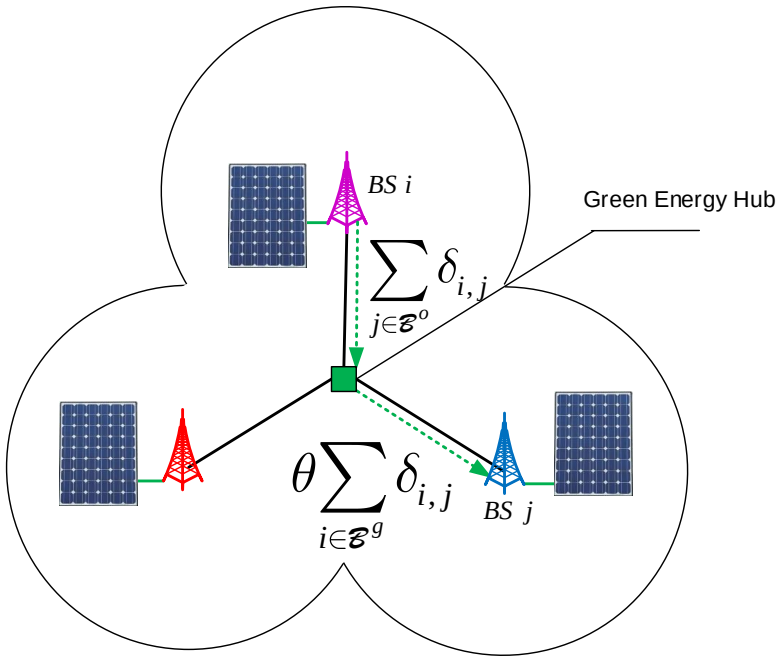

Figure 4.3 Inter-BS green energy flow with the green energy hub.

power supplements from BSs, and distribute the green energy to other BSs in need of energy.

The above approximation analysis allows BPO problem in (4.16) to be decomposed into the following two consecutive steps.

Step I: With (4.23), the objective function in (4.16) becomes

$$\sum_{i\in\mathcal{B}^o}\frac{P_i-E_i}{\theta_{0,i}}-\theta\sum_{i\in\mathcal{B}^o}\sum_{j\in\mathcal{B}^g}\delta_{j,i}$$

Consequently, instead of identifying the energy flows among all BS pairs, the following naive power supplement scheme will minimize the total on-grid power consumption.

1) BS i, $i\in\mathcal{B}^g$, will simply forward all the remaining energy, E_i-P_i, to the green energy hub. 2) BS i, $i\in\mathcal{B}^o$, will draw at most $(P_i-E_i)/(\theta_{0,i}\theta)$ amount of energy from the green energy hub.

With the above power supplement scheme, the BPO problem is expressed as the following weighted user-BS association (WUA) problem.

$$\min_{(\boldsymbol{\rho},\mathcal{B}^o,\mathcal{B}^g)} \sum_{i\in\mathcal{B}^o} \frac{P_i-E_i}{\theta_{0,i}} - \sum_{i\in\mathcal{B}^g} \theta(E_i-P_i) \tag{4.24}$$

$$s.t. \qquad (4.17), (4.18), (4.19)$$

$$E_i \geq P_i, i \in \mathcal{B}^g \tag{4.25}$$

$$P_i \geq E_i, i \in \mathcal{B}^o \tag{4.26}$$

where $\sum_{i\in\mathcal{B}^g} E_i - P_i$ is the total amount of power that BSs send to the green energy hub.

Note that in the objective function of (4.24), there will be no on-grid brown energy consumption when $\sum_{i\in\mathcal{B}^g} E_i - P_i \geq \sum_{i\in\mathcal{B}^o}(P_i - E_i)/\theta_{0,i}$. However, the corresponding $\{\boldsymbol{\rho}, \mathcal{B}^o, \mathcal{B}^g\}$ will still be optimal.

Step II: The on-grid power consumption in (4.16) is further reduced by lifting the assumption of (4.23). With the traffic load $\boldsymbol{\rho}$ and the power consumption P_i returned by (4.24), the BS energy sharing (BES) problem is designed to obtain the energy flows among all BS pairs.

$$\min_{\boldsymbol{\delta}} \sum_{i\in\mathcal{B}^o} \frac{P_i-E_i}{\theta_{0,i}} - \sum_{i\in\mathcal{B}^o}\sum_{j\in\mathcal{B}^g} \frac{\theta_{j,i}\delta_{j,i}}{\theta_{0,i}} \tag{4.27}$$

$$s.t. \qquad (4.20), (4.21)$$

The decomposition reduces the complexity of solving the BPO problem because in each step, only a subset of the variables needs to be optimized. Moreover, it increases the flexibility of the proposed wireless communications system to be accommodated by the smart grid.

For example, when BSs deposit and withdraw credits from the green energy hub in Figure 4.3, the credit is of common value to each BS. If smart grid schedules the locally available on-grid energy to the BSs that withdraw the credit, the second step is not needed. On the other hand, when the wired green energy transfer is scheduled

by smart grid between the BS pairs, the on-grid power consumption of the network can be optimized by solving the problems in Step I and Step II sequentially.

4.3 An Approximate Solution

In this section, heuristic algorithms are proposed to solve the WUA problem and BES problem.

4.3.1 Wired and Wireless Energy Transfer

For the mixed integer programming problem in Equation (4.24), instead of iterating all possible $\mathcal{B}^o$ and $\mathcal{B}^g$, we note that in order to reduce the on-grid brown power consumption of BSs in $\mathcal{B}^o$, the design of the optimal traffic load $\boldsymbol{\rho}$ has to reflect the following two schemes.

First, the *green energy supplement scheme* will try to decrease ρ_i, $i \in \mathcal{B}^g$, so that more leftover green power, i.e., $E_i - P_i$, will be transferred to BSs in $\mathcal{B}^o$. The wired energy transfer directly balances the available green energy of each BS. On the other hand, the *traffic offloading scheme* will try to increase ρ_i, $i \in \mathcal{B}^g$. It allows BSs with more green energy to serve more mobile users, and reduces the traffic load of BSs in $\mathcal{B}^o$.

Since we assume power supplement and traffic offloading are both feasible in area $\mathcal{A}$, how BSs choose the optimal traffic load and minimize the on-grid brown energy consumption depends on the energy loss factor of both methods. As compared with the wired energy transfer efficiency defined for power supplement in (4.9), the energy loss associated with traffic offloading is owing to the wireless channel gain.

As shown in Figure 4.4, with maximum SINR association scheme $\widetilde{\boldsymbol{\eta}}(x)$, UE located at x is in the coverage of BS i^*, i.e., the channel gain in Equation (4.2) is $g_{i^*}(x) = \max_{i \in \mathcal{B}} g_i(x)$. Suppose with the traffic offloading scheme, UE x is offloaded to BS i. With $g_i(x) < g_{i^*}(x)$, to serve the same traffic demand of UE x, BS i will spend more power than BS i^*. The additional power consumption can be recognized

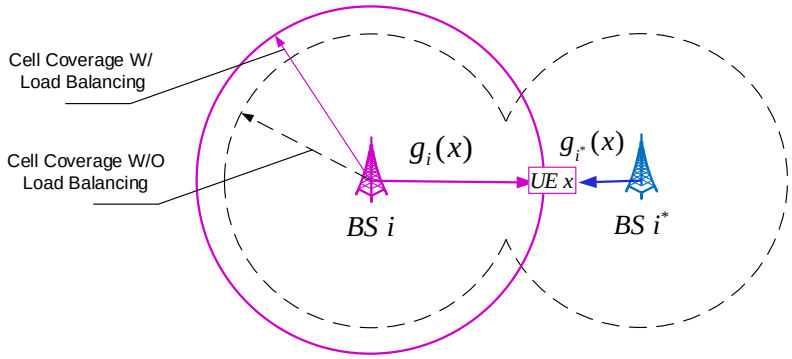

Figure 4.4 Wireless energy transfer of traffic offloading.

as the power loss caused by traffic offloading. Hence, in a way, traffic offloading can be considered as wireless transfer of energy from BS i to BS i^*, and BS i^* will use the received energy to serve the offloaded users. The "wireless energy transfer efficiency" defined for traffic offloading is also less than 1.

As shown in Figure 4.5, the wireless energy transfer efficiency will increase with traffic load $\rho_{i^*} < \widetilde{\rho}_{i^*}$. In particular, with $\rho^1_{i^*} > \rho^2_{i^*}$, we have $g_{i^*}(x_1)/g_i(x_1) < g_{i^*}(x_2)/g_i(x_2)$. Thus, offloading UE at x_2 will cost more energy than offloading UE at x_1.

4.3.2 Analysis of the WUA Problem

By comparing the wireless energy transfer efficiency incurred by traffic offloading and the wired energy transfer efficiency via smart grid, we propose to find the traffic load ρ in (4.24) by sequentially optimizing the traffic offloading scheme and the green energy sharing scheme. First, when the wireless energy transfer efficiency is greater than the wired energy transfer efficiency, a BS's surplus green energy should be utilized to serve more user traffic. When the neighbors' nearby traffic is absorbed, the wireless energy transfer efficiency will be lower, and a BS's surplus green energy should be shared with other BSs via the smart grid.

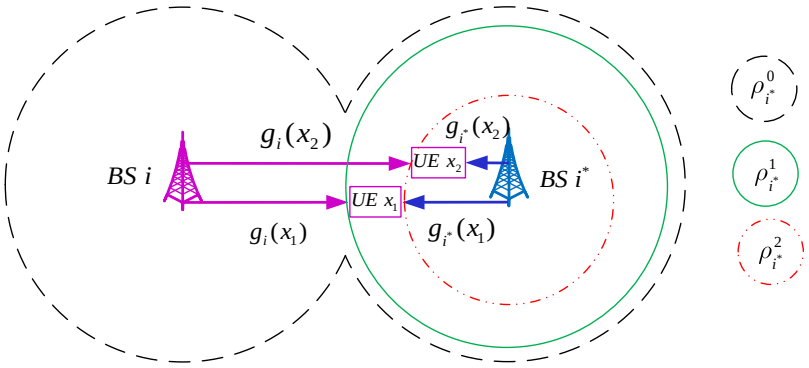

Figure 4.5 Wireless energy transfer efficiency vs. ρ_{i^*}.

The decoupling between wired and wireless energy transfer requires traffic load of each BS to be greater than a certain value, such that the energy loss caused by offloading ($g_i(x) < g_{i^*}(x)$) is less than directly transferring energy from BS i to BS i^*.

$$\boldsymbol{\rho} \geq \widetilde{\boldsymbol{\omega}}\widetilde{\boldsymbol{\rho}} \tag{4.28}$$

where $\widetilde{\boldsymbol{\omega}} = (\widetilde{\omega}_1, \cdots, \widetilde{\omega}_N) \leq \mathbf{1}$ is the threshold set for the wireless energy efficiency in terms of traffic load, and $\widetilde{\boldsymbol{\rho}}$ is the unbalanced traffic load, i.e., the traffic load of each BS when users are connected to BSs according to the maximum SINR association scheme $\widetilde{\boldsymbol{\eta}}(x)$.

The corresponding weighted user-BS association problem in (4.24) can be expressed as

$$\begin{aligned} &\min_{(\boldsymbol{\rho}, \mathcal{B}^o, \mathcal{B}^g)} \sum_{i \in \mathcal{B}^o} \frac{P_i - E_i}{\theta_{0,i}} \\ &s.t. \quad (4.17), (4.18), (4.19), (4.25), (4.26), (4.28) \end{aligned} \tag{4.29}$$

Lemma 10. *The optimal traffic load $\boldsymbol{\rho}$ and the corresponding $\mathcal{B}^o$ and $\mathcal{B}^g$ for (4.29) must be the optimal solution to the WUA problem in (4.24).*

The proof of Lemma 10 is given in Appendix A.6. The lower bound of ρ_i in (4.28) can be realized by setting a constraint on a user's minimum data rate at

location x.

$$r(\boldsymbol{\eta}, x) \geq \omega \widetilde{r}(x), x \in \mathcal{A} \tag{4.30}$$

where $r(\boldsymbol{\eta}, x)$ is the data rate of a user located at x with user association scheme $\boldsymbol{\eta}$, and $\widetilde{r}(x) = \max \sum_{i \in \mathcal{B}} r_i(x)$ is denoted as the data rate of UE at x with the maximum SINR association scheme. $0 < \omega < 1$ is a linear coefficient that constrains the minimum data rate of a user at location x. By changing ω, we can limit the wireless energy transfer efficiency to be larger than θ.

Note that (4.30) is consistent with the design of prevailing wireless access systems. In LTE systems, for example, to ensure the energy efficiency of base station and mobile devices, downlink sensitivity and uplink sensitivity are set such that a mobile user can only associate with the BSs to which the user's pathloss is smaller than the predefined thresholds [93].

4.3.3 Solving the WUA Problem

In this section, we present the energy loss and latency aware (ELLA) user association scheme that solves the WUA problem in (4.29). First, the constraints (4.18), (4.19), (4.25), and (4.26) in (4.29) can be converted back to the positive function in the objective function as follows.

$$\begin{aligned} &\min_{\boldsymbol{\rho}} \sum_{i \in \mathcal{B}} \frac{\{P_i - E_i\}^+}{\theta_{0,i}} \\ &s.t. \quad (4.17), (4.28) \end{aligned} \tag{4.31}$$

In the ELLA scheme, we approximate $\{P_i - E_i\}^+ / \theta_{0,i}$ as $\log(e^{(P_i - E_i)/\theta_{0,i}} + 1)$, and approximately reformulate the WUA problem using the logarithmic barrier function [94]. Then, the approximate WUA (AWUA) problem is

$$\begin{aligned} &\min F(\boldsymbol{\rho}) \\ &s.t. \quad (4.28) \end{aligned} \tag{4.32}$$

where $F(\boldsymbol{\rho})$ is the redefined objective function.

$$F(\boldsymbol{\rho}) = \sum_{i \in \mathcal{B}} \log(e^{\frac{P_i - E_i}{\theta_{0,i}}} + 1) - \frac{1}{t} \sum_{i \in \mathcal{B}} \log(\frac{\tau^*}{\tau^* + 1} - \rho_i) \tag{4.33}$$

where $t > 0$ is a parameter that sets the accuracy of the approximation. The quality of the approximation increases as t grows.

Lemma 11. *With $\rho_i \in [\widetilde{\omega}_i \widetilde{\rho}_i, \frac{\tau^*}{\tau^*+1}]$, $i \in \mathcal{B}$, $F(\boldsymbol{\rho})$ is a convex function of $\boldsymbol{\rho}$.*

The convexity of $F(\boldsymbol{\rho})$ can be proved by showing $\bigtriangledown^2 F(\boldsymbol{\rho}) > 0$. To solve (4.32), the sub-gradient algorithm is adopted, in which the objective function $F(\boldsymbol{\rho})$ will decrease as the traffic load $\boldsymbol{\rho}$ iterates in the ***descent direction*** $\hat{\boldsymbol{\rho}}(k) - \boldsymbol{\rho}(k)$.

$$\boldsymbol{\rho}(k+1) = \boldsymbol{\rho}(k) + \xi_k(\hat{\boldsymbol{\rho}}(k) - \boldsymbol{\rho}(k)) \tag{4.34}$$

where $\boldsymbol{\rho}(k) = (\rho_1(k), \rho_2(k), \cdots, \rho_N(k))$ is the advertised traffic load at the k-th iteration, and $\hat{\boldsymbol{\rho}}(k) = (\hat{\rho}_1(k), \hat{\rho}_2(k), \cdots, \hat{\rho}_N(k))$ is the instantaneous traffic load at the k-th iteration. Moreover, $0 < \xi_k < 1$ is the step size calculated by BS via backtracking line search [94], such that

$$F(\boldsymbol{\rho}(k+1)) \leq F(\boldsymbol{\rho}(k)) + \xi_k \zeta \langle \bigtriangledown F(\boldsymbol{\rho})|_{\boldsymbol{\rho}=\boldsymbol{\rho}(k)}, \hat{\boldsymbol{\rho}}(k) - \boldsymbol{\rho}(k) \rangle \tag{4.35}$$

where $0 < \zeta < 0.5$ is a constant, $\langle , \rangle$ denotes the inner product, and the gradient of the convex function $F(\boldsymbol{\rho})$ at $\boldsymbol{\rho}(k)$ is

$$\bigtriangledown F(\boldsymbol{\rho})|_{\boldsymbol{\rho}=\boldsymbol{\rho}(k)} = (\bigtriangledown F(\rho_1(k)), \bigtriangledown F(\rho_2(k)), \cdots, \bigtriangledown F(\rho_N(k)))$$

According to Equation (4.4), traffic load is a function of the binary UE-BS association indicator $\boldsymbol{\eta}(x)$. Define $\hat{\boldsymbol{\eta}}(x)$ as the association indicator for the instantaneous traffic load $\hat{\boldsymbol{\rho}}(k)$:

$$\hat{\boldsymbol{\eta}}(x) = (\hat{\eta}_1(x), \hat{\eta}_2(x), \cdots, \hat{\eta}_N(x)), \ x \in \mathcal{A} \tag{4.36}$$

Lemma 12. *The following binary UE-BS association indicator will provide a descent direction at the k-th iteration.*

$$\hat{\eta}_i(x) = \begin{cases} 1, \ i = \arg\max\limits_{j \in \mathcal{B}} \frac{r_j(x)}{\bigtriangledown F(\rho_j(k))} \\ 0, \ else \end{cases} \tag{4.37}$$

As illustrated in Appendix A.7, (4.37) is derived by finding a search direction which yields a negative inner product with $\bigtriangledown F(\boldsymbol{\rho})|_{\boldsymbol{\rho}=\boldsymbol{\rho}(k)}$. The corresponding ELLA algorithm is given in Alg. 4. The convergence and optimality of the ELLA algorithm are presented in the following theorems, which are proved in Appendices B.1-B.2.

Theorem 1. *There exists a traffic load vector with* $\boldsymbol{\rho}^*(k+1) = \boldsymbol{\rho}^*(k)$.

Theorem 2. *The traffic load vector* $\boldsymbol{\rho}$ *converges to the optimal traffic load vector* $\boldsymbol{\rho}^*$ *that minimizes* $F(\boldsymbol{\rho})$.

4.3.4 Solving the BES Problem

To obtain the optimal energy sharing among BSs, we use the optimal association scheme and corresponding power consumption obtained from the AWUA problem. Since $\sum_{i \in \mathcal{B}^o}(P_i - E_i)/\theta_{0,i}$ in (4.27) is known, the BES problem equals to the following linear programming problem that can be efficiently solved using an optimization software such as CVX [95].

$$\begin{aligned} &\max_{\boldsymbol{\delta}} \sum_{i \in \mathcal{B}^o} \sum_{j \in \mathcal{B}^g} \frac{\theta_{j,i}\delta_{j,i}}{\theta_{0,i}} \\ s.t. \quad &(4.20), (4.21) \end{aligned} \tag{4.41}$$

4.4 Implementation

When jointly designing the BS operation and power distribution, the cooperation between wireless access networks and smart grid is essential. The following sections will introduce how to cooperatively implement both systems to realize the optimal performance.

Algorithm 4: ELLA Algorithm

1 $k = 1$;
2 $\boldsymbol{\rho}(k) = \mathbf{0}$;
3 **while** $\boldsymbol{\rho}(k) \neq \boldsymbol{\rho}(k+1)$ **do**
4 $\quad k = k + 1$;
5 $\quad$ **for** $x \in \mathcal{A}$ **do**
6 $\quad\quad \mathcal{B} = \{1, \cdots, N\}$;
7 $\quad\quad$ Calculate temporary BS for UE located at x;

$$i^* = \arg\max_{i \in \mathcal{B}} \frac{r_i(x)}{\bigtriangledown F(\rho_i(k))}$$

8 $\quad\quad$ **if** $r_{i^*}(x) \geq \omega \widetilde{r}(x)$ **then**
9 $\quad\quad\quad$ Update UE-BS association indication function;

$$\hat{\eta}_i(x) = \begin{cases} 1, \ i = i^* \\ 0, \ else \end{cases}$$

10 $\quad\quad$ **else**
11 $\quad\quad\quad \mathcal{B} = \mathcal{B} \backslash i^*$;
12 $\quad\quad\quad$ Go to Step 7;
13 $\quad$ **for** $i \in \mathcal{B}$ **do**
14 $\quad\quad$ Update instantaneous traffic load $\hat{\rho}_i(k)$;

$$\hat{\rho}_i(k) = \min(\int_{x \in \mathcal{A}} \frac{\lambda(x) s(x) \hat{\eta}_i(x)}{r_i(x)} dx, \frac{\tau^*}{\tau^* + 1} - \epsilon) \tag{4.38}$$

15 $\quad\quad \xi_k = 1$;
16 $\quad\quad$ **while** *(4.35) is not true* **do**
17 $\quad\quad\quad$ Update step size ;

$$\xi_k = \psi \xi_k \tag{4.39}$$

18 $\quad\quad$ Update traffic offload $\rho_i(k+1)$ according to (4.34);

$$\rho_i(k+1) = \rho_i(k) + \xi_k(\hat{\rho}_i(k) - \rho_i(k)) \tag{4.40}$$

19 *Remark 1:* In (4.38), ϵ is an arbitrary small positive constant to guarantee $\rho_i < \frac{\tau^*}{\tau^*+1}$;
20 *Remark 2:* In (4.39), $0 < \psi < 1$ is a real number;

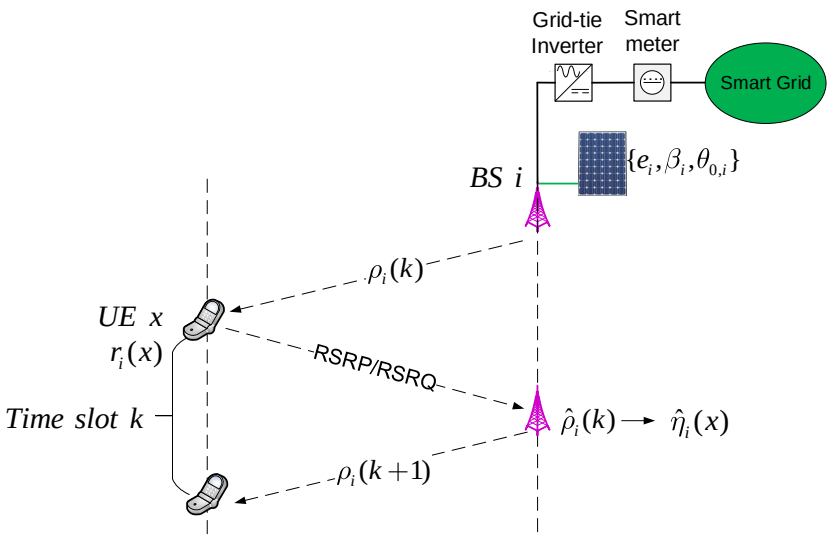

Figure 4.6 Distributed ELLA algorithm.

4.4.1 Wireless Access Network Operation

To provide mobility support, the protocols of the current 3GPP LTE system has addressed mobility management issues such as searching for base station, cell reselection and handover decision parameters based on Reference Signal Received Power/Reference Signal Received Quality (RSRP/RSRQ), service cost, load balancing, and UE speed. For the cell selection and handover procedures, the Radio Resource Control (RRC) protocol mandates that 1) UE measures downlink signal strength and processes the measurement result; 2) UE sends the measurement report to the serving base station; 3) the serving base station makes the cell selection or handover decision based on the received measurement reports [96, 97].

4.4.1.1 Distributive ELLA algorithm To accommodate the user association protocol in the currently deployed wireless access networks, we propose to implement the ELLA scheme in a distributed fashion, which consists of a *user side algorithm* and a *BS side algorithm*.

As shown in Figure 4.6, the user side algorithm measures the instantaneous data rate $r_i(x)$ of the physical downlink shared channel and RSRP/RSRQ of the

reference signals. The BS side measures the current traffic load $\hat{\boldsymbol{\rho}}(k)$. Based on the measurements, the BS side decides $\hat{\boldsymbol{\eta}}(x)$, i.e., selects the optimal BS to minimize the objective function of the AWUA problem, and updates its advertised traffic load $\boldsymbol{\rho}(k+1)$ for the future.

In order to guarantee convergence of the distributed user-BS association scheme, we assume that the time scale of the traffic arrival and departure process is faster relatively to that of BSs in advertising their traffic loads. In other words, BSs broadcast their traffic loads after the system exhibits the stationary performance.

We assume that all the BSs are synchronized and advertise their traffic loads simultaneously, and the time interval between two consecutive traffic load advertisements is defined as a *time slot*. Each time slot accommodates one iteration of the ELLA scheme. Moreover, the green energy generation rate is consistent during the time period of establishing a stable user-BS association.[3]

4.4.2 Smart Grid Operation

The traditional power grid model consists of power generation, transmission, dispatching and consuming links. For the market based power grid, the economic power dispatch model controls "the operation of generation facilities to produce energy at the lowest cost to reliably serve consumers, recognizing any operational limits of generation and transmission facilities" [99]. To integrate distributed harvested renewable energy with the grid, the green power dispatch function is continuously removing priority dispatch for brown energy sources, such as coal. It will be distributed into the emerging microgrids, which are small scale power systems with local generation resources, storage devices and loads [100].

[3]Since the time scale of the traffic arrival and departure process is typically less than several minutes, the user-BS association process is at a time scale of several minutes. The solar power generation is usually modeled at a time scale of a hour. Thus, this assumption is reasonable [98].

In particular, the communications network between the local energy harvester and microgrid controller is capable of exchanging data, and the controller will centrally make power scheduling calculations and manage the power flows in electric grids accordingly. Owing to the significant growth in the on-site renewable energy sources, a less complex distributed energy scheduling scheme has been developed to tap the distributed computing power of energy devices [101].

4.4.2.1 Distributive algorithm for the BES problem Once the traffic load of each BS converges to the optimal $\boldsymbol{\rho}$, BSs in $\mathcal{B}^g$ will forward all the residual green energy $P_i - E_i$ into the grid, and BSs in $\mathcal{B}^o$ will demand $E_i - P_i$ amount of energy. The net energy metering will collect the data and transmit them to the deployed microgrid control center, where the optimal energy routing algorithm $\delta_{i,j}$ is obtained by solving (4.41).

4.5 Simulation Results

Simulations are set up to evaluate the performance of the proposed approximate solution in a mobile network with 12 BSs deployed in a $6km \times 6km$ area. The BS's transmit power is $P_i^t = 20\ W$. The BS's static power consumption is 700 W and $\beta_i = 500,\ i \in \mathcal{B}$ [85]. We adopt COST 231 Walfisch-Ikegami [102] as the propagation model with 9 dB rayleigh fading and 5 dB shadowing fading. The carrier frequency is 2110 MHz, the bandwidth is 5 MHz, the antenna feeder loss is 3 dB, the transmitter gain is 1 dB, the noise power level is -104 dBm, and the receiver sensitivity is -97 dBm. The green energy generation rate is consistent during the simulation.

We compare the proposed algorithm with the green energy aware and latency aware (GALA) scheme [103], which optimizes the user-BS association by considering both the green energy utilization and average traffic delivery latency. The energy-latency coefficient $\theta^* \in [0, 1]$ in GALA balances the weight of the latency and green energy. When θ^* is set as zero, the BS's desired traffic loads are its actual traffic loads

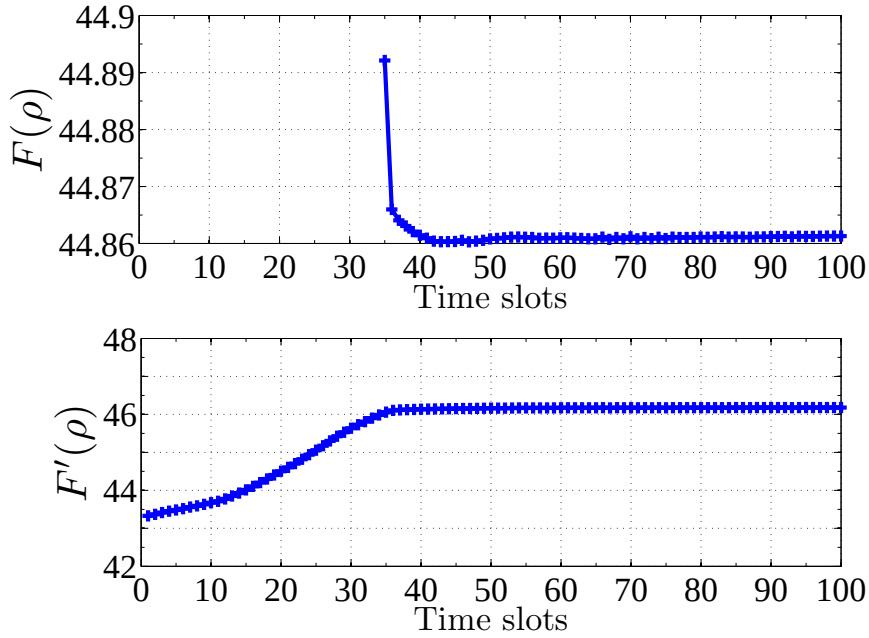

Figure 4.7 ELLA's convergence.

without considering green energy. In this case, we consider the BS being latency-sensitive; otherwise, if θ^* is equal to one, the BS's desired traffic loads are dominated by its green traffic capacity and thus the BS is energy-sensitive. More details of the GALA scheme is referred to [103].

The convergence of the ELLA algorithm is shown in Figure 4.7, where the on-grid brown power consumption part in (4.33) is defined as follows

$$F'(\boldsymbol{\rho}) = \sum_{i \in \mathcal{B}} \log(e^{\frac{P_i - E_i}{\theta_{0,i}}} + 1) \tag{4.42}$$

As we can see, at the beginning of the ELLA algorithm (the first 35 time slots), $F(\boldsymbol{\rho})$ tends to infinity. This is because at the beginning of the ELLA algorithm, traffic demands are directed to the BSs with higher green energy generation rates, and thus these BSs' QoS constraints are violated. Since traffic loads concentrate on the BSs with higher green energy rates, the on-grid power consumption is low. Therefore, $F'(\boldsymbol{\rho})$ is small at the beginning of the ELLA algorithm. As the ELLA algorithm evolves, traffic demands are gradually offloaded from the congested BSs to other BSs

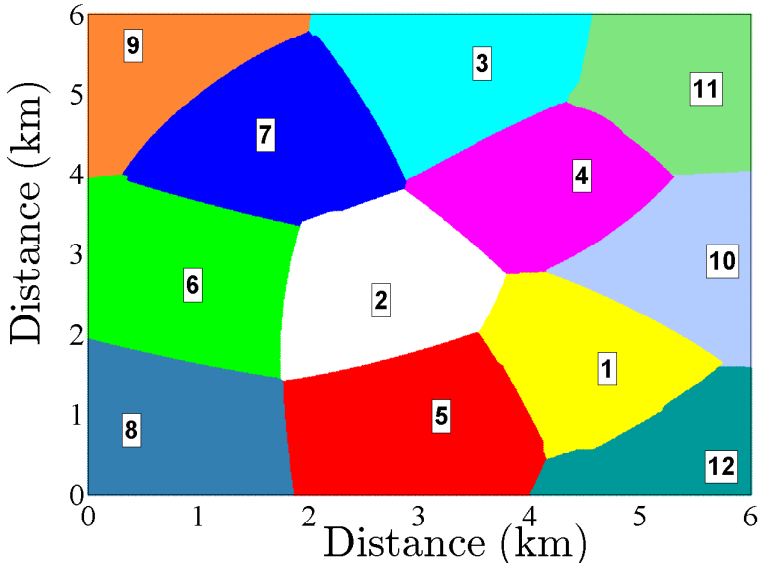

Figure 4.8 Coverage area ($\tau^* = 8$).

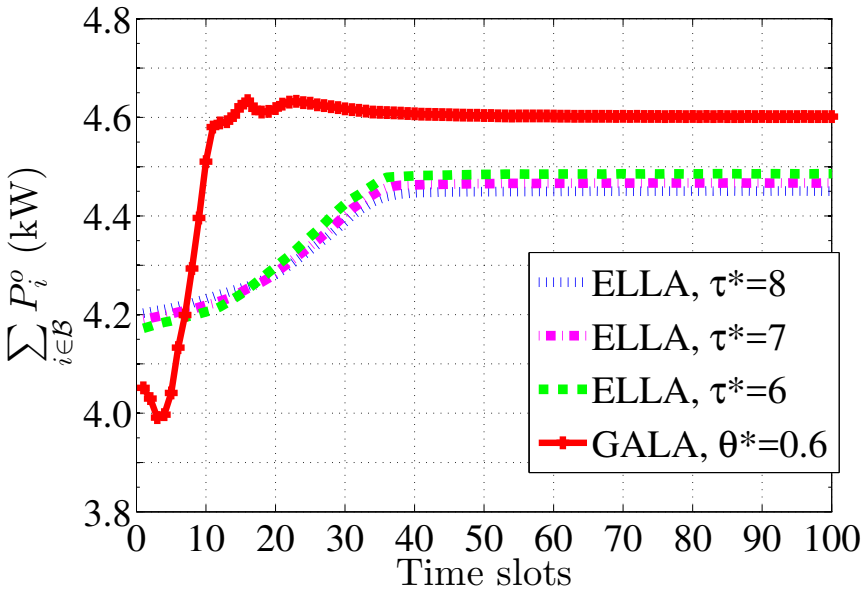

Figure 4.9 On-grid power consumption.

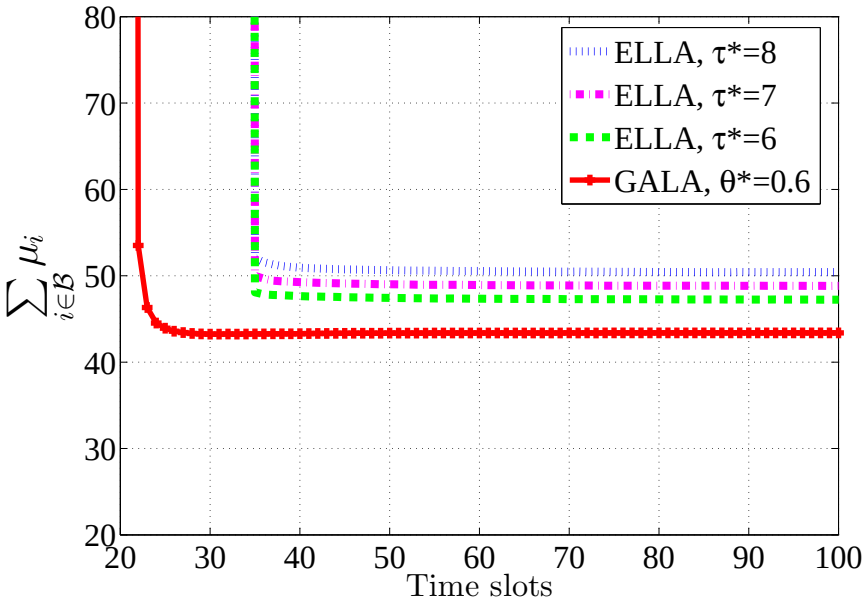

Figure 4.10 Traffic delivery latency.

until the BSs' QoS requirements are satisfied. The ELLA algorithm converges after around 40 time slots.

The coverage area of the ELLA algorithm is shown in Figure 4.8. In associating users with BSs, the ELLA algorithm considers the energy efficiency of traffic offloading, the green energy generation rates, and the wired power transmission efficiency. By considering the wireless energy transfer efficiency of traffic offloading, the maximum coverage area of a BS is constrained. By accommodating the green energy generation rate and the wired power transmission efficiency, more traffic is directed to the BSs with higher green energy generation rate and power transmission efficiency. In this simulation, as compared with its neighboring BSs, the fifth BS has a higher green energy generation rate and power transmission efficiency. Thus, the fifth BS covers a relatively larger area.

Figures 4.9 and 4.10 compare the on-grid power consumption and the traffic delivery latency of the ELLA and GALA algorithms, respectively. As shown in Figure 4.9, as compared with the GALA algorithm, the ELLA algorithm achieves additional on-grid power savings. The amount of power savings reduces as τ^* decreases. When

$\tau^* = 8$, the ELLA algorithm achieves about 150 W power savings as compared with the GALA algorithm. The power saving is not very significant because 1) we constrain the maximum coverage area of each BS to restrict the energy efficiency of traffic offloading being higher than that of sharing energy among BSs; 2) the GALA algorithm is also green energy aware and is designed to optimize the green energy utilization. In Figure 4.10, the traffic delivery latency of the ELLA algorithm is larger than that of the GALA algorithm because the ELLA algorithm aims to minimize the on-grid power consumption with a targeted traffic delivery latency while the GALA algorithm tries to optimize the trade-off between the on-grid power consumption and the traffic delivery latency.

By solving the BES problem, the optimal power sharing among BSs is derived. With the BS energy sharing, the network's on-grid power consumption is further reduced as shown in Table 4.2. As compared with the GALA algorithm which only optimizes the BS operation, the proposed approximate solution to solve the BPO problem saves around 18% on-grid power.

Table 4.2 On-grid Power Consumption of BSs (kw)

GALA	BPO ($\tau^* = 6$)	BPO ($\tau^* = 7$)	BPO ($\tau^* = 8$)
4.6	3.80	3.77	3.76

4.6 Sumamry

In this chapter, we have proposed to jointly optimize the BS operation and power distribution for mobile networks powered by smart grid. The joint **B**S operation and **P**ower distribution **O**ptimization (BPO) problem is difficult to solve because of the highly coupling of the BS operation and the power distribution. We have proposed an approximate solution that solves the BPO problem, which saves about 18% on-grid power as compared with the solutions that only optimize the BS operation.

CHAPTER 5

FUTURE WORK

The performance of wireless mobile edge in terms of energy efficiency can be improved by leveraging the radio resource cooperation in Chapter 2 and the renewable energy sharing discussed in Chapters 3 and 4. In this chapter, we briefly discuss how network cooperation can improve the latency and security performances of wireless communication and networking.

5.1 Communications and Storage Resources Trading

For the cooperative mobile edge, we have made the implicit assumption that each device is willing to cooperate and can be trusted. When this assumption is lifted, the network performance depends on incentive scheme and network security, because the base stations, cloudlets, or even users can be reluctant to share their own resources or they could be dishonest even malicious. In this section, we will discuss the communication and storage trading scheme that motivates the mobile edge cooperation.

5.1.1 Communications Resource Trading

Wired energy trading between BSs can facilitate the radio resource exchange between the grid-connected wireless access nodes [104, 105]. Bayram *et al.* [105] introduced the energy trading framework for smart grid with distributed energy harvesters. By dynamically scheduling the green energy in the smart grid, the energy usage can be balanced among the grid-tied consumers. With high energy efficiency and low carbon output, energy trading is a win-win solution for end users and smart grid, and various pricing schemes have been proposed [106]. Chen *et al.* [107] introduced the energy storage unit attached to the energy consumer, and Wang *et al.* [108] proposed a game

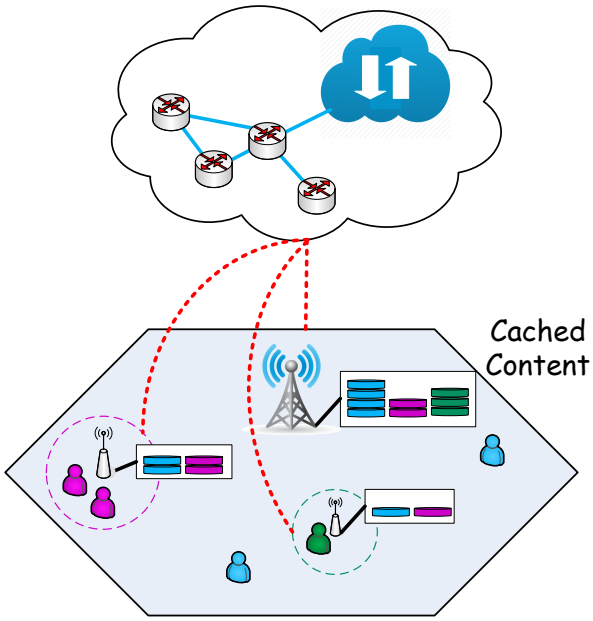

Figure 5.1 Mobile edge with distributed storage resources.

theoretic model to design the dynamic pricing scheme between multiple buyers and sellers.

5.1.2 Storage Resource Sharing

Wireless content distribution is facilitating many emerging applications for smart phone users, such as live streaming and on-demand video streaming [109, 110]. To improve the user experience in terms of delay and battery life, mobile edge computing has been proposed for the next generation network architecture to bridge the end users and contents in the remote cloud [111,112]. The local mobile edge servers equip the wireless access networks with distributed caching memories and computational resources [113,114]. Leveraging the ultra-dense deployment of small cells and advances in device-to-device communications, the mobile edge serving nodes can be adapted from the legacy network nodes, such as mobile users and low power nodes, which are willing to cooperatively transmit files to other end users.

To explore the limited caching capabilities at the serving nodes, *cache placement schemes* have been proposed to study which files should be stored in advance at which serving nodes. Considering the popularity of the file requests, various cache placement schemes have been proposed to maximize the probability of finding the desired file through the local serving nodes instead of going to the second tier cache. In the mobile edge, however, offloading traffic from a macro base station to nearby second/third tier serving nodes is not necessarily a good option. The reason is that the radio resources such as spectrum and power available at each serving node is limited; too many user requests aggregated at one local serving node may cause traffic congestion and deteriorate the quality of service in terms of longer delay, and multiple closely located serving nodes may cause intolerable device to device interference or inter-tier interference.

To further improve the storage and communications resource utilization in serving nodes, *content delivery schemes* have explored the content request overlap, such that the traffic offload within the network is reduced [115]. For each serving node, the naive multicasting of the same file to a group of users can save the radio resources [116]. For a group of serving nodes, the coded caching scheme has been proposed to split the files and produce content overlap at the caches [117].

5.1.3 Incentive Scheme Design

For smart grid powered wireless access networks with distributed data storage and energy harvesters, we propose to study 1) the content delivery scheme by considering both the content exchange and energy sharing among grid-tied base stations, and 2) the dynamic spectrum access system, where the smart grid connected primary base station and secondary system are independently equipped with green energy harvesters. The secondary base station will gain spectrum usage by forwarding primary data or transfer its saved on-grid energy credit to the primary base station.

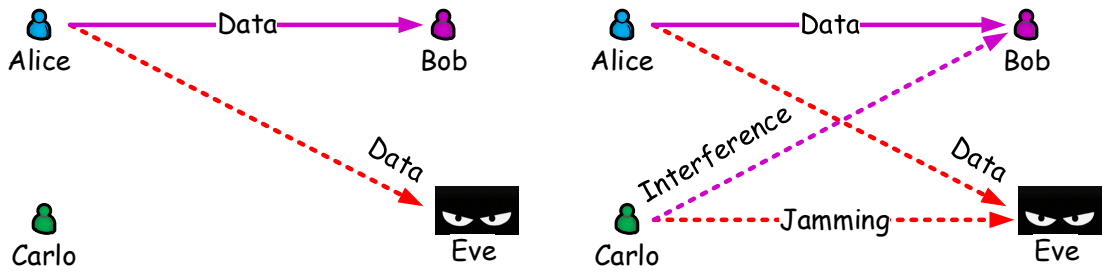

(a) (b)

Figure 5.2 Energy efficiency v.s. data confidentiality.

5.2 Secure Multi-party Communications and Computation

In this section, the uncertainly in terms of untrustworthy is introduced into the system, and security issue will be discussed from two perspectives: data confidentiality and data privacy.

5.2.1 Physical Layer Security

As illustrated in Chapter 2, in terms of energy efficiency, the receiver will simultaneously connect with multiple transmitters only when the radio resource is not sufficient to support the data transmission. However, the single point to point data transmission is vulnerable to passive attacks. For instance, Eve in Figure 5.2a can eavesdrop the data transmission between Alice and Bob. To protect the data confidentiality, current physical layer security schemes explore the dynamics of the wireless channels. As shown in Figure 5.2b, Carlo will be leveraged to transmit signals and jam the data reception of Eve.

However, the energy efficiency of the system will decrease owing to the additional power consumption required by Carlo and extra interference introduced to Bob. Consequently, we propose to leverage the characteristics of radio frequency signals, and better balance energy efficiency and data confidentiality. RF signals can be used to transmit data, cause unwanted interference, and jam the data reception. As

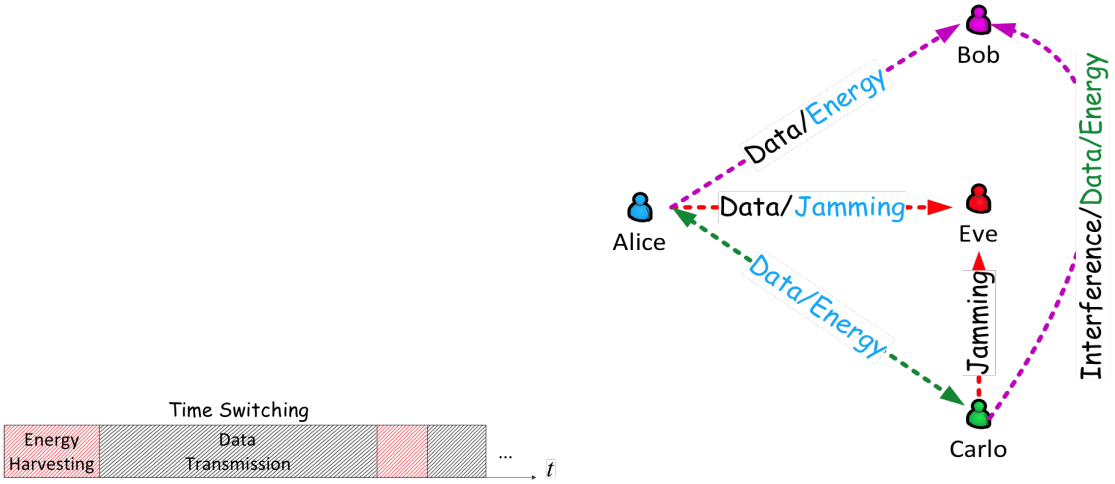

(a) (b)

Figure 5.3 Energy harvesting enabled physical layer security.

discussed in Chapter 3, it can also be used to transmit energy. Consequently, Alice can shift between energy harvesting and data transmission. As long as the time switching pattern in Figure 5.3a is confidential between Alice and Bob, Alice can jam the data reception of Eve by herself, because Eve cannot distinguish between data and energy transfer. Moreover, as illustrated in Figure 5.3b, Carlo can also shift between data and energy to Bob, instead of causing pure interference. Similarly, Alice can harvest energy from Bob.

5.2.2 Multi-party Privacy

With the advancement of internet of things technologies, users are more actively creating their own data and sharing the resources among themselves [118, 119]. It is crucial to investigate a privacy preserving multi-party communications and computation protocol, which synergizes the merits of both the distributively located resources and crowdsourced data. Existing privacy preserving schemes include anonymization, trusted computation, cryptographic computation, verifiable computation, and perturbation. They cannot be applied directly to the IoT system

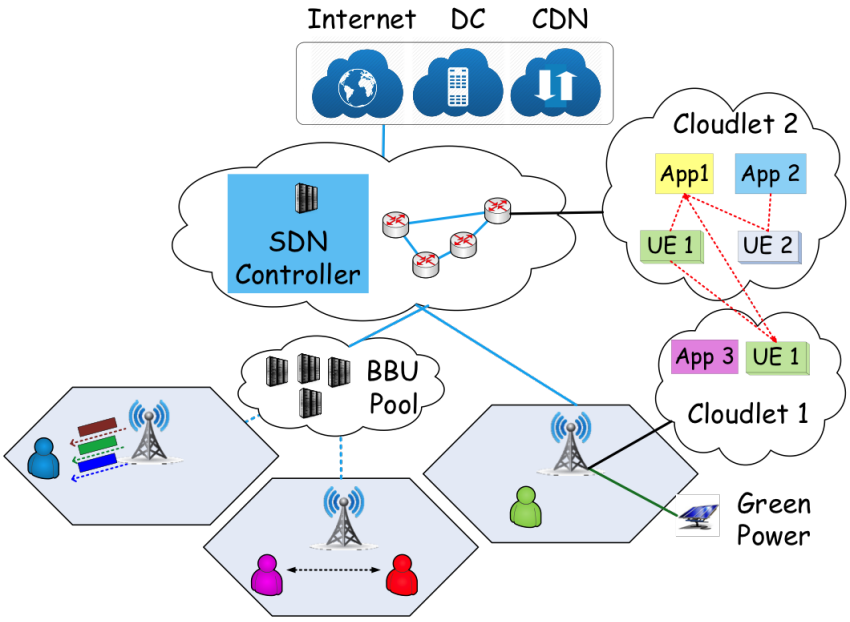

Figure 5.4 Privacy enhanced cooperative framework.

architecture, where the parties involved are often resource limited. As shown in Figure 5.4, each user may own multiple devices and rent multiple virtual machines. Therefore, by grouping the parties with no privacy concern, the system can scale down and there is more room to maneuver the privacy enhancement scheme.

APPENDIX A

PROOFS OF LEMMAS

A.1 Proof of Lemma 1

First, we will prove that Lemma 1 is true for $M = 2$. Then, mathematical induction is used to prove the scenario for $M \geq 3$.

A.1.1 $M = 2$

Since all of the N users need power, either from BS 1, BS 2, or both, then at least N elements of $\mathbf{X}$ are non-zero. To prove Lemma 1, we need to prove that the minimum power consumption can be guaranteed when at most one of the N users is served by two BSs simultaneously.

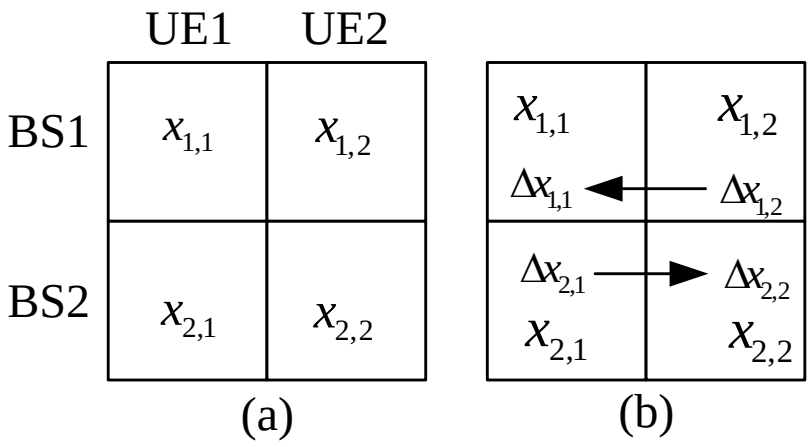

Figure A.1 Power shift in the 2-BS cooperative wireless system.

We use *reductio ad absurdum* here. Suppose in the optimal solution $\{\mathbf{X}, \mathbf{Y}\}$, both UE 1 and UE 2 are powered by BS 1 and BS 2, i.e., $x_{i,j} > 0$, $(i, j = 1, 2)$. Then, any power shift $\Delta x_{i,j} \neq 0$, $(i, j = 1, 2)$ in Figure A.1 (b) will result in higher total

power consumption.

$$\begin{cases} x'_{1,1} = x_{1,1} + \Delta x_{1,1}, x'_{1,2} = x_{1,2} - \Delta x_{1,2} \\ x'_{2,1} = x_{2,1} - \Delta x_{2,1}, x'_{2,2} = x_{2,2} + \Delta x_{2,2} \end{cases}$$

To guarantee the throughput requirement, $\sum_{i=1}^{M} \gamma_{i,j} x_{i,j}$ should remain the same after the power shift, which yields

$$\begin{cases} \gamma_{1,1}\Delta x_{1,1} - \gamma_{2,1}\Delta x_{2,1} = 0 \\ \gamma_{2,2}\Delta x_{2,2} - \gamma_{1,2}\Delta x_{1,2} = 0 \end{cases}$$

If $\gamma_{1,1}\gamma_{2,2} - \gamma_{1,2}\gamma_{2,1} \geq 0$, there always exists a power shift to ensure $\Delta x_{1,2} + \Delta x_{2,1} - \Delta x_{1,1} - \Delta x_{2,2} \geq 0$, where

$$\begin{cases} \Delta x_{2,1} \geq \Delta x_{2,2} \geq 0, \Delta x_{1,1} = \Delta x_{1,2} \geq 0 \\ \Delta x_{1,2} \geq \Delta x_{1,1} \geq 0, \Delta x_{2,1} = \Delta x_{2,2} \geq 0 \end{cases}$$

Similarly, for $\gamma_{1,1}\gamma_{2,2} - \gamma_{1,2}\gamma_{2,1} \leq 0$, the following $\Delta x_{i,j}$ is always feasible such that the total power consumption will decrease after the power shifting.

$$\begin{cases} \Delta x_{2,2} \leq \Delta x_{2,1} \leq 0, \Delta x_{1,1} = \Delta x_{1,2} \leq 0 \\ \Delta x_{1,1} \leq \Delta x_{1,2} \leq 0, \Delta x_{2,1} = \Delta x_{2,2} \leq 0 \end{cases}$$

This contradicts with the assumption.

If there is a set consisting of more than two users powered by BS 1 and 2 simultaneously, we can iteratively group these users into pairs, and do power shifting as in the two-user case. The remaining users that are powered by two BSs form a new user set. Finally, we will get at most one user being served by the two BSs simultaneously.

Note 1: 1) For $\gamma_{1,1}\gamma_{2,2} - \gamma_{1,2}\gamma_{2,1} < 0$, it is always more power efficient if BS 1 schedules more power to UE 2, while UE 1 prefers BS 2; the optimal power allocation must be the case when at least one of $x'_{1,1}$ and $x'_{2,2}$ is zero. 2) For $\gamma_{1,1}\gamma_{2,2} - \gamma_{1,2}\gamma_{2,1} > 0$,

the optimal power allocation must be the case when at least one of $x'_{1,2}$ and $x'_{2,1}$ is zero. 3) For $\gamma_{1,1}\gamma_{2,2} - \gamma_{1,2}\gamma_{2,1} = 0$, if the power keeps shifting until at least one of $x_{i,j}$ $(i, j = 1, 2)$ becomes zero, it can still guarantee the minimum power consumption because power shifting brings no increment in the total power consumption.

A.1.2 $M \geq 3$

Assume Lemma 1 is true for the scenario with $M - 1$ BSs.

For the scenario with M BSs and N UEs, we represent the power allocation solution as an $M \times N$ area, similar to the 3×4 area in Figure A.2 (a).

Suppose there are more than $MN - (M-1)(N-1) = M + N - 1$ non-zero cells in the $M \times N$ area, taking $M + N$ non-zero cells for example. Since each UE, i.e., column, has at least one non-zero cell, then at least $N - M$ UEs will be powered by individual BSs.

Suppose columns $\{M + 1, \cdots, N\}$ of the $M \times N$ area represent UEs that are powered by individual BSs, then there must be $2M$ non-zero cells in the $M \times M$ square formed by the first M columns of the $M \times N$ area (similar to the first 3×3 square in Figure A.2 (b)).

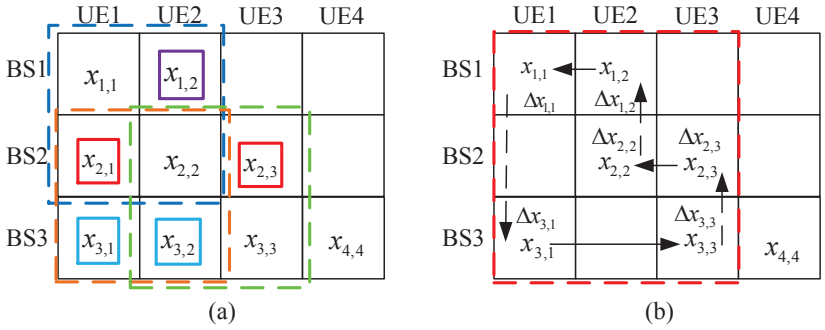

Figure A.2 Power shift in the 3-BS cooperative wireless system.

Denote T_i, $i \in \{1, \cdots, M\}$ as the number of non-zeros elements in the i-th row of the $M \times M$ square. Since $\sum_{i=1}^{M} T_i \leq 2M$ and Lemma 1 is true for $M - 1$ BSs, then

in the $M \times M$ square, we can get

$$2M - T_i \leq (M-1) + (M-1), \forall i \in \{1, \cdots, M\}$$

The above equation implies $T_i = 2, \forall i \in \{1, \cdots, M\}$, i.e., each row has two non-zero cells in the $M \times M$ square. If there are columns that have only one non-zero cell, delete these columns and the corresponding rows where these non-zero cells are located. Finally, an $m \times m$, $(M \geq m \geq 2)$ sub-square which has two non-zero cells in each column and each row must exist. Divide the $2m$ non-zeros cells into two groups, each with m non-zero elements. Within each group, each row is distinct and so is each column.

Taking the 3×3 dotted sub-square in Figure A.2 (b) for example. Group 1 includes $\{x_{1,1}, x_{2,2}, x_{3,3}\}$ and group 2 includes $\{x_{3,1}, x_{1,2}, x_{2,3}\}$. It can be proved that in the optimal solution, the number of non-zero elements in the 3×3 sub-square should be no greater than $2 \times 3 - 1$ [120].

In summary, if the product of $\gamma_{i,j}$ of cells in group 1 is greater than the product of SNR of group 2, then a power shift from group 2 to group 1 that will decrease the total power consumption exists. If the product of group 1 is no more than the group 2's product, then there exists a power shift from group 1 to group 2 that will bring no increment to the total power consumption.

In either case, the power shifting will continue until at least one of the cells becomes zero. So, the number of non-zero cells in the $m \times m$ square will be no more than $2M - 1$. The number of non-zero cells in the $M \times N$ area will be no more than $(2M-1) + (N-M) = M + N - 1$. Accordingly, the number of zeros cells will be greater than $MN - (N + M - 1) = (M-1)(N-1)$.

When there are more than $M + N$ non-zero cells in the $M \times N$ area, we can always iteratively take $M + N$ non-zero cells and do power shifting to make the number of the non-zero cells no more than $M + N - 1$.

A.2 Proof of Lemma 2

We will prove that Lemma 2 is true for the scenarios for $M = 2, 3$. For scenarios with $M > 3$, the same argument can be utilized to arrive at the same conclusion.

A.2.1 $M = 2$, $\boldsymbol{J^{CC}} = [j_{1,2}]$

To prove Lemma 2, we need to show in the optimal clusters J_1 and J_2, when users are sorted in descending order of $\gamma_{1,2}^j$,

$$\max_{j \in J_1}\{j\} < \min_{j \in J_2}\{j\} \tag{A.1}$$

For the initial clusters $J_1^0 = \{1, \cdots, j_0\}$ and $J_2^0 = \{j_0 + 1, \cdots, N\}$, let $j_{1,2} = j_0$.

For the optimal clusters, suppose there are two users $j_1^* \in J_1, j_2^* \in J_2$, and $j_1^* > j_2^*$, as shown in Figure A.3. Since $\gamma_{1,j_1^*}\gamma_{2,j_2^*} - \gamma_{2,j_1^*}\gamma_{1,j_2^*} < 0$, power shifting between the two users will result in only one of the following scenarios (*Note 1*):

Scenario 1: As shown in Figure A.3 (a), $J_1 = J_1^0$, $J_2 = J_2^0$.

Scenario 2: One of the users is powered by two base stations; take j_2^* for example, as shown in Figure A.3 (b). Then, the power shifting between UE j_2^* and j_0 will result in Figure A.3 (c), where $x'_{2,j_2^*}x'_{1,j_0} = 0$.

1) If $x'_{2,j_2^*} = 0$, we will have $J_1 = \{1, \cdots, j_0 - 1\}$, $\{j_0 + 1, \cdots, N\} \subset J_2$.

2) If $x'_{2,j_2^*} > 0$, $x'_{1,j_0} = 0$, then UE j_2^* will continue to do power shifting with UE $\{j_0 - 1, j_0 - 2, \cdots, j_2^* + 1\}$ until either $x'_{2,j_2^*} = 0$ or $J_2 = \{j_2^* + 1, \cdots, N\}$. In either case, for any $j_1 \in J_1$ and $j_2 \in J_2$, there will be $j_1 < j_2$.

Furthermore, at least $N-1$ UEs will belong to J_1 or J_2 (Lemma 1), if $J_1 \bigcup J_2 = \{1, \cdots, N\}$, $j_{1,2} = \max_{j \in J_1}\{j\}$. If UE j^* is powered by both BS 1 and BS 2 simultaneously, $j_{1,2} = j^*$.

A.2.2 $M = 3$, $\boldsymbol{J^{CC}} = [j_{1,2}, j_{1,3}, j_{2,3}]$

The UE-BS association scheme in the optimal solution must fall in one of the categories in Figure A.4, where a solid arrow represents power coordination (providing power

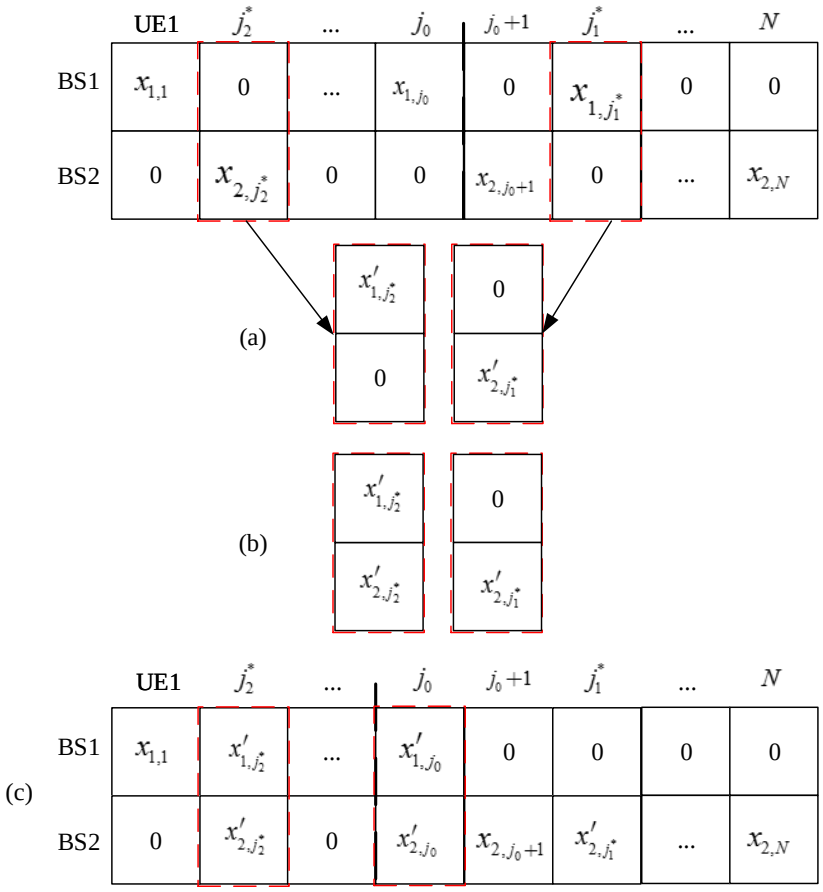

Figure A.3 UE-BS association in the 2-BS cooperative wireless system.

for other BS's UE), and a dashed line means spectrum coordination only (increasing the transmission power of its own UE to spare more spectrum for other BSs). For each category, we can find the corresponding $\boldsymbol{J^{CC}}$ which satisfies Lemma 2. Readers are referred to [120] for details.

A.3 Proof of Lemma 3

If $S_1 = S_2$, then they must be the optimal solution because relaxing the constraints by limiting the transmit power of only one BS brings no benefits to the total power consumption.

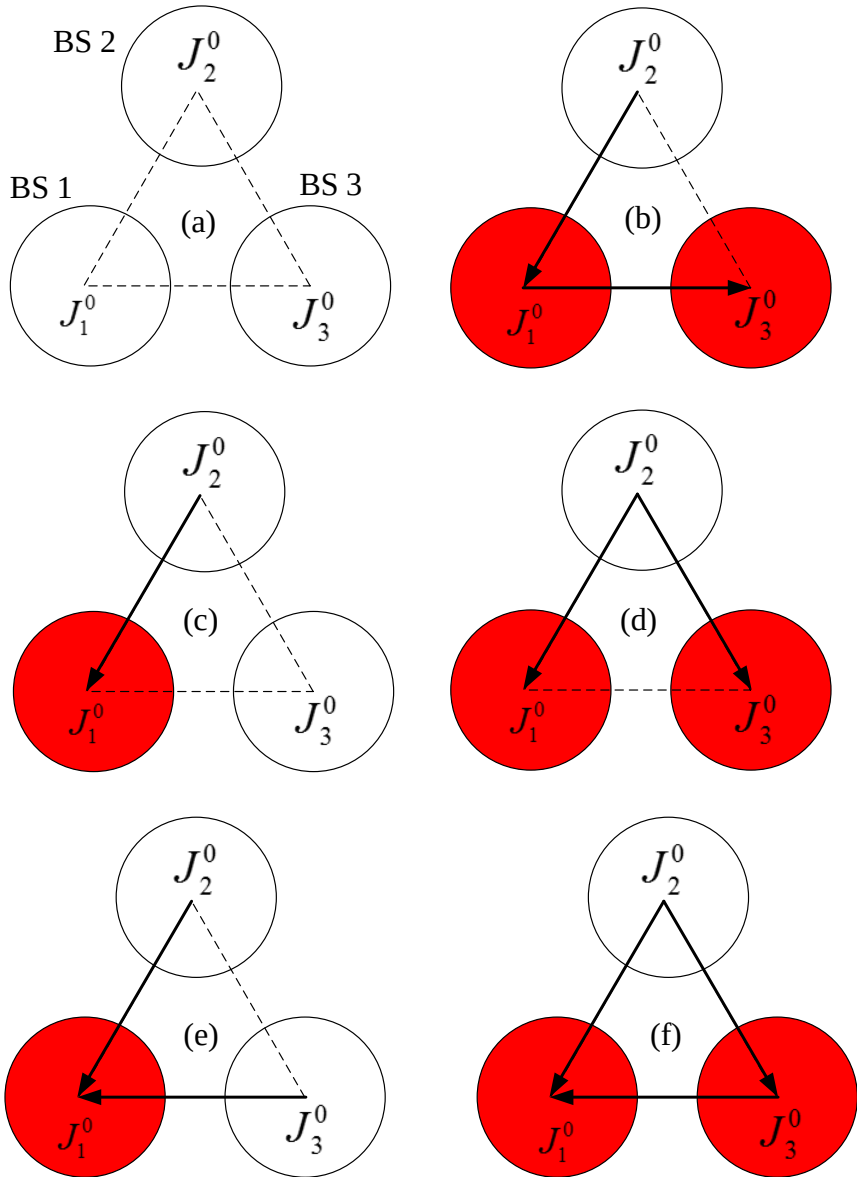

Figure A.4 Spectrum and power coordination in the 3-BS cooperative wireless system (red BS means power consumption is 1).

Then, we only prove part 2) with $S_1 > (1, 1)$, as part 3) can be similarly proved. Suppose in the CC vector $\boldsymbol{J^{CC}}$ which corresponds to the optimal solution $\{x^*_{i,j}\}$, we have $j_{1,2} < j'_1$, then the optimal cluster $J^*_1 \subseteq \{1, \cdots, j'_1 - 2\} \subset J^0_1$.

1) For the optimal solution $\{x^*_{i,j}\}$, we can find the corresponding mapping $\{x'_{i,j}\}$ by relaxing the constraint of BS 1 as follows:

$$\begin{cases} x'_{1,j} = x^*_{1,j} + \gamma^j_{2,1} x^*_{2,j}, & x'_{2,j} = 0, \qquad j \in J^0_1 \backslash J^*_1 \\ x'_{1,j} = x^*_{1,j}, & x'_{2,j} = x^*_{2,j}, \quad j \in J^*_1 \bigcup J^0_2 \end{cases} \tag{A.2}$$

Since $\{x_{i,j}\}$ in S_1 is the optimal relaxed solution, $\{x'_{i,j}\}$ must fall into the shadowed region of Figure A.5,

$$\sum_{j \in J^0_1} x'_{1,j} + \sum_{j \in J^0_2} x'_{2,j} > \sum_{j \in J^0_1} x_{1,j} + \sum_{j \in J^0_2} x_{2,j} \tag{A.3}$$

Based on (A.3), we have the following result

$$\sum_{j=1}^{j'_1 - 1} \left(x'_{1,j} - x_{1,j} \right) > \sum_{j=j'_1}^{j_0} \left(x_{1,j} - x'_{1,j} \right) + \sum_{j \in J^0_2} \left(x_{2,j} - x'_{2,j} \right) \tag{A.4}$$

2) For $\{x_{i,j}\}$, the relaxed solution in S_1, we can find the corresponding mapping $\{x^{*'}_{i,j}\}$ by considering the power constraint of BS 1. The power allocation with power constraints for each BS becomes

$$\begin{cases} x^{*'}_{1,j} = x_{1,j},\ x^{*'}_{2,j} = 0,\ j \in \{1, \cdots, j'_1 - 1\} \\ x^{*'}_{1,j} = \beta x_{1,j},\ x^{*'}_{2,j} = \gamma^j_{1,2}(1-\beta) x_{1,j},\ j = j'_1 \\ x^{*'}_{1,j} = 0,\ x^{*'}_{2,j} = \gamma^j_{1,2} x_{1,j},\ j \in \{j'_1 + 1, \cdots, j_0\} \\ x^{*'}_{1,j} = 0,\ x^{*'}_{2,j} = x_{2,j},\ j \in J^0_2 \end{cases} \tag{A.5}$$

where $\beta = (1 - \sum_{j=1}^{j'_1 - 1} x_{1,j}) / x_{1,j'_1}$. From (A.2) and (A.5), we have

$$\begin{cases} \sum_{i=1}^{2} \sum_{j=1}^{j'_1 - 1} \left(x^*_{i,j} - x'^*_{i,j} \right) \geq \left(\sum_{j=1}^{j'_1 - 1} x^*_{1,j} + (\sum_{j=1}^{j'_1 - 1} x'_{1,j} - \sum_{j=1}^{j'_1 - 1} x^*_{1,j}) \gamma^{j'-1}_{1,2} \right) - \sum_{j=1}^{j'_1 - 1} x_{1,j} \\ \sum_{i=1}^{2} \sum_{j=j'_1}^{N} \left(x'^*_{i,j} - x^*_{i,j} \right) = \left((1 - \gamma^{j'_1}_{1,2}) \beta x_{1,j'_1} + \sum_{j=j'_1}^{j_0} \gamma^j_{1,2} x_{1,j} + \sum_{j \in J^0_2} x_{2,j} \right) - \\ \qquad \left(\sum_{j=j'_1}^{j_0} \gamma^j_{1,2} x'_{1,j} + \sum_{j \in J^0_2} x'_{2,j} \right) \end{cases} \tag{A.6}$$

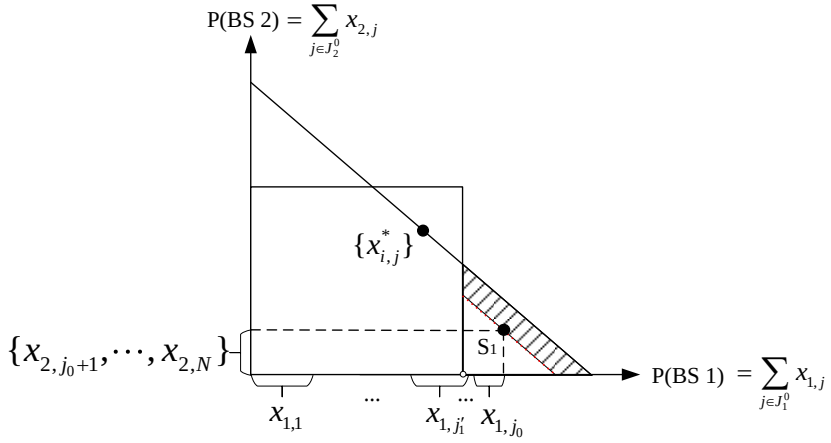

Figure A.5 Solution mapping, slop=1.

Substituting $\sum_{j=1}^{j_1'-1} x^*_{1,j} = 1 = \sum_{j=1}^{j_1'-1} x_{1,j} + \beta x_{1,j_1'}$ into (A.6), we can see

$$\begin{cases} \sum_{i=1}^{2}\sum_{j=1}^{j_1'-1}\left(x^*_{i,j} - x'^*_{i,j}\right) \geq \beta x_{1,j_1'} + \left(\sum_{j=1}^{j_1'-1}\left(x'_{1,j} - x_{1,j}\right) - \beta x_{1,j_1'}\right)\gamma_{1,2}^{j_1'-1} \\ \sum_{i=1}^{2}\sum_{j=j_1'}^{N}\left(x'^*_{i,j} - x^*_{i,j}\right) \leq \beta x_{1,j_1'} + \left(\sum_{j=j_1'}^{j_0}\left(x_{1,j} - x'_{1,j}\right) - \beta x_{1,j_1'}\right)\gamma_{1,2}^{j_1'} + \sum_{j\in J_2^0}\left(x_{2,j} - x'_{2,j}\right) \end{cases} \tag{A.7}$$

According to the sorting rule of UE, $\gamma_{1,2}^{j_1'-1} \geq \gamma_{1,2}^{j_1'}$. From (A.4) and (A.7), we have

$$\sum_{i=1}^{2}\sum_{j=1}^{j_1'-1}\left(x^*_{i,j} - x'^*_{1,j}\right) \geq \sum_{i=1}^{2}\sum_{j=j_1'}^{N}\left(x'^*_{1,j} - x^*_{i,j}\right)$$

Consequently, the following result, which contradicts with the assumption that $\{x^*_{i,j}\}$ is the optimal solution, can be obtained.

$$\sum_{i=1}^{2}\sum_{j=1}^{N} x^*_{i,j} \geq \sum_{i=1}^{2}\sum_{j=1}^{N} x'^*_{i,j}$$

A.4 Proof of Lemma 8

The lemma can be proved by contradiction. Suppose for a given power consumption profile of each BS, i.e., P_i, $i \in \mathcal{B}$, BS i_1 will have to draw brown power from the grid, and then transmit it to other BSs. BS i_2 is one of the power supplement recipients

from BS i_1.

$$\delta_{i_1,i_2} + \sum\nolimits_{j\in\mathcal{B}\setminus i_2} \delta_{i_1,j} > E_{i_1} + \sum\nolimits_{j\in\mathcal{B}\setminus i_2} \delta_{j,i_1}\theta_{j,i_1} + \delta_{i_2,i_1}\theta_{i_2,i_1}$$

where $\delta_{i_2,i_1} = 0$.

Then, the corresponding on-grid power consumption of BSs i_1 and i_2 are given in (A.4).

$$P^o_{i_1} = \frac{P_{i_1}+\delta_{i_1,i_2}-(E_{i_1}+\sum_{j\in\mathcal{B}\setminus i_2}\delta_{j,i_1}\theta_{j,i_1}-\sum_{j\in\mathcal{B}\setminus i_2}\delta_{i_1,j})}{\theta_{0,i_1}}$$
$$P^o_{i_2} = \frac{\{P_{i_2}-\delta_{i_1,i_2}\theta_{i_1,i_2}-(E_{i_2}+\sum_{j\in\mathcal{B}\setminus i_1}\delta_{j,i_2}\theta_{j,i_2}-\sum_{j\in\mathcal{B}\setminus i_1}\delta_{i_2,j})\}^+}{\theta_{0,i_2}}$$

Next, we decrease $\delta_{i_1,i}$ by $\Delta\delta_{i_1,i}$. The corresponding power consumption of the two BSs are updated as follows.

$$P^{o'}_{i_1} + P^{o'}_{i_2} \leq P^o_{i_1} - \frac{\Delta\delta_{i_1,i_2}}{\theta_{0,i_1}} + P^o_{i_2} + \frac{\Delta\delta_{i_1,i_2}\theta_{i_1,i_2}}{\theta_{0,i_2}} \tag{A.8}$$

Since in (4.10), we have assumed the brown power flow within the smart grid should be optimal in terms of the power transmission efficiency, $\theta_{0,i_1}\theta_{i_1,i_2} < \theta_{0,i_2}$, we can conclude that reducing δ_{i_1,i_2} will yield less $P^{o'}_{i_1} + P^{o'}_{i_2}$.

This contradicts with the assumption and hence it is not optimal for BS i_1 to draw brown power from the grid and then transmit it to BS i_2.

Consequently, there is no reason for any base station to provide brown energy supplement to other BSs.

A.5 Proof of Lemma 9

Lemma 2 can be proved using the technique similar to proving Lemma 1. Suppose BS i will first withdraw green energy from BS i_1, and then transmit it to BS i_2, as shown in Figure A.6. The corresponding power consumption of those three BSs are given in (A.5).

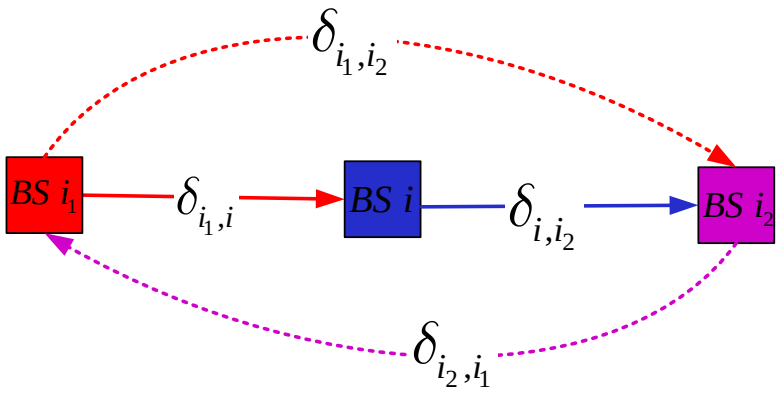

Figure A.6 Power supplements among BSs.

$$P_{i_1}^o = \frac{\{P_{i_1}+\delta_{i_1,i}+\delta_{i_1,i_2}-\delta_{i_2,i_1}\theta_{i_2,i_1}-(E_{i_1}+\sum_{j\in\mathcal{B}\setminus\{i,i_2\}}\delta_{j,i_1}\theta_{j,i_1}-\sum_{j\in\mathcal{B}\setminus\{i,i_2\}}\delta_{i_1,j})\}^+}{\theta_{0,i_1}}$$
$$P_{i}^o = \frac{\{P_{i}+\delta_{i,i_2}-\delta_{i_1,i}\theta_{i_1,i}-(E_{i}+\sum_{j\in\mathcal{B}\setminus\{i_1,i_2\}}\delta_{j,i}\theta_{j,i}-\sum_{j\in\mathcal{B}\setminus\{i_1,i_2\}}\delta_{i,j})\}^+}{\theta_{0,i}}$$
$$P_{i_2}^o = \frac{\{P_{i_2}+\delta_{i_2,i_1}-\delta_{i_1,i_2}\theta_{i_1,i_2}-\delta_{i,i_2}\theta_{i,i_2}-(E_{i_2}+\sum_{j\in\mathcal{B}\setminus\{i,i_1\}}\delta_{j,i_2}\theta_{j,i_2}-\sum_{j\in\mathcal{B}\setminus\{i,i_1\}}\delta_{i_2,j})\}^+}{\theta_{0,i_2}}$$

Next, we design two power shift schemes for the two cases.

Case I: $\delta_{i_2,i_1}=0$. We decrease $\delta_{i_1,i}$ by $\Delta\delta_{i_1,i}$. To keep the power consumption of BSs i_1 and i, the following power shift can be obtained.

$$\begin{cases} \delta'_{i_1,i}=\delta_{i_1,i}-\Delta\delta_{i_1,i},\ \delta'_{i_1,i_2}=\delta_{i_1,i_2}+\Delta\delta_{i_1,i} \\ \delta'_{i_1,i}=\delta_{i_1,i}-\Delta\delta_{i_1,i},\ \delta'_{i,i_2}=\delta_{i,i_2}-\Delta\delta_{i_1,i}\theta_{i_1,i} \end{cases} \tag{A.9}$$

Then, the corresponding power consumption of BS i_2 is updated as follows.

$$P_{i_2}^{o'} = P_{i_2}^o + \frac{-\Delta\delta_{i_1,i}\theta_{i_1,i_2}+\Delta\delta_{i_1,i}\theta_{i_1,i}\theta_{i,i_2}}{\theta_{0,i_2}}$$

According to (4.10), $\theta_{i_1,i_2} > \theta_{i_1,i}\theta_{i,i_2}$. So, $P_{i_2}^{o'} \le P_{i_2}^o$. This contradicts with the assumption.

Case II: $\delta_{i_1,i_2}=0$. We decrease $\delta_{i_1,i}$ by $\Delta\delta_{i_1,i}$. To keep the power consumption of BSs i_1 and i, the following power shift can be obtained.

$$\begin{cases} \delta'_{i_1,i}=\delta_{i_1,i}-\Delta\delta_{i_1,i},\ \delta'_{i_2,i_1}=\delta_{i_2,i_1}-\frac{\Delta\delta_{i_1,i}}{\theta_{i_2,i_1}} \\ \delta'_{i_1,i}=\delta_{i_1,i}-\Delta\delta_{i_1,i},\ \delta'_{i,i_2}=\delta_{i,i_2}-\Delta\delta_{i_1,i}\theta_{i_1,i} \end{cases} \tag{A.10}$$

Then, the corresponding power consumption of BS i_2 is updated as follows.

$$P^{o'}_{i_2}=P^{o}_{i_2}+\frac{-\frac{\Delta\delta_{i_1,i}}{\theta_{i_1,i_2}}+\Delta\delta_{i_1,i}\theta_{i_1,i}\theta_{i,i_2}}{\theta_{0,i_2}}$$

According to (4.9), $1/\theta_{i_1,i_2}>1>\theta_{i_1,i}\theta_{i,i_2}$. So, $P^{o'}_{i_2}\leq P^{o}_{i_2}$. This also contradict with the assumption.

To sum up, each BS will never receive green power supplement from one BS while providing power supplement to another BS.

A.6 Proof of Lemma 10

Lemma 3 is proved by the following two steps.

Step I: We prove that the optimal solution to the following problem must also be optimal to the original WUA problem in (4.24).

$$\begin{aligned} &\min_{(\boldsymbol{\rho},\mathcal{B}^o,\mathcal{B}^g)} \sum_{i\in\mathcal{B}^o}\tfrac{P_i-E_i}{\theta_{0,i}}-\sum_{i\in\mathcal{B}^g}\theta(E_i-P_i) \\ &s.t.\quad (4.17),(4.18),(4.19),(4.25),(4.26),(4.28) \end{aligned} \tag{A.11}$$

By comparing the objective functions and constraints of (4.24) and (A.11), we only need to prove that the optimal solution to (4.24) satisfies the newly added traffic load constraint in (4.28).

Suppose the optimal traffic load of BS i^* of the original WUA problem is less than the threshold in (4.28), $\rho_{i^*}<\widetilde{\omega}_{i^*}\widetilde{\rho}_{i^*}$. Since $\widetilde{\omega}_{i^*}\leq 1$, increasing ρ_{i^*} by $\Delta\rho_{i^*}$ is still feasible, i.e., meeting the latency ratio requirement in (4.17).

Then, the traffic load of other BSs which serve the users in the coverage of BS i^* will decrease by $\Delta\rho_i$, $i\in\mathcal{B}\backslash i^*$. The increased traffic load will be less than the

decreased traffic load because $g_{i^*}(x) > g_i(x)$.

$$\Delta\rho_{i^*} < \sum_{i\in\mathcal{B}\setminus i^*} \Delta\rho_i \tag{A.12}$$

The objective function of the WUA problem will change with $\Delta\rho_i$, as illustrated in (A.13).

$$\begin{cases} \frac{(P_{i^*}+\Delta P_{i^*})-E_{i^*}}{\theta_{0,i}} = \frac{P_{i^*}-E_{i^*}}{\theta_{0,i^*}} + \frac{\beta_{i^*}\Delta\rho_{i^*}}{\theta_{0,i^*}}, & i^* \in \mathcal{B}^o \\ -\theta(E_{i^*} - (P_{i^*} + \Delta P_{i^*})) = -\theta(E_{i^*} - P_{i^*}) + \theta\beta_{i^*}\Delta\rho_{i^*}, & i^* \in \mathcal{B}^g \\ \sum\limits_{i\in\mathcal{B}^o\setminus i^*} \frac{(P_i-\Delta P_i)-E_i}{\theta_{0,i}} - \sum\limits_{i\in\mathcal{B}^g\setminus i^*} \theta(E_i - (P_i - \Delta P_i)) = \sum\limits_{i\in\mathcal{B}^o\setminus i^*} \frac{P_i-E_i}{\theta_{0,i}} - \sum\limits_{i\in\mathcal{B}^g\setminus i^*} \theta(E_i - P_i) - \\ \qquad\qquad \left(\sum\limits_{i\in\mathcal{B}^o\setminus i^*} \frac{\beta_i\Delta\rho_i}{\theta_{0,i}} + \sum\limits_{i\in\mathcal{B}^g\setminus i^*} \theta\beta_i\Delta\rho_i\right) \end{cases} \tag{A.13}$$

With $i^* \in \mathcal{B}^g$, when $\widetilde{\omega}_{i^*}$ is set to make sure the difference between $\Delta\rho_{i^*}$ and $\sum_{i\in\mathcal{B}\setminus i^*} \Delta\rho_i$ is big enough, (A.13) will yield smaller result for the WUA problem.

$$\begin{aligned} &\theta\beta_i^*\Delta\rho_{i^*} - \left(\sum_{i\in\mathcal{B}^o\setminus i^*} \frac{\beta_i\Delta\rho_i}{\theta_{0,i}} + \sum_{i\in\mathcal{B}^g\setminus i^*} \theta\beta_i\Delta\rho_i\right) < \\ &\theta\beta_i^*\Delta\rho_{i^*} - \left(\sum_{i\in\mathcal{B}^o\setminus i^*} \theta\beta_i\Delta\rho_i + \sum_{i\in\mathcal{B}^g\setminus i^*} \theta\beta_i\Delta\rho_i\right) < 0 \end{aligned}$$

where $1/\theta_{0,i} > \theta_{i,j}/\theta_{0,i} = \theta$.

Similar conclusion can be derived for $i^* \in \mathcal{B}^o$.

$$\frac{\beta_i^*\Delta\rho_{i^*}}{\theta_{0,i^*}} - \left(\sum_{i\in\mathcal{B}^o\setminus i^*} \frac{\beta_i\Delta\rho_i}{\theta_{0,i}} + \sum_{i\in\mathcal{B}^g\setminus i^*} \theta\beta_i\Delta\rho_i\right) < 0$$

The above results contradict with the assumption and hence the solution with $\rho_{i^*} < \widetilde{\omega}_{i^*}\widetilde{\rho}_{i^*}$ is not optimal. The objective function will decrease until $\rho_{i^*} + \Delta\rho_{i^*} \geq \widetilde{\omega}_{i^*}\widetilde{\rho}_{i^*}$.

Step II: We prove the optimal solution to the redefined WUA problem in (4.29) must be the optimal solution to (A.11). Since the feasible area defined by the

constraints of (4.29) and (A.11) are the same, to prove they have the same optimal solutions, we only need to prove that the optimal solution of the redefined WUA problem will result in the maximum $\sum_{i\in\mathcal{B}^g}\theta(P_i-E_i)$, i.e., maximum $\sum_{i\in\mathcal{B}^g}P_i$.

The traffic load requirement in (4.28) has imposed BSs with sufficient green energy to serve as many mobile UEs as possible, because offloading traffic has the highest energy transfer efficiency. So, to achieve the smallest $\sum_{i\in\mathcal{B}^o}(P_i-E_i)/\theta_{0,i}$, i.e., smallest traffic load for BSs belonging to $\mathcal{B}^o$, there must be maximum $\sum_{i\in\mathcal{B}^g}\theta(P_i-E_i)$. So, (4.28) eliminates $\sum_{i\in\mathcal{B}^g}P_i-E_i$ in (A.11).

In conclusion, the WUA problem can solved by finding the optimal solution to (4.29).

A.7 Proof of Lemma 12

Since $F(\boldsymbol{\rho})$ is a convex function, the descent direction $\hat{\boldsymbol{\rho}}(k)-\boldsymbol{\rho}(k)$ should make an acute angle with the negative gradient as follows [94].

$$\langle\bigtriangledown F(\boldsymbol{\rho})|_{\boldsymbol{\rho}=\boldsymbol{\rho}(k)},\hat{\boldsymbol{\rho}}(k)-\boldsymbol{\rho}(k)\rangle<0 \tag{A.14}$$

where the gradient of $F(\boldsymbol{\rho})$ at $\boldsymbol{\rho}(k)$ is

$$\bigtriangledown F(\rho_i(k))=\frac{f(\rho_i(k))(\beta_i t(\tau^*-\rho_i(k)\tau^*-\rho_i(k))+(\tau^*+1)\theta_{0,i})+(\tau^*+1)\theta_{0,i}}{\theta_{0,i}t(\tau^*-\rho_i(k)\tau^*-\rho_i(k))(f(\rho_i(k))+1)} \tag{A.15}$$

where $f(\rho_i(k))=e^{\frac{\beta_i\rho_i(k)+P_i^S-E_i}{\theta_{0,i}}}$.

According to the definition of traffic load in (4.4), the following can be obtained.

$$\begin{aligned}&\langle\bigtriangledown F(\boldsymbol{\rho})|_{\boldsymbol{\rho}=\boldsymbol{\rho}(k)},\hat{\boldsymbol{\rho}}(k)-\boldsymbol{\rho}(k)\rangle=\textstyle\sum_{i\in\mathcal{B}}\bigtriangledown F(\rho_i(k))(\hat{\rho}_i(k)-\rho_i(k))=\\&\textstyle\int_{x\in\mathcal{A}}\lambda(x)s(x)\sum_{i\in\mathcal{B}}\frac{\bigtriangledown F(\rho_i(k))(\hat{\eta}_i(x)-\eta_i(x))}{r_i(x)}dx\end{aligned} \tag{A.16}$$

To make the inner product in (A.16) negative, we need

$$\begin{aligned}&\textstyle\sum_{i\in\mathcal{B}}\frac{(\hat{\eta}_i(x)-\eta_i(x))\bigtriangledown F(\rho_i(k))}{r_i(x)}=\\&\textstyle\sum_{i\in\mathcal{B}}\frac{\hat{\eta}_i(x)\bigtriangledown F(\rho_i(k))}{r_i(x)}-\sum_{i\in\mathcal{B}}\frac{\eta_i(x)\bigtriangledown F(\rho_i(k))}{r_i(x)}<0\end{aligned} \tag{A.17}$$

The above inequality will hold when the binary UE-BS association indicator is set as follows:

$$\hat{\eta}_i(x) = \begin{cases} 1, \ i = \arg\max\limits_{j \in \mathcal{B}} \frac{r_j(x)}{\bigtriangledown F(\rho_j(k))} \\ 0, \ else \end{cases}$$

Hence, Lemma 12 is proved.

APPENDIX B

PROOFS OF THEOREMS

B.1 Proof of Theorem 1

According to the definition of $\hat{\boldsymbol{\rho}}(k)$ in (4.38) of the ELLA algorithm, both $\hat{\boldsymbol{\rho}}(k)$ and $\boldsymbol{\rho}(k)$ are defined on $[0, \tau^*/(\tau^*+1) - \epsilon]$. So, $\hat{\boldsymbol{\rho}}(k)$ is a continuous mapping to itself. Based on the Brouwer's fixed-point theorem, there exists a solution that satisfies $\hat{\boldsymbol{\rho}}^*(k) = \boldsymbol{\rho}^*(k)$, and the corresponding $\boldsymbol{\rho}^*(k+1)$ in (4.34) is also equal to $\boldsymbol{\rho}^*(k)$.

B.2 Proof of Theorem 2

According to (4.34),

$$\boldsymbol{\rho}(k+1) - \boldsymbol{\rho}(k) = \xi_k(\hat{\boldsymbol{\rho}}(k) - \boldsymbol{\rho}(k)) \tag{B.1}$$

Since $0 < \xi_k < 1$, and $\hat{\boldsymbol{\rho}}(k) - \boldsymbol{\rho}(k)$ is the descent direction at $\boldsymbol{\rho}(k)$, we can get

$$\langle \bigtriangledown F(\boldsymbol{\rho})|_{\boldsymbol{\rho}=\boldsymbol{\rho}(k)}, \boldsymbol{\rho}(k+1) - \boldsymbol{\rho}(k) \rangle < 0 \tag{B.2}$$

As we can see, $\boldsymbol{\rho}(k+1) - \boldsymbol{\rho}(k)$ also provides a descent direction of $F(\boldsymbol{\rho})$ at $\boldsymbol{\rho}(k)$. This indicates $F(\boldsymbol{\rho}(k+1)) < F(\boldsymbol{\rho}(k))$ until $\boldsymbol{\rho}(k+1) = \boldsymbol{\rho}(k)$.

According to Chapter 9.3 in [94], with a descent direction, linear convergence can be achieved such that $\boldsymbol{\rho}(k)$ converges to the optimal traffic load vector $\boldsymbol{\rho}^*$ that minimizes $F(\boldsymbol{\rho})$ at least as fast as a geometric series. By properly selecting the backtracking line search parameters ζ and ψ, the number of iterations required for the convergence can be reduced. However, how to optimize these two parameters is beyond the scope of this dissertation.

BIBLIOGRAPHY

[1] Recommendation ITU-R M.2083-0, "IMT Vision - Framework and overall objectives of the future development of IMT for 2020 and beyond," https://www.itu.int/rec/R-REC-M.2083-0-201509-I/en (accessed on April 22, 2017).

[2] D. Bharadia, E. McMilin, and S. Katti, "Full duplex radios," in *Proceedings of the ACM SIGCOMM*, October 2013, pp. 375–386.

[3] M. Jain, J. I. Choi, T. Kim, D. Bharadia, S. Seth, K. Srinivasan, P. Levis, S. Katti, and P. Sinha, "Practical, real-time, full duplex wireless," in *Proceedings of the 17th Annual ACM International Conference on Mobile Computing and Networking (MobiCom)*, September 2011, pp. 301–312.

[4] A. Osseiran, F. Boccardi, V. Braun, K. Kusume, P. Marsch, M. Maternia, O. Queseth, M. Schellmann, H. Schotten, H. Taoka, H. Tullberg, M. Uusitalo, B. Timus, and M. Fallgren, "Scenarios for 5G mobile and wireless communications: the vision of the METIS project," *IEEE Communications Magazine*, vol. 52, no. 5, pp. 26–35, May 2014.

[5] Z. Gao, L. Dai, D. Mi, Z. Wang, M. Imran, and M. Shakir, "MmWave massive-MIMO-based wireless backhaul for the 5G ultra-dense network," *IEEE Wireless Communications*, vol. 22, no. 5, pp. 13–21, October 2015.

[6] A. Gotsis, S. Stefanatos, and A. Alexiou, "Spatial coordination strategies in future ultra-dense wireless networks," in *Proceedings of the 11th IEEE International Symposium on Wireless Communications Systems (ISWCS)*, August 2014, pp. 801–807.

[7] E. Hossain, M. Rasti, H. Tabassum, and A. Abdelnasser, "Evolution toward 5G multi-tier cellular wireless networks: An interference management perspective," *IEEE Wireless Communications*, vol. 21, no. 3, pp. 118–127, June 2014.

[8] M. Peng, Y. Li, T. Quek, and C. Wang, "Device-to-device underlaid cellular networks under Rician fading channels," *IEEE Transactions on Wireless Communications*, vol. 13, no. 8, pp. 4247–4259, August 2014.

[9] A. Asadi, Q. Wang, and V. Mancuso, "A survey on Device-to-Device communication in cellular networks," *IEEE Communications Surveys and Tutorials*, vol. 16, no. 4, pp. 1801–1819, Fourth Quarter 2014.

[10] M. Tehrani, M. Uysal, and H. Yanikomeroglu, "Device-to-device communication in 5G cellular networks: challenges, solutions, and future directions," *IEEE Communications Magazine*, vol. 52, no. 5, pp. 86–92, May 2014.

[11] M. Satyanarayanan, P. Bahl, R. Caceres, and N. Davies, "The case for VM-based cloudlets in mobile computing," *IEEE Pervasive Computing*, vol. 8, no. 4, pp. 14–23, October 2009.

[12] M. Satyanarayanan, R. Schuster, M. Ebling, G. Fettweis, H. Flinck, K. Joshi, and K. Sabnani, "An open ecosystem for mobile-cloud convergence," *IEEE Communications Magazine*, vol. 53, no. 3, pp. 63–70, March 2015.

[13] M. Satyanarayanan, Z. Chen, K. Ha, W. Hu, W. Richter, and P. Pillai, "Cloudlets: at the leading edge of mobile-cloud convergence," in *Proceedings of the 6th IEEE International Conference on Mobile Computing, Applications and Services (MobiCASE)*, November 2014, pp. 1–9.

[14] S. Clinch, J. Harkes, A. Friday, N. Davies, and M. Satyanarayanan, "How close is close enough? understanding the role of cloudlets in supporting display appropriation by mobile users," in *Proceedings of the IEEE International Conference on Pervasive Computing and Communications (PerCom)*, March 2012, pp. 122–127.

[15] G. Lewis, S. Simanta, M. Novakouski, G. Cahill, J. Boleng, E. Morris, and J. Root, "Architecture patterns for mobile systems in resource-constrained environments," in *Proceedings of the IEEE Military Communications Conference (MILCOM)*, November 2013, pp. 680–685.

[16] D. Li, W. Saad, I. Guvenc, A. Mehbodniya, and F. Adachi, "Decentralized energy allocation for wireless networks with renewable energy powered base stations," *IEEE Transactions on Communications*, vol. 63, no. 6, pp. 2126–2142, June 2015.

[17] "EAGER: REPWiNet: Renewable Energy Powered Wireless Networks - Architecture, Protocols and Implementations," http://nsf.gov/awardsearch/showAward?AWD_ID=1147602 (accessed on September 22, 2013), National Science Foundation.

[18] X. Huang, T. Han, and N. Ansari, "On green energy powered cognitive radio networks," *IEEE Communications Surveys and Tutorials*, vol. 17, no. 2, pp. 827–842, Second Quarter 2015.

[19] C. Liang and F. Yu, "Wireless network virtualization: A survey, some research issues and challenges," *IEEE Communications Surveys and Tutorials*, vol. 17, no. 1, pp. 358–380, First Quarter 2015.

[20] R. Kokku, R. Mahindra, H. Zhang, and S. Rangarajan, "NVS: A substrate for virtualizing wireless resources in cellular networks," *IEEE/ACM Transactions on Networking*, vol. 20, no. 5, pp. 1333–1346, October 2012.

[21] K. Nakauchi, K. Ishizu, H. Murakami, A. Nakao, and H. Harada, "AMPHIBIA: A cognitive virtualization platform for end-to-end slicing," in *Proceedings of the IEEE International Conference on Communications (ICC)*, June 2011, pp. 1–5.

[22] A. Manzalini, R. Minerva, F. Callegati, W. Cerroni, and A. Campi, "Clouds of virtual machines in edge networks," *IEEE Communications Magazine*, vol. 51, no. 7, pp. 63–70, July 2013.

[23] Q. Duan, N. Ansari, and M. Toy, "Software-defined network virtualization: an architectural framework for integrating SDN and NFV for service provisioning in future networks," *IEEE Network*, vol. 30, no. 5, pp. 10–16, September 2016.

[24] K. Sundaresan, M. Y. Arslan, S. Singh, S. Rangarajan, and S. V. Krishnamurthy, "FluidNet: A flexible cloud-based radio access network for small cells," *IEEE/ACM Transactions on Networking*, vol. 24, no. 2, pp. 915–928, April 2016.

[25] "ECOMP (enhanced control, orchestration, management & policy) architecture white paper," Url/http://about.att.com/content/dam/snrdocs/ecomp.pdf (accessed on April 11, 2017), AT&T Inc., Dallas, TX.

[26] S. Bu, F. Yu, Y. Cai, and X. Liu, "When the smart grid meets energy-efficient communications: Green wireless cellular networks powered by the smart grid," *IEEE Transactions on Wireless Communications*, vol. 11, no. 8, pp. 3014–3024, August 2012.

[27] C.-H. Lo and N. Ansari, "The progressive smart grid system from both power and communications aspects," *IEEE Communications Surveys Tutorials*, vol. 14, no. 3, pp. 799–821, 2012.

[28] E. Vincent and S. Yusuf, "Integrating renewable energy and smart grid technology into the nigerian electricity grid system," *Scientific Research Smart Grid and Renewable Energy*, vol. 5, no. 9, pp. 220–238, September 2014.

[29] "Grid-connected renewable energy systems," http://energy.gov/energysaver/grid-connected-renewable-energy-systems (accessed on April 22, 2017), Department of Energy, Washington, DC.

[30] X. Huang and N. Ansari, "Energy sharing within EH-enabled wireless communication networks," *IEEE Wireless Communications*, vol. 22, no. 3, pp. 144–149, June 2015.

[31] "C-RAN: The road towards green radio access network, white paper," http://labs.chinamobile.com/cran/category/file-download/ (accessed on September 22, 2013), China Mobile Research Institute, Beijing, China.

[32] L. E. Li, Z. M. Mao, and J. Rexford, "Toward software-defined cellular networks," in *Proceedings of the IEEE European Workshop on Software Defined Networking*, Oct 2012, pp. 7–12.

[33] 3GPP TR 36.814 V0.4.1., "Further Advancements for E-UTRA Physical Layer Aspects," http://www.3gpp.org/ftp/Specs/html-info/36814.htm (accessed on September 22, 2013).

[34] S. E. Elayoubi, O. B. Haddada, and B. Fourestie, "Performance evaluation of frequency planning schemes in OFDMA-based networks," *IEEE Transactions on Wireless Communications*, vol. 7, no. 5, pp. 1623–1633, 2008.

[35] M. Qian, W. Hardjawana, Y. Li, B. Vucetic, J. Shi, and X. Yang, "Inter-cell interference coordination through adaptive soft frequency reuse in LTE networks," in *Proceedings of the IEEE Wireless Communications and Networking Conference (WCNC)*, 2012, pp. 1618–1623.

[36] D. Yang, X. Fang, and G. Xue, "Game theory in cooperative communications," *IEEE Wireless Communications*, vol. 19, no. 2, pp. 44–49, April 2012.

[37] Q. Zhang, J. Jia, and J. Zhang, "Cooperative relay to improve diversity in cognitive radio networks," *IEEE Communications Magazine*, vol. 47, no. 2, pp. 111–117, 2009.

[38] P. Li, S. Guo, Z. Cheng, and A. Vasilakos, "Joint relay assignment and channel allocation for energy-efficient cooperative communications," in *Proceedings of the IEEE Wireless Communications and Networking Conference (WCNC)*, 2013, pp. 626–630.

[39] H. Zhu and J. Wang, "Radio Resource Allocation in Multiuser Distributed Antenna Systems," *IEEE Journal on Selected Areas in Communications*, vol. 31, no. 10, pp. 2058–2066, October 2013.

[40] Q. Cui, B. Luo, X. Huang, A. Dowhuszko, and J. Jiang, "Closed-form solution for minimizing power consumption in coordinated transmissions," *EURASIP Journal on Wireless Communications and Networking*, vol. 2012, no. 1, pp. 1–14, 2012.

[41] J. Zhao, T. Quek, and Z. Lei, "Coordinated multipoint transmission with limited backhaul data transfer," *IEEE Transactions on Wireless Communications*, vol. 12, no. 6, pp. 2762–2775, 2013.

[42] V. Varma, S. Elayoubi, M. Debbah, and s. Lasaulce, "On the energy efficiency of virtual mimo systems," in *Proceedings of the IEEE 24th International Symposium on Personal, Indoor and Mobile Radio Communications (PIMRC Workshops)*, Sept 2013, pp. 11–15.

[43] 3GPP R1-050507, "Soft frequency reuse scheme for UTRAN LTE," http://www.3gpp.org/ftp/tsg_ran/wg1_rl1/TSGR1_41/Docs/ (accessed on September 22, 2013).

[44] E. Liu, Q. Zhang, and K. Leung, "Relay-Assisted Transmission with Fairness Constraint for Cellular Networks," *IEEE Transactions on Mobile Computing*, vol. 11, no. 2, pp. 230–239, Feb 2012.

[45] D. Wang, X. Xu, X. Chen, and X. Tao, "Joint scheduling and resource allocation based on genetic algorithm for coordinated multi-point transmission using adaptive modulation," in *Proceedings of the 23rd IEEE International Symposium on Personal Indoor and Mobile Radio Communications (PIMRC)*, Sept 2012, pp. 220–225.

[46] G. Li, Z. Xu, C. Xiong, C. Yang, S. Zhang, Y. Chen, and S. Xu, "Energy-efficient wireless communications: tutorial, survey, and open issues," *IEEE Wireless Communications*, vol. 18, no. 6, pp. 28–35, December 2011.

[47] S. Cui, A. Goldsmith, and A. Bahai, "Energy-constrained modulation optimization," *IEEE Transactions on Wireless Communications*, vol. 4, no. 5, pp. 2349–2360, Sept 2005.

[48] F. Brah, A. Zaidi, J. Louveaux, and L. Vandendorpe, "On the Lambert-W function for constrained resource allocation in cooperative networks," *EURASIP Journal on Wireless Communications and Networking*, vol. 19, no. 1, pp. 1–13, 2011.

[49] S. Boyd and L. Vandenberghe, *Convex Optimization*. Cambridge University Press, 2004.

[50] X. Huang and N. Ansari, "Joint spectrum and power allocation for multi-node cooperative wireless systems," *IEEE Transactions on Mobile Computing*, vol. 14, no. 10, pp. 2034–2044, October 2015.

[51] ——, "RF energy harvesting enabled power sharing in relay networks," in *Proceedings of the IEEE Online Conference on Green Communications (OnlineGreencomm)*, November 2014, pp. 1–6.

[52] A. Sakr and E. Hossain, "Location-aware cross-tier coordinated multipoint transmission in two-tier cellular networks," *IEEE Transactions on Wireless Communications*, vol. 13, no. 11, pp. 6311–6325, Nov 2014.

[53] X. Huang and N. Ansari, "Optimal cooperative power allocation for energy-harvesting-enabled relay networks," *IEEE Transactions on Vehicular Technology*, vol. 65, no. 4, pp. 2424–2434, April 2016.

[54] K. Tutuncuoglu and A. Yener, "Multiple access and two-way channels with energy harvesting and bi-directional energy cooperation," in *Proceedings of the IEEE Information Theory and Applications Workshop (ITA)*, Feb 2013, pp. 1–8.

[55] ——, "The energy harvesting and energy cooperating two-way channel with finite-sized batteries," in *Proceedings of the IEEE Global Communications Conference (GLOBECOM)*, Dec 2014, pp. 1424–1429.

[56] J. Xu and R. Zhang, "CoMP meets smart grid: A new communication and energy cooperation paradigm," *IEEE Transactions on Vehicular Technology*, vol. 64, no. 6, pp. 2476–2488, June 2015.

[57] B. Gurakan, O. Ozel, J. Yang, and S. Ulukus, "Energy cooperation in energy harvesting wireless communications," in *Proceedings of the IEEE International Symposium on Information Theory Proceedings (ISIT)*, July 2012, pp. 965–969.

[58] K. Tutuncuoglu and A. Yener, "Cooperative energy harvesting communications with relaying and energy sharing," in *Proceedings of the IEEE Information Theory Workshop (ITW)*, Sept 2013, pp. 1–5.

[59] D. Michalopoulos, H. Suraweera, and R. Schober, "Relay selection for simultaneous information transmission and wireless energy transfer: A tradeoff perspective," *IEEE Journal on Selected Areas in Communications*, vol. 33, no. 8, pp. 1578–1594, Aug 2015.

[60] J. Laneman, D. Tse, and G. W. Wornell, "Cooperative diversity in wireless networks: Efficient protocols and outage behavior," *IEEE Transactions on Information Theory*, vol. 50, no. 12, pp. 3062–3080, 2004.

[61] C.-N. Hsu, H.-J. Su, and P.-H. Lin, "Joint subcarrier pairing and power allocation for ofdm transmission with decode-and-forward relaying," *IEEE Transactions on Signal Processing*, vol. 59, no. 1, pp. 399–414, 2011.

[62] L. Vandendorpe, R. Duran, J. Louveaux, and A. Zaidi, "Power allocation for OFDM transmission with DF relaying," in *Proceedings of the IEEE International Conference on Communications (ICC)*, May 2008, pp. 3795–3800.

[63] Z. Ding, S. Perlaza, I. Esnaola, and H. Poor, "Power allocation strategies in energy harvesting wireless cooperative networks," *IEEE Transactions on Wireless Communications*, vol. 13, no. 2, pp. 846–860, February 2014.

[64] T. Han and N. Ansari, "Smart grid enabled mobile networks: Jointly optimizing bs operation and power distribution," in *Proceedings of the IEEE International Conference on Communications (ICC)*, June 2014, pp. 2624–2629.

[65] E. Oh, B. Krishnamachari, X. Liu, and Z. Niu, "Toward dynamic energy-efficient operation of cellular network infrastructure," *IEEE Communications Magazine*, vol. 49, no. 6, pp. 56–61, June 2011.

[66] N. Ansari and T. Han, *Green Mobile Networks: A Networking Perspective*. Wiley-IEEE Press, 2017.

[67] O. Blume, D. Zeller, and U. Barth, "Approaches to energy efficient wireless access networks," in *Proceedings of the 4th IEEE International Symposium on Communications, Control and Signal Processing (ISCCSP)*, March 2010, pp. 1–5.

[68] X. Huang and N. Ansari, "Data and energy cooperation in relay-enhanced ofdm systems," in *Proceedings of the IEEE International Conference on Communications (ICC)*, May 2016.

[69] G. Miao, N. Himayat, Y. G. Li, and A. Swami, "Cross-layer optimization for energy-efficient wireless communications: a survey," *Wireless Communications and Mobile Computing*, vol. 9, no. 4, pp. 529–542, April 2009.

[70] "Sustainable energy use in mobile communications (white paper)," www.ericsson.com/technology/whitepapers/sustainable_energy.pdf (accessed on April 11, 2008), Ericson Inc., Stockholm, Sweden.

[71] Y. Mao, Y. Luo, J. Zhang, and K. Letaief, "Energy harvesting small cell networks: feasibility, deployment, and operation," *IEEE Communications Magazine*, vol. 53, no. 6, pp. 94–101, June 2015.

[72] T. Han and N. Ansari, "On optimizing green energy utilization for cellular networks with hybrid energy supplies," *IEEE Transactions on Wireless Communications*, vol. 12, no. 8, pp. 3872–3882, Aug. 2013.

[73] T. Han, X. Huang, and N. Ansari, "Energy agile packet scheduling to leverage green energy for next generation cellular networks," in *Proceedings of the IEEE International Conference on Communications (ICC)*, June 2013, pp. 3650–3654.

[74] X. Huang and N. Ansari, "Content caching and distribution in smart grid enabled wireless networks," *IEEE Internet of Things Journal*, vol. 4, no. 2, pp. 513–520, April 2017.

[75] M. Hong and H. Zhu, "Power-efficient operation of wireless heterogeneous networks using smart grids," in *Proceedings of the IEEE International Conference on Smart Grid Communications (SmartGridComm)*, Nov 2014, pp. 236–241.

[76] P. Vytelingum, S. D. Ramchurn, T. D. Voice, A. Rogers, and N. R. Jennings, "Trading agents for the smart electricity grid," in *Proceedings of the 9th International Conference on Autonomous Agents and Multiagent Systems*, May 2010, pp. 897–904.

[77] S. Bu, F. Yu, Y. Cai, and X. Liu, "When the smart grid meets energy-efficient communications: Green wireless cellular networks powered by the smart grid," *IEEE Transactions on Wireless Communications*, vol. 11, no. 8, pp. 3014–3024, 2012.

[78] X. Huang and N. Ansari, "Resource exchange in smart grid connected cooperative cognitive radio networks," *IEEE Transactions on Vehicular Technology*, DOT: 10.1109/TVT.2016.2642902, 2016.

[79] H. Kim, G. de Veciana, X. Yang, and M. Venkatachalam, "Distributed $\alpha-$optimal user association and cell load balancing in wireless networks," *IEEE/ACM Transactions on Networking*, vol. 20, no. 1, pp. 177–190, Feb. 2012.

[80] J. Lavaei and S. Low, "Zero duality gap in optimal power flow problem," *IEEE Transactions on Power Systems*, vol. 27, no. 1, pp. 92–107, 2012.

[81] T. J. Overbye, X. Cheng, and Y. Sun, "A comparison of the ac and dc power flow models for lmp calculations," in *Proceedings of the 37th Annual IEEE Hawaii International Conference on System Sciences*, Jan 2004, pp. 1–9.

[82] I. n. Goiri, K. Le, T. D. Nguyen, J. Guitart, J. Torres, and R. Bianchini, "Greenhadoop: leveraging green energy in data-processing frameworks," in *Proceedings of the 7th ACM European Conference on Computer Systems*, Apr. 2012, pp. 57–70.

[83] 3GPP TS 136 213 V8.8.0, "Physical layer procedures (release 8)," http://www.etsi.org/deliver/etsi_ts/136200_136299/136213/08.08.00_60/ts_136213v080800p.pdf (accessed on September 22, 2013).

[84] L. Kleinrock, *Queueing Systems: Computer applications*. Wiley-Interscience, 1976.

[85] G. Auer, V. Giannini, C. Desset, I. Godor, P. Skillermark, M. Olsson, M. Imran, D. Sabella, M. Gonzalez, O. Blume, and A. Fehske, "How much energy is needed to run a wireless network?" *IEEE Wireless Communications*, vol. 18, no. 5, pp. 40 –49, Oct. 2011.

[86] R. Parasher, "Load flow analysis of radial distribution network using linear data structure," *CoRR*, vol. abs/1403.4702, 2014, http://arxiv.org/abs/1403.4702 (accessed on April 22, 2017).

[87] "Energy efficiency in the U.S. power grid," http://www.abb.com/cawp/seitp202/64cee3203250d1b7c12572c8003b2b48.aspx (accessed on April 22, 2017), ABB Inc., Zrich, Switzerland.

[88] R. Baldick, "Variation of distribution factors with loading," *IEEE Transactions on Power Systems*, vol. 18, no. 4, pp. 1316–1323, Nov 2003.

[89] Y. C. Chen, S. V. Dhople, A. D. Domínguez-García, and P. W. Sauer, "Generalized injection shift factors," *IEEE Transactions on Smart Grid*, vol. PP, no. 99, pp. 1–10, 2016.

[90] N. Cai, "Linearized and distributed methods for power flow analysis and control in smart grids and microgrids," http://search.proquest.com/docview/1612601356?accountid=35725 (accessed on April 22, 2017), p. 148, 2014.

[91] M. Liu and G. Gross, "Effectiveness of the distribution factor approximations used in congestion modeling," in *Proceedings of the 14th Power Systems Computation Conference*, June 2002, pp. 1–7.

[92] "Implementing EPA's clean power plan: A menu of options," http://www.4cleanair.org/NACAA_Menu_of_Options (accessed on April 21, 2017), NACAA, Washington, D.C.

[93] 3GPP TS 36.101 version 8.4.0 Release 8, "LTE; evolved universal terrestrial radio access (E-UTRA); user equipment (UE) radio transmission and reception," http://www.etsi.org/deliver/etsi_ts/136100_136199/136101/08.04.00_60/ts_136101v080400p.pdf (accessed on September 22, 2013).

[94] S. Boyd and L. Vandenberghe, *Convex Optimization*. Cambridge University Press, 2004.

[95] M. Grant and S. Boyd, "CVX: Matlab software for disciplined convex programming, version 2.0 beta," http://cvxr.com/cvx (accessed April 11, 2014).

[96] T. Suyash, K. Vinay, and A. K., "LTE E-UTRAN and its access side protocols," *Radisys White Paper*, September 2011.

[97] A. Ulvan, R. Bestak, and M. Ulvan, "Handover procedure and decision strategy in lte-based femtocell network," *Telecommunication Systems*, vol. 52, no. 4, pp. 2733–2748, 2013.

[98] "Solar integration data sets," http://www.nrel.gov/electricity/transmission/solar_integration_methodology.html (accessed on April 11, 2017), NREL, Golden, CO.

[99] "Energy Policy Act 2005," http://web.archive.org/web/20110429035824/http://www.doi.gov/pam/EnergyPolicyAct2005.pdf (accessed on April 11, 2017).

[100] H. Kanchev, D. Lu, F. Colas, V. Lazarov, and B. Francois, "Energy management and operational planning of a microgrid with a pv-based active generator for smart grid applications," *IEEE Transactions on Industrial Electronics*, vol. 58, no. 10, pp. 4583–4592, Oct 2011.

[101] M.-Y. C. Navid Rahbari-Asr, Yuan Zhang, "Cooperative distributed scheduling for storage devices in microgrids using dynamic KKT multipliers and consensus networks," in *Proceedings of the IEEE PES General Meeting*, July 2015.

[102] "Digital mobile radio towards future generation systems: COST 231 final report," http://grow.tecnico.ulisboa.pt/~grow.daemon/cost231/ (accessed on April 22, 2017).

[103] T. Han and N. Ansari, "Green-energy aware and latency aware user associations in heterogeneous cellular networks," in *Proceedings of IEEE Global Telecommunications Conference (GLOBECOM)*, Atlanta, GA, USA, Dec. 2013.

[104] Z. M. Fadlullah, M. M. Fouda, N. Kato, A. Takeuchi, N. Iwasaki, and Y. Nozaki, "Toward intelligent machine-to-machine communications in smart grid," *IEEE Communications Magazine*, vol. 49, no. 4, pp. 60–65, April 2011.

[105] I. S. Bayram, M. Z. Shakir, M. Abdallah, and K. Qaraqe, "A survey on energy trading in smart grid," in *Proceedings of the IEEE Global Conference on Signal and Information Processing (GlobalSIP)*, Dec 2014, pp. 258–262.

[106] W. Tushar, C. Yuen, D. B. Smith, and H. V. Poor, "Price discrimination for energy trading in smart grid: A game theoretic approach," *IEEE Transactions on Smart Grid*, vol. PP, no. 99, pp. 1–12, 2016.

[107] S. Chen, N. B. Shroff, and P. Sinha, "Energy trading in the smart grid: From end-user's perspective," in *Proceedings of the Asilomar Conference on Signals, Systems and Computers*, Nov 2013, pp. 327–331.

[108] Y. Wang, W. Saad, Z. Han, H. V. Poor, and T. Başar, "A game-theoretic approach to energy trading in the smart grid," *IEEE Transactions on Smart Grid*, vol. 5, no. 3, pp. 1439–1450, May 2014.

[109] X. Huang and N. Ansari, "Content caching and user scheduling in heterogeneous wireless networks," in *Proceedings of the IEEE Global Communications Conference (GLOBECOM)*, Dec 2016, pp. 1–6.

[110] N. Abedini and S. Shakkottai, "Content caching and scheduling in wireless networks with elastic and inelastic traffic," *IEEE/ACM Transactions on Networking*, vol. 22, no. 3, pp. 864–874, June 2014.

[111] X. Vasilakos, V. A. Siris, G. C. Polyzos, and M. Pomonis, "Proactive selective neighbor caching for enhancing mobility support in information-centric networks," in *Proceedings of the Second Edition of the ACM ICN Workshop on Information-centric Networking*, August 2012, pp. 61–66.

[112] B. Ejder, B. Mehdi, K. Marios, and D. Mrouane, "Cache-enabled small cell networks: Modeling and tradeoffs," *EURASIP Journal on Wireless Communications and Networking*, vol. 2015, no. 26, p. 41, February 2015.

[113] X. Sun, N. Ansari, and Q. Fan, "Green energy aware avatar migration strategy in green cloudlet networks," in *Proceedings of the 7th IEEE International Conference on Cloud Computing Technology and Science (CloudCom)*, Nov 2015, pp. 139–146.

[114] T. H. Luan, L. Gao, Z. Li, Y. Xiang, and L. Sun, "Fog computing: Focusing on mobile users at the edge," *CoRR*, vol. abs/1502.01815, 2015, http://arxiv.org/abs/1502.01815 (accessed on April 22, 2017).

[115] A. Sengupta, R. Tandon, and O. Simeone, "Cache aided wireless networks: Tradeoffs between storage and latency," in *Proceedings of the Annual IEEE Conference on Information Science and Systems (CISS)*, March 2016, pp. 320–325.

[116] L. Al-Kanj, Z. Dawy, W. Saad, and E. Kutanoglu, "Energy-aware cooperative content distribution over wireless networks: Optimized and distributed approaches," *IEEE Transactions on Vehicular Technology*, vol. 62, no. 8, pp. 3828–3847, Oct 2013.

[117] M. A. Maddah-Ali and U. Niesen, "Cache-aided interference channels," in *Proceedings of the IEEE International Symposium on Information Theory (ISIT)*, June 2015, pp. 809–813.

[118] B. Li, Z. Wang, J. Liu, and W. Zhu, "Two decades of internet video streaming: A retrospective view," *ACM Transactions on Multimedia Computing, Communications and Applications*, vol. 9, no. 1s, pp. 33:1–33:20, Oct. 2013.

[119] F. Chen, C. Zhang, F. Wang, and J. Liu, "Crowdsourced live streaming over the cloud," in *Proceedings of the IEEE Conference on Computer Communications (INFOCOM)*, April 2015, pp. 2524–2532.

[120] X. Huang and N. Ansari, "Joint spectrum and power allocation for multi-node cooperative wireless systems," *IEEE Transactions on Mobile Computing*, vol. 14, no. 10, pp. 2034–2044, Oct 2015.